

Beyond ***The Standard Model of Cosmology***

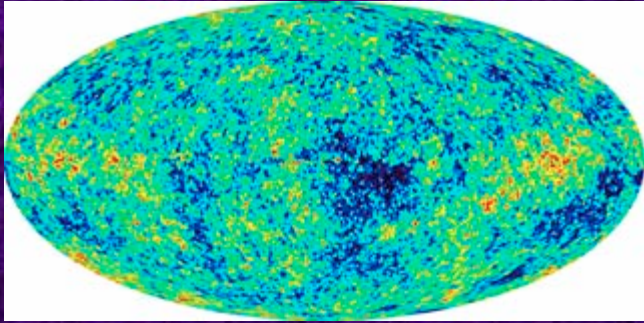
Arman Shafieloo

Korea Astronomy and Space Science Institute

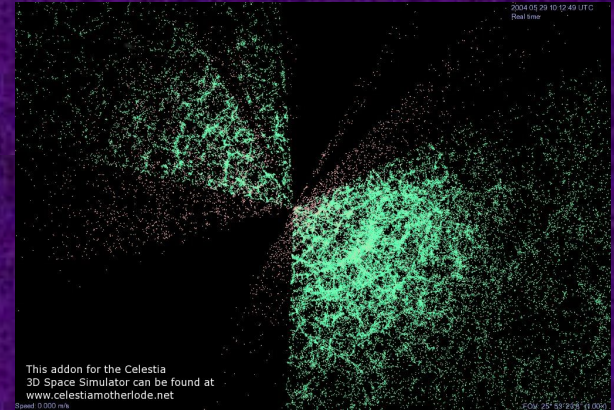
IBS-KASI Joint Workshop, CTPU-IBS, Daejeon

August 2015 ,

Cosmology, from *fiction* to being *science*.....



Cosmic Microwave Background (CMB)



Large-scale structure

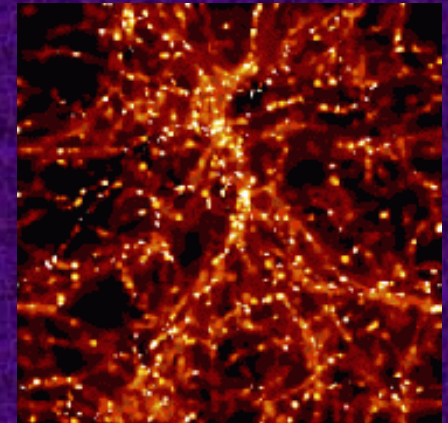
Cosmological Observations



Gravitational Lensing



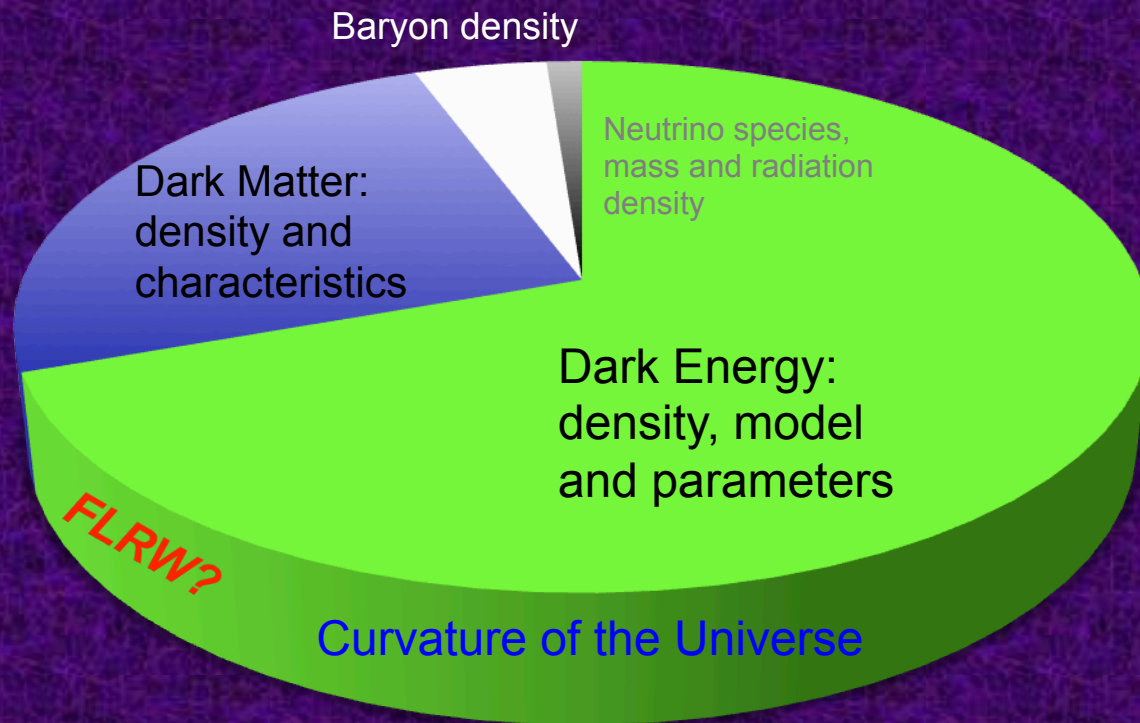
Type Ia supernovae



Lyman Alpha Forest

Era of Precision Cosmology

Combining theoretical works with new measurements and using statistical techniques to place sharp constraints on cosmological models and their parameters.



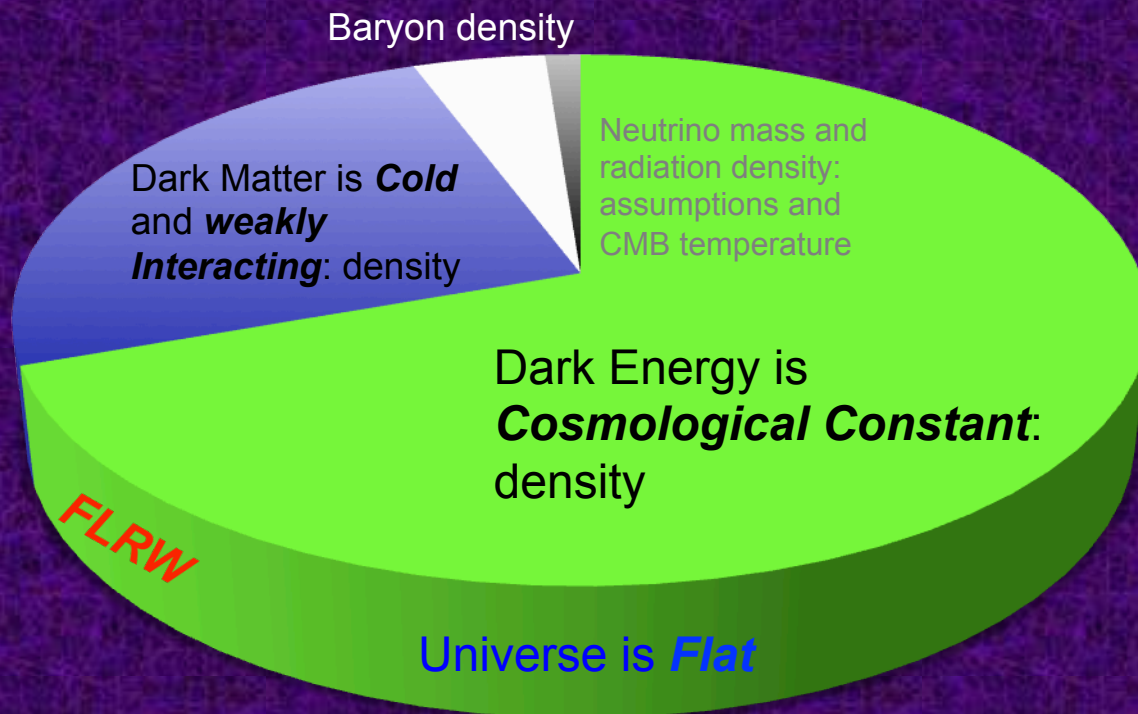
Initial Conditions:
Form of the Primordial
Spectrum and Model of
Inflation and its Parameters

Epoch of reionization

Hubble Parameter and
the Rate of Expansion

Standard Model of Cosmology

Using measurements and statistical techniques to place sharp constraints on parameters of the standard cosmological models.



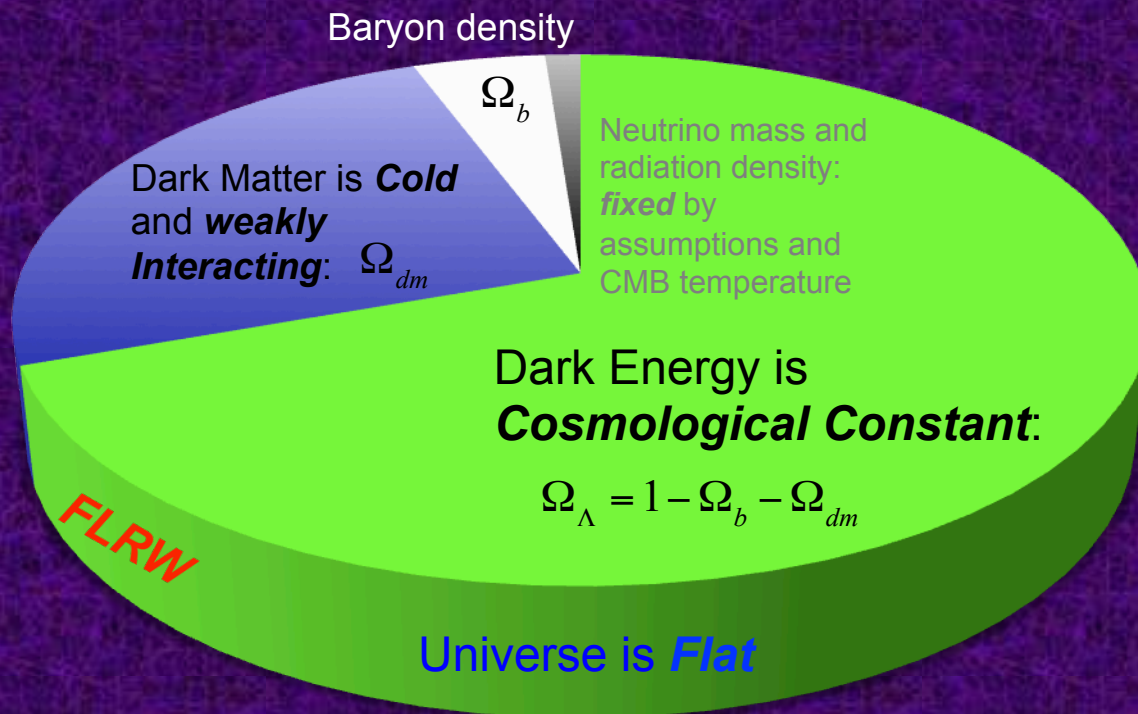
Initial Conditions:
Form of the Primordial
Spectrum is **Power-law**

Epoch of reionization

Hubble Parameter and
the Rate of Expansion

Standard Model of Cosmology

Using measurements and statistical techniques to place sharp constraints on parameters of the standard cosmological model.



Initial Conditions:
Form of the Primordial
Spectrum is **Power-law**

$$n_s, A_s$$

Epoch of reionization

$$\tau$$

Hubble Parameter and
the Rate of Expansion

$$H_0$$

Standard Model of Cosmology

Using measurements and statistical techniques to place sharp constraints on parameters of the standard cosmological model.

Baryon density

Combination of Assumptions

Dark Energy is
Cosmological Constant:

$$\Omega_{\Lambda} = 1 - \Omega_b - \Omega_{dm}$$

Universe is *Flat*

FLRW

Epoch of reionization

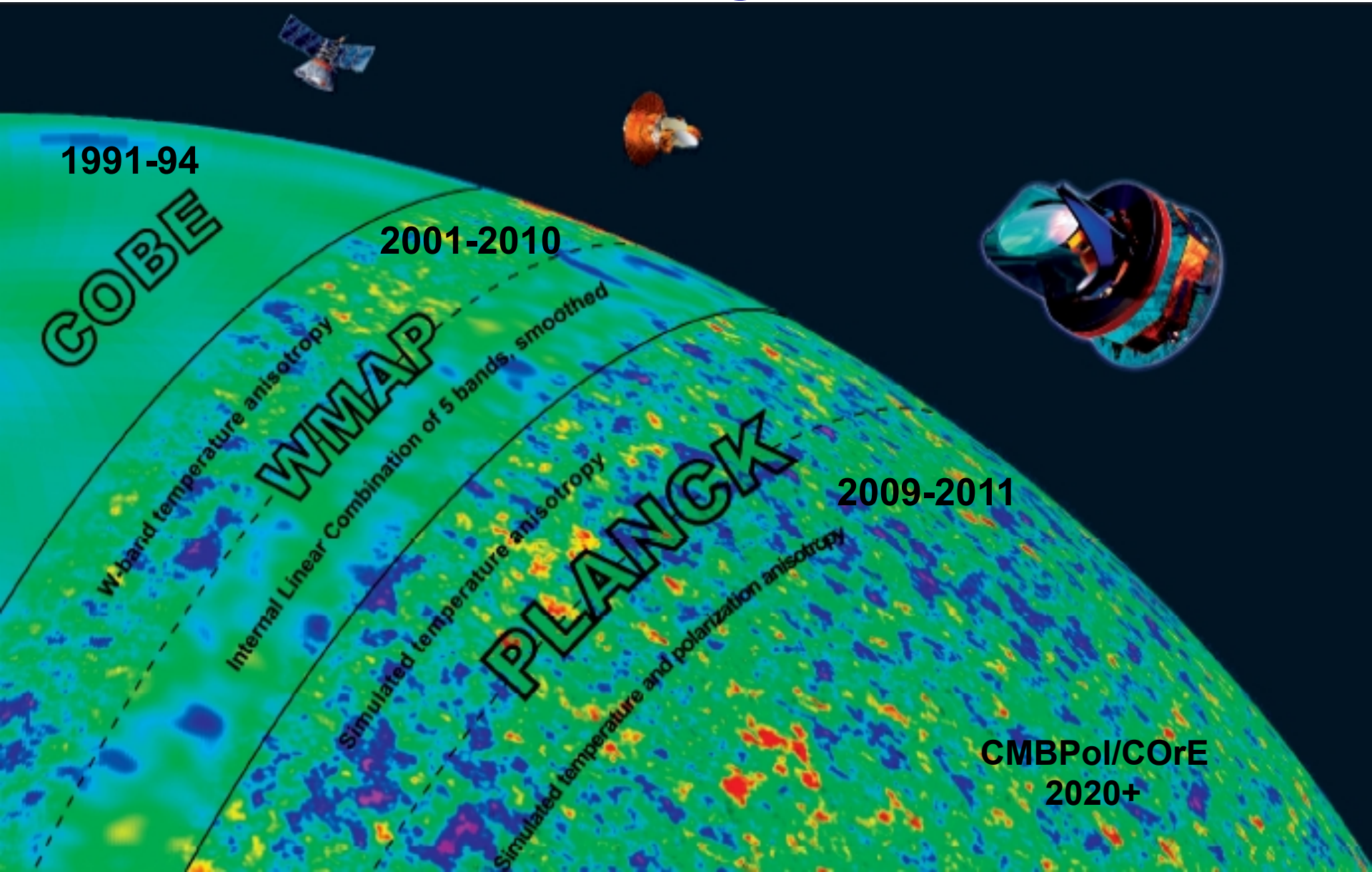
τ

Hubble Parameter and
the Rate of Expansion

H_0

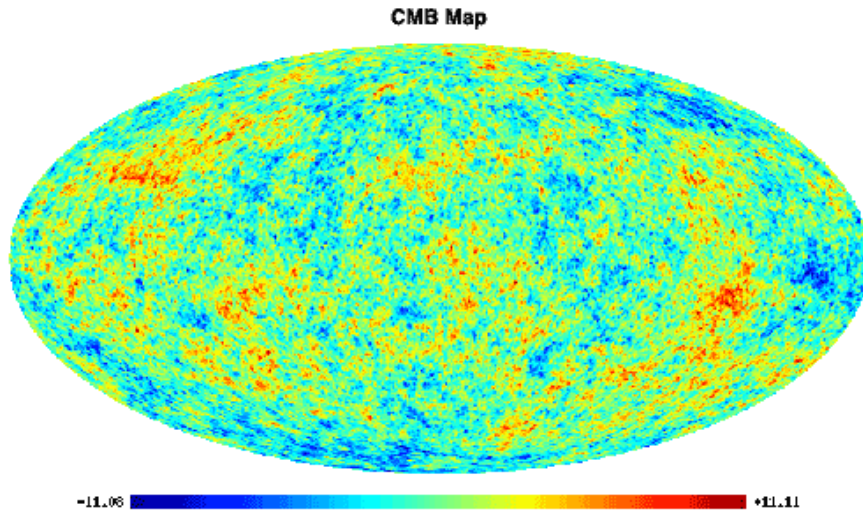
Why such assumptions?

Hints from Cosmological Observations



Statistics of CMB

CMB Anisotropy Sky map \Rightarrow Spherical Harmonic decomposition

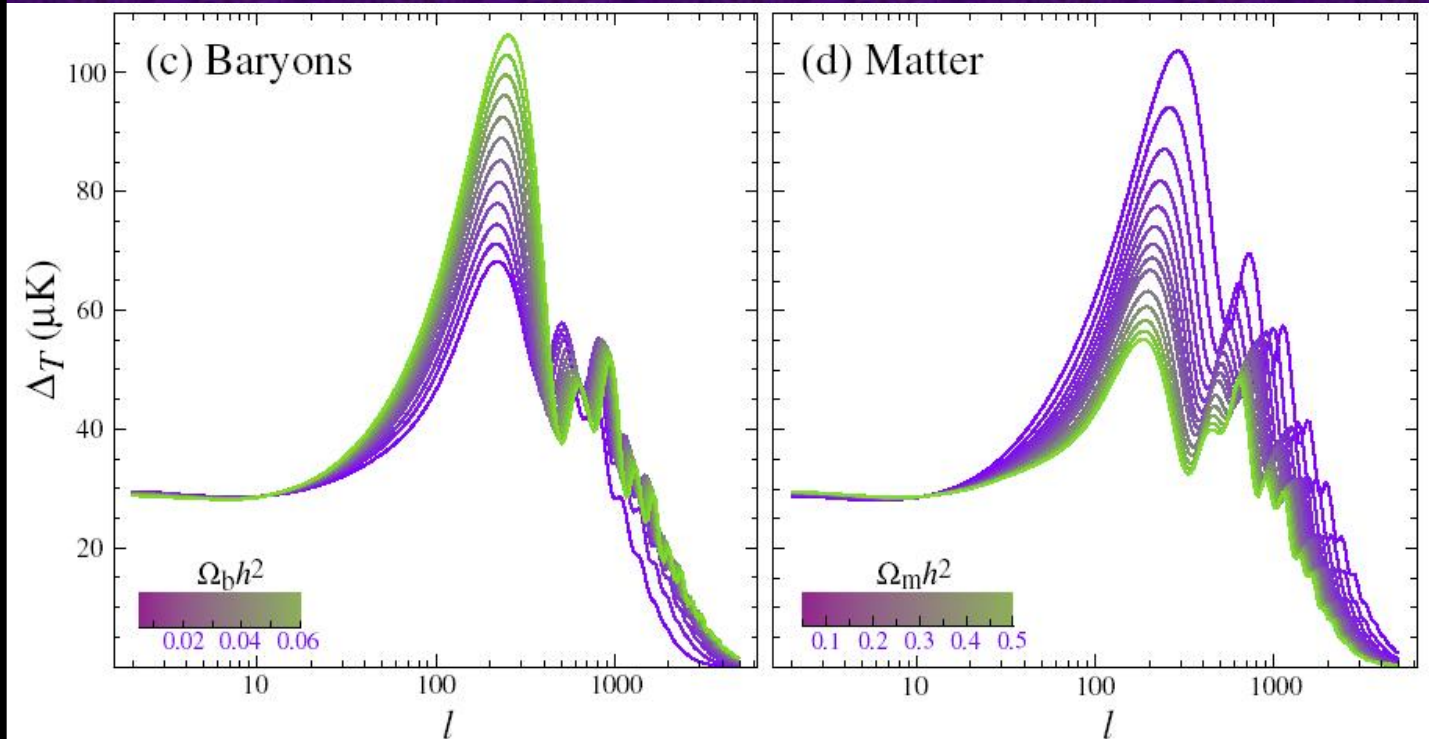
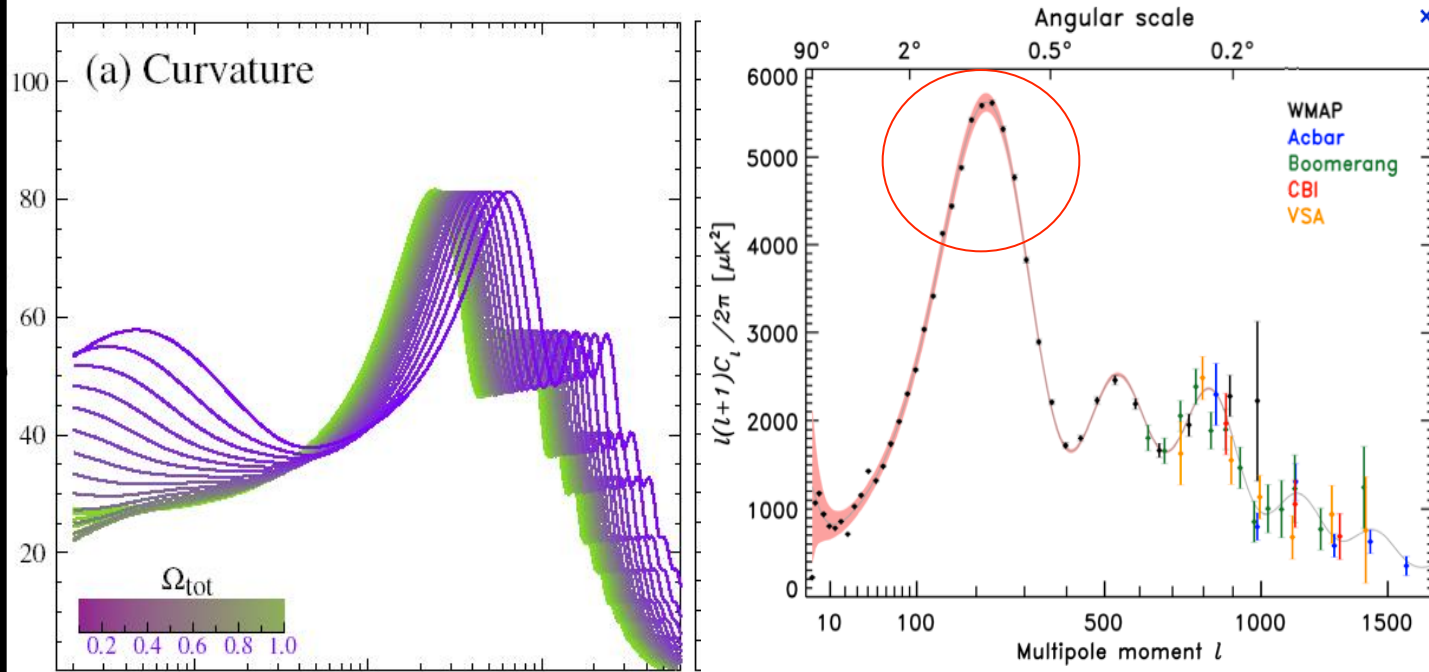


$$\Delta T(\theta, \phi) = \sum_{l=2}^{\infty} \sum_{m=-l}^l a_{lm} Y_{lm}(\theta, \phi)$$

$$\langle a_{lm} a_{l'm'}^* \rangle = C_l \delta_{ll'} \delta_{mm'}$$

Gaussian Random field \Rightarrow Completely specified by
angular power spectrum $l(l+1)C_l$:

Power in fluctuations on angular scales of $\sim \pi/l$



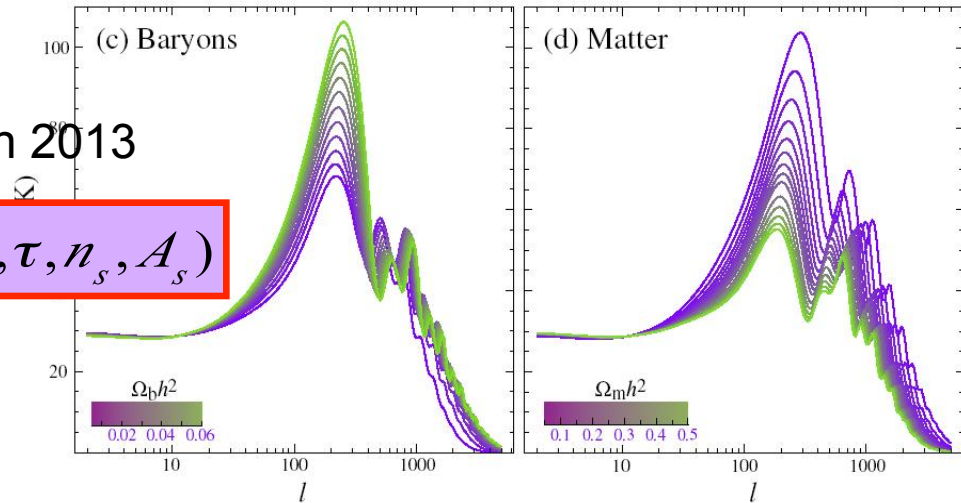
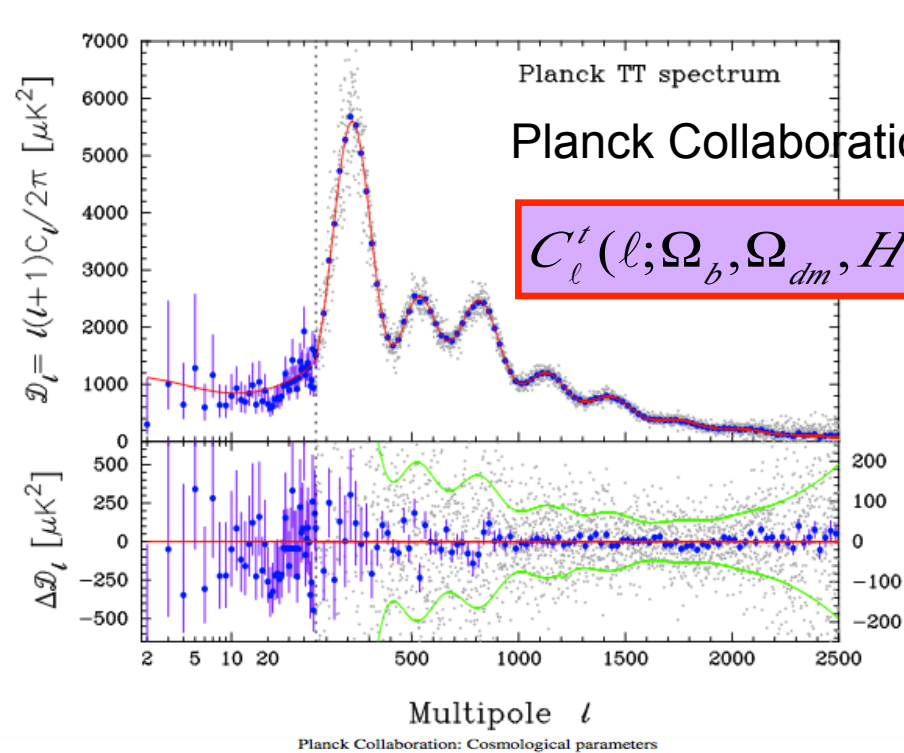
Sensitivity of the CMB acoustic temperature spectrum to four fundamental cosmological parameters.

Total density

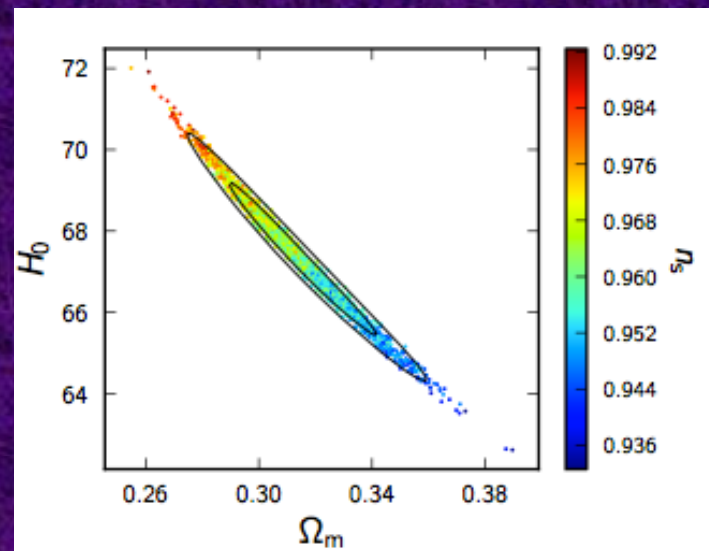
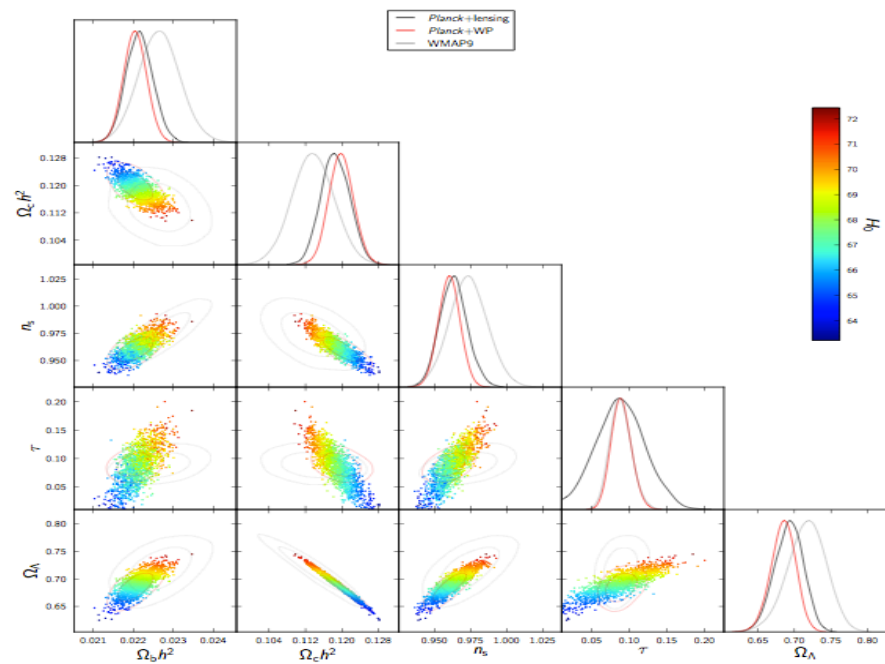
Dark Energy

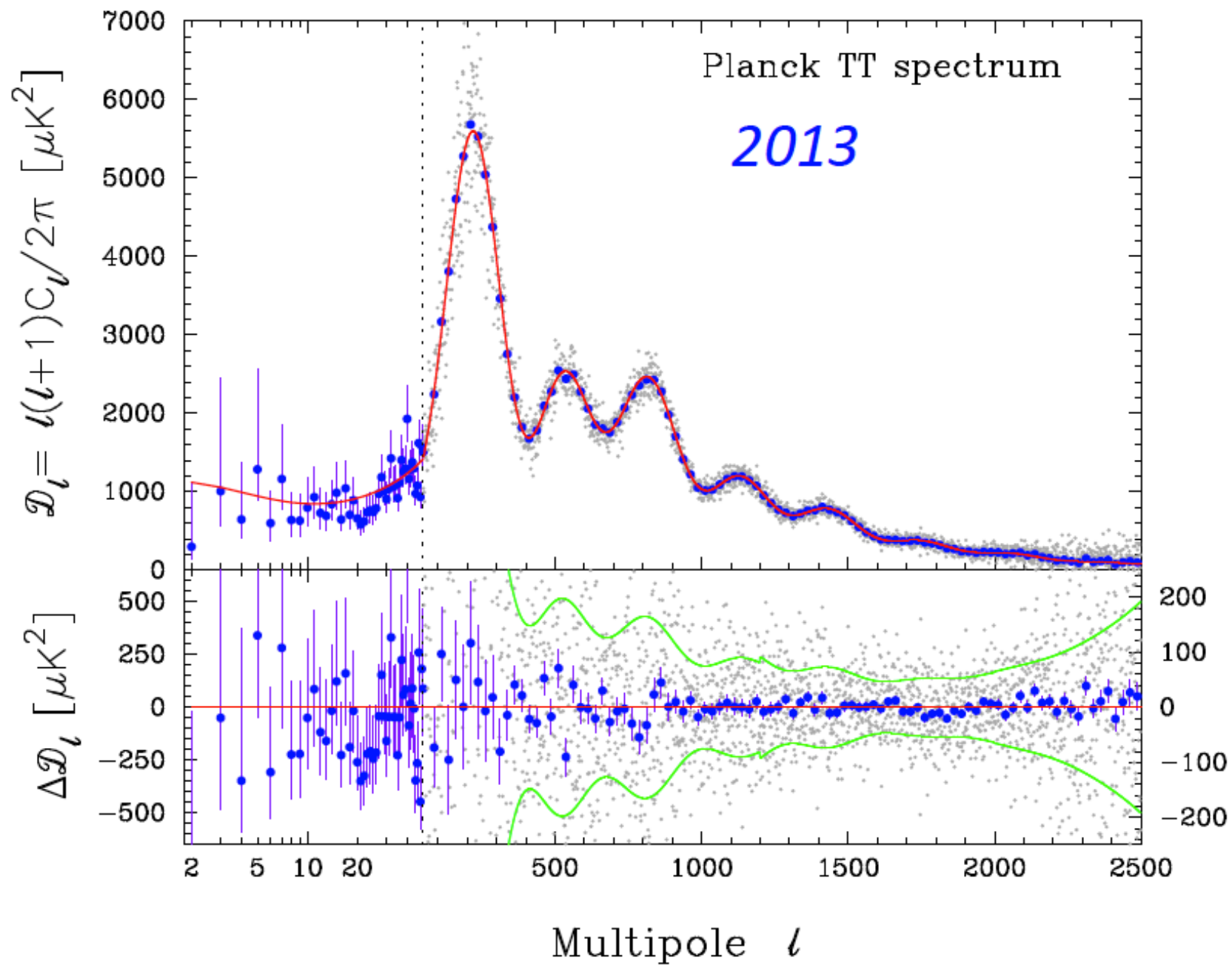
Baryon density and

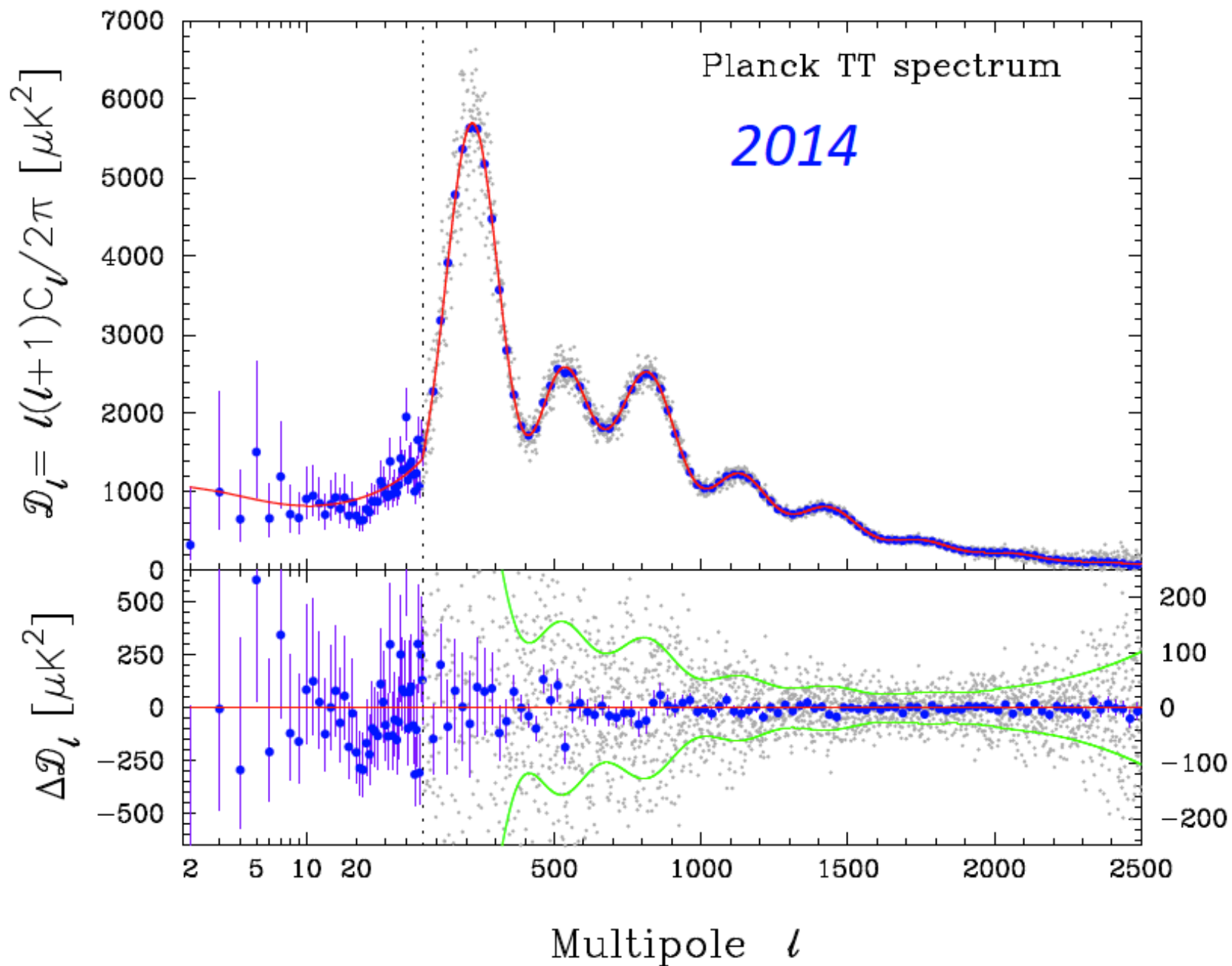
Matter density.



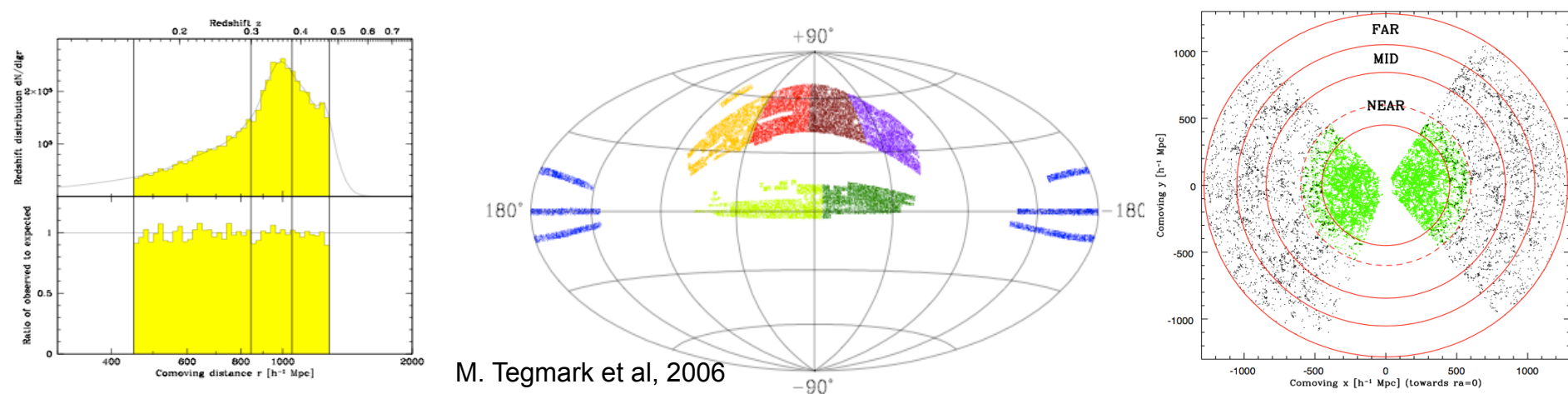
$$\chi^2 = \sum_{\ell=2}^N (C_\ell^t - C_\ell^e)^T Cov^{-1} (C_\ell^t - C_\ell^e)$$





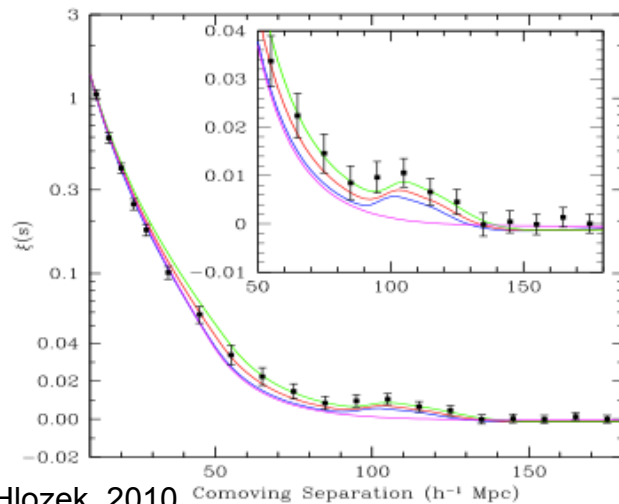


preliminary



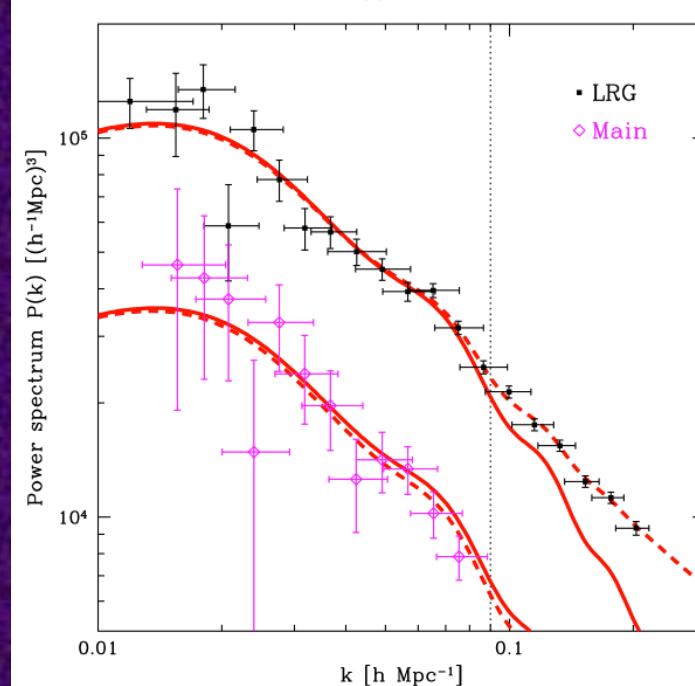
Large Scale Structure Data and Distribution of Galaxies

$$P(k) = \int_{-\infty}^{\infty} \xi(r) \exp(-ikr) r^2 dr.$$



Bassett & Hlozek, 2010

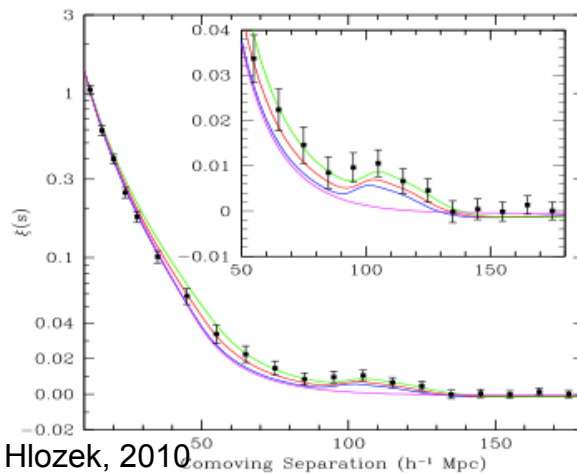
Fig. 1.1. The Baryon Acoustic Peak (BAP) in the correlation function – the BAP is visible in the clustering of the SDSS LRG galaxy sample, and is sensitive to the matter density (shown are models with $\Omega_m h^2 = 0.12$ (top), 0.13 (second) and 0.14 (third), all with $\Omega_b h^2 = 0.024$). The bottom line without a BAP is the correlation function in the pure CDM model, with $\Omega_b = 0$. From Eisenstein *et al.*, 2005 (52).



Large Scale Structure Data and Distribution of Galaxies

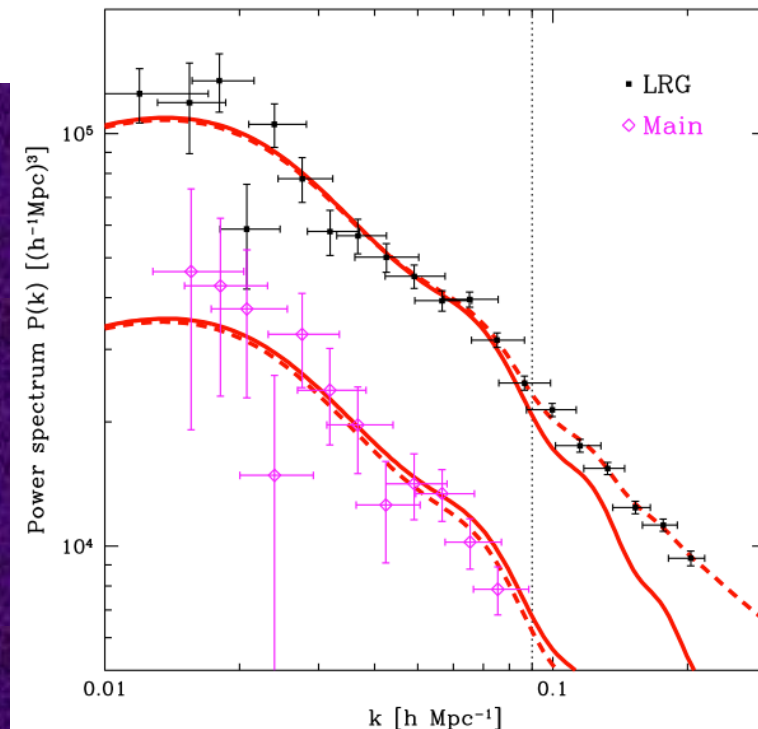
$$P(k) = \int_{-\infty}^{\infty} \xi(r) \exp(-ikr) r^2 dr.$$

Fig. 1.5. Rings of power superposed. Schematic galaxy distribution formed by placing the galaxies on rings of the same characteristic radius L . The preferred radial scale is clearly visible in the left hand panel with many galaxies per ring. The right hand panel shows a more realistic scenario - with many rings and relatively few galaxies per ring, implying that the preferred scale can only be recovered statistically.



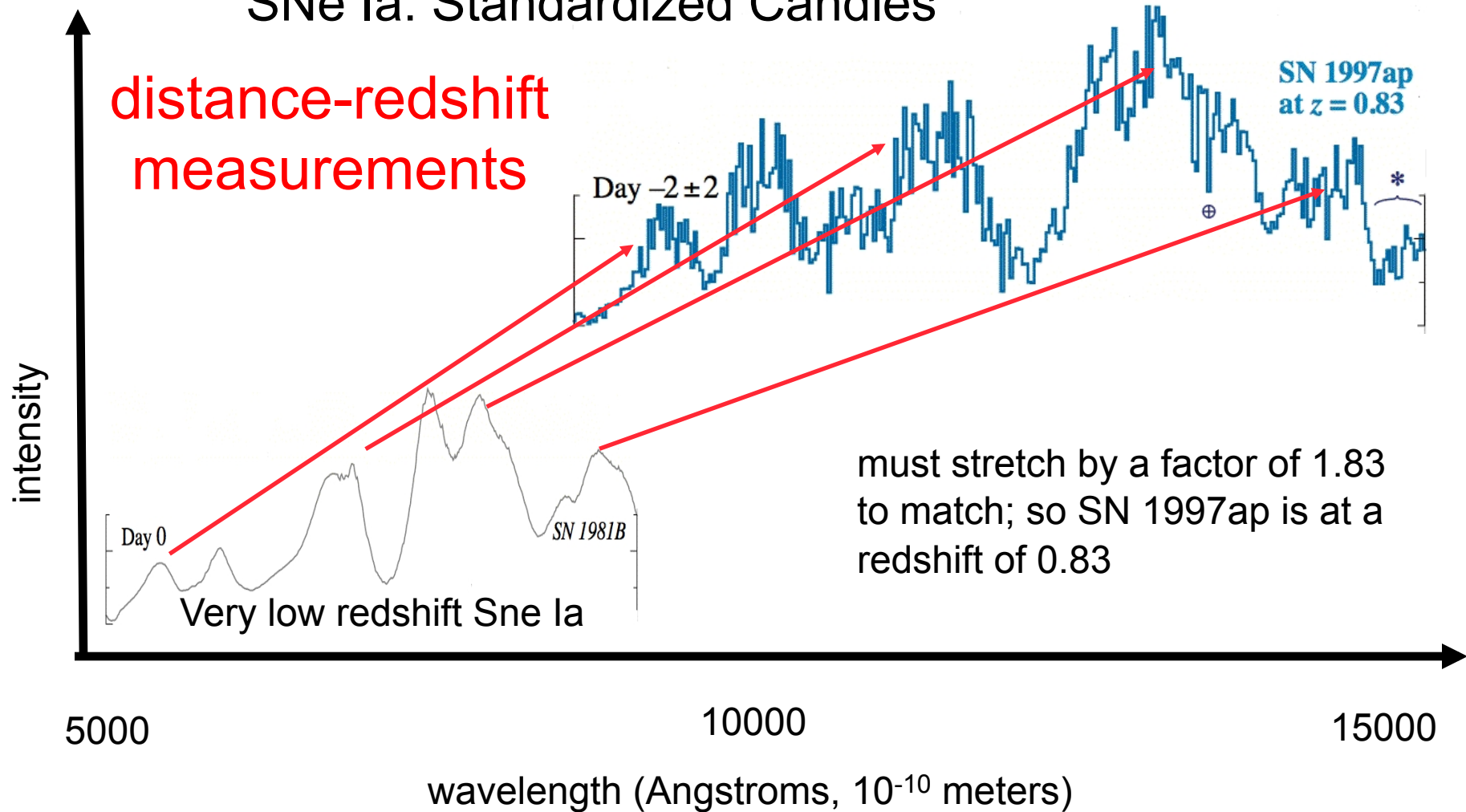
Bassett & Hlozek, 2010

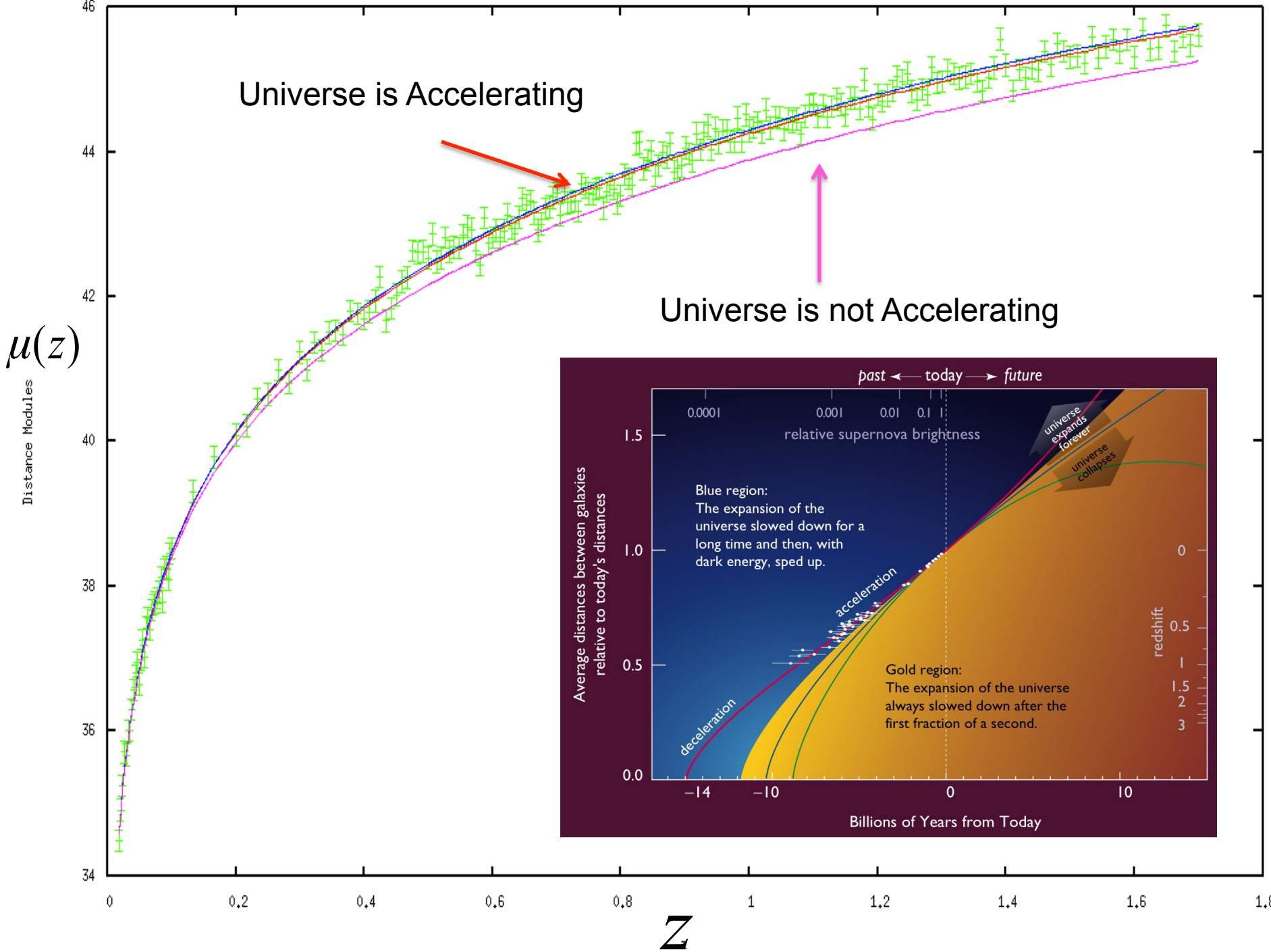
Fig. 1.1. The Baryon Acoustic Peak (BAP) in the correlation function – the BAP is visible in the clustering of the SDSS LRG galaxy sample, and is sensitive to the matter density (shown are models with $\Omega_m h^2 = 0.12$ (top), 0.13 (second) and 0.14 (third), all with $\Omega_b h^2 = 0.024$). The bottom line without a BAP is the correlation function in the pure CDM model, with $\Omega_b = 0$. From Eisenstein *et al.*, 2005 (52).



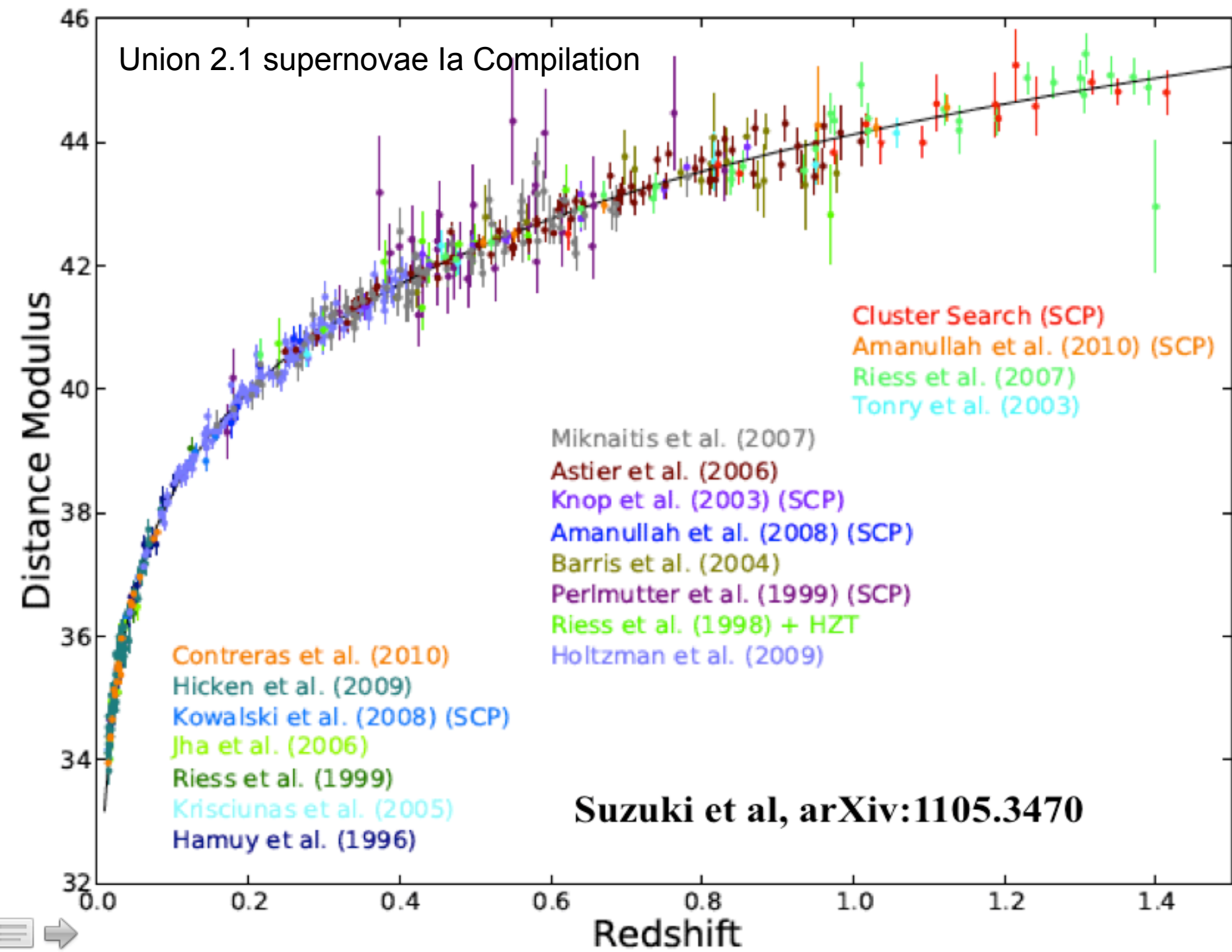
Measuring Distances in Astronomy

SNe Ia: Standardized Candles



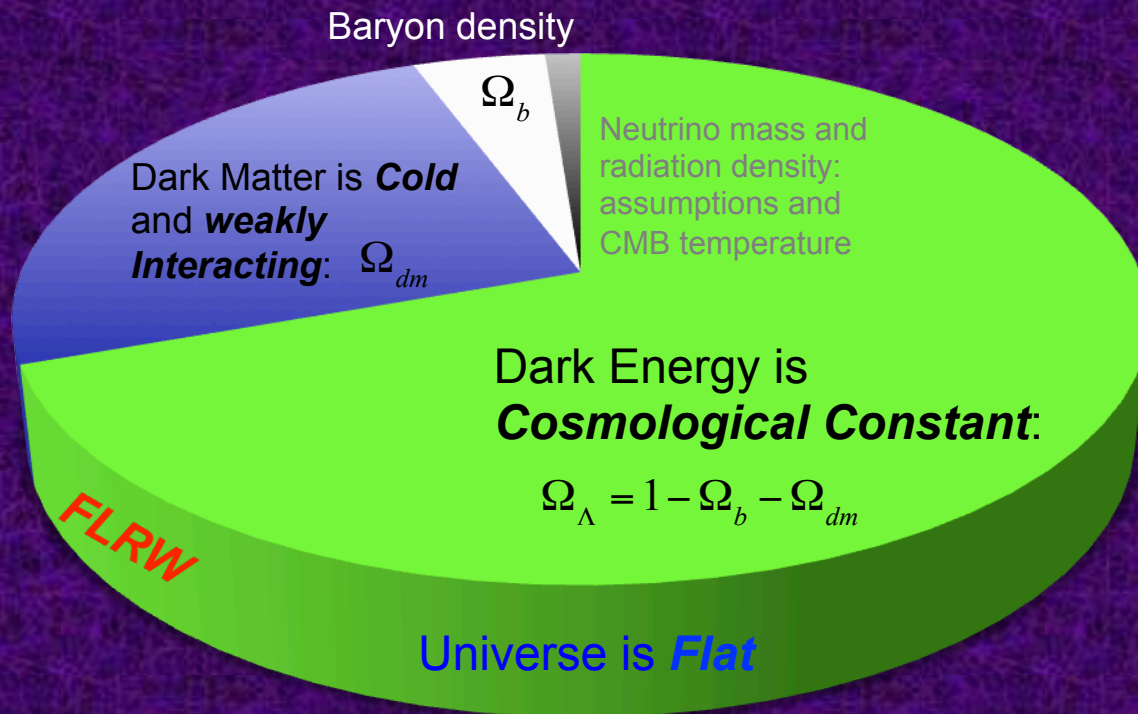


Union 2.1 supernovae Ia Compilation



Standard Model of Cosmology

combination of *reasonable* assumptions, but.....



Initial Conditions:
Form of the Primordial Spectrum is **Power-law**

$$n_s, A_s$$

Epoch of reionization

$$\tau$$

Hubble Parameter and the Rate of Expansion

$$H_0$$

Beyond the Standard Model of Cosmology

- The universe might be more complicated than its current standard model (Vanilla Model).
- There might be some extensions to the standard model in defining the cosmological quantities.
- This needs proper investigation, using advanced statistical methods, high performance computational facilities and high quality observational data.

(Present)_t

Standard Model of Cosmology

Universe is Flat

Universe is Isotropic

Universe is Homogeneous (large scales)

Dark Energy is Lambda ($w=-1$)

Power-Law primordial spectrum ($n_s=\text{const}$)

Dark Matter is cold

All within framework of FLRW

Inflation

- Extreme accelerated expansion of the early universe.
- It can be realized by scalar fields (or some other mechanisms).
- So far the best theory that can resolve the magnetic monopole problem (absence of relics), flatness problem, horizon problem and explain the initial perturbations from quantum fluctuations.
- It has many many models.
- These models are different in their statistical properties and we may be able to distinguish between them using cosmological observations.

Constraints on inflationary scenarios from cosmological observations:

- Form of the primordial spectrum (*degenerate with other cosmological quantities*).
- Tensor-to-scalar ratio of perturbation amplitudes (*near future potential probe*)
- Primordial non-Gaussianities (*near future potential probe*)

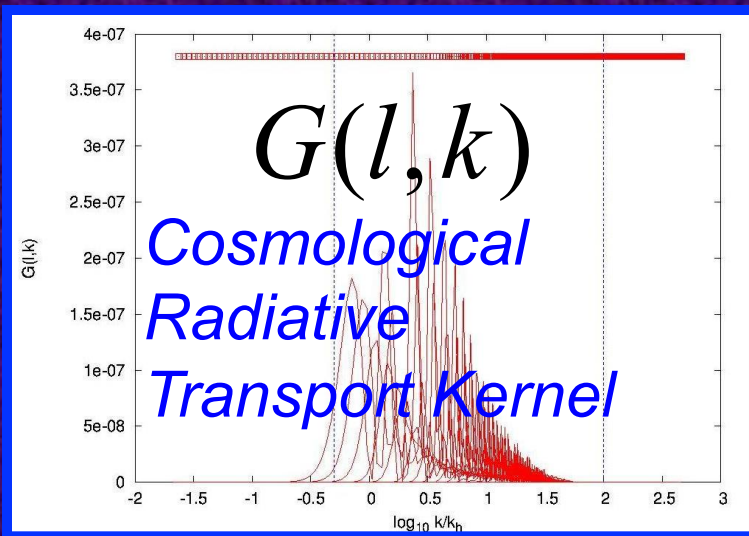
Parameterization and Model Fitting

$P(k)$
Primordial Power
Spectrum

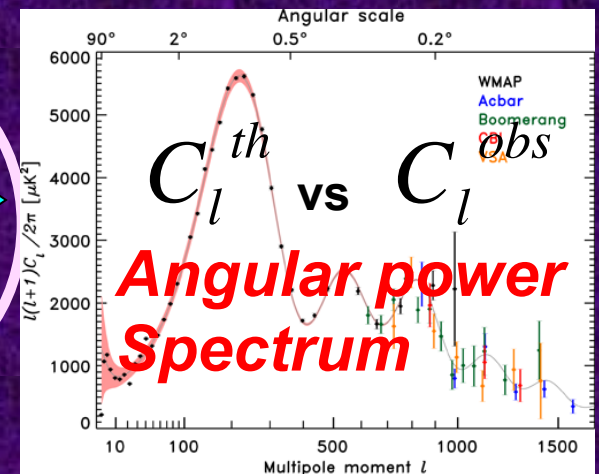
Suggested by Model of Inflation

$$C_l = \sum G(l, k) P(k)$$

Determined by background model
and cosmological parameters

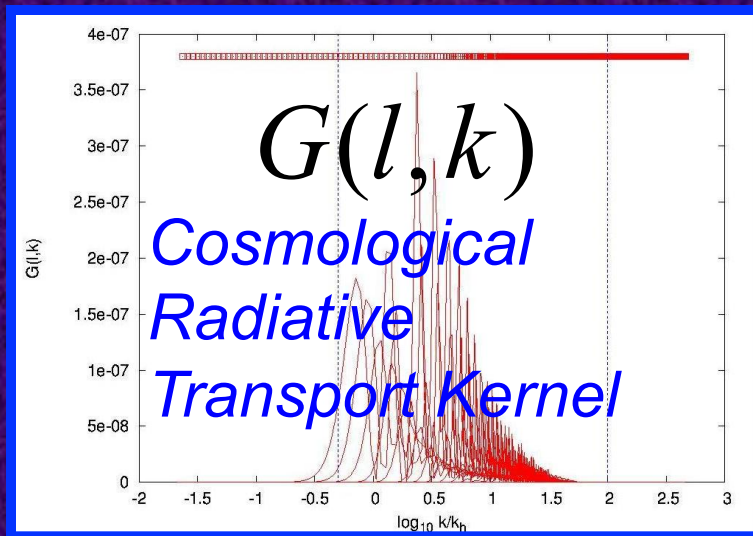


Detected by observation



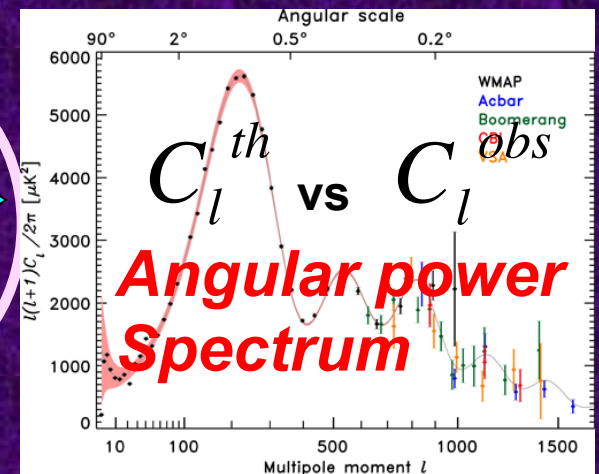
We cannot anticipate the unexpected !!

$$C_l = \sum G(l, k) P(k)$$



Determined by background model and cosmological parameters

Detected by observation



DIRECT TOP DOWN Reconstruction

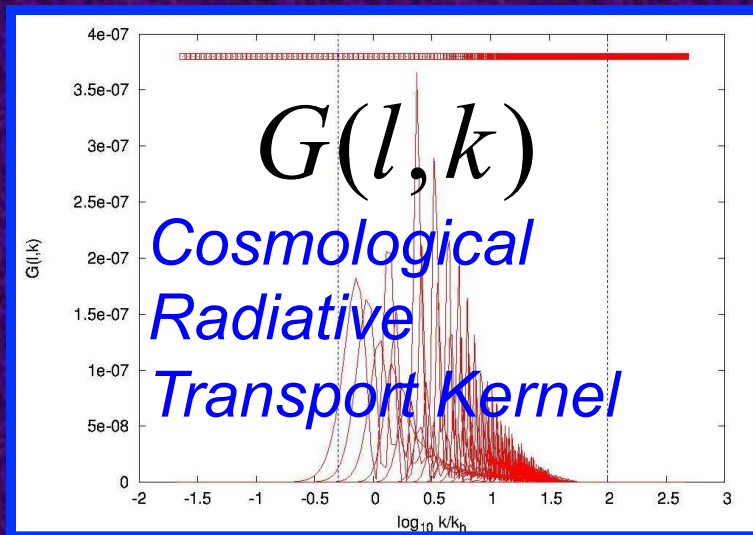
$P(k)$
Primordial Power
Spectrum

?

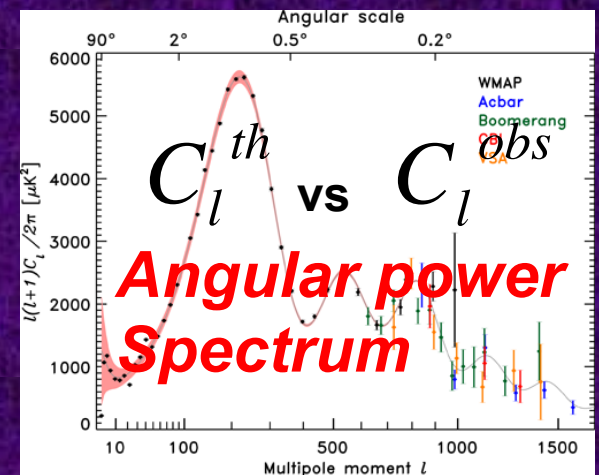
Reconstructed by Observations

$$C_l = \sum G(l, k) P(k)$$

Determined by background model
and cosmological parameters



Detected by observation



Modified Richardson-Lucy Deconvolution

- Iterative algorithm.
- Not sensitive to the initial guess.
- Enforce positivity of $P(k)$.

[$G(l, k)$ is positive definite and C_l is positive]

$$C_\ell = \sum_i G_{\ell k_i} P_{k_i}$$

$$P_k^{(i+1)} - P_k^{(i)} = P_k^{(i)} \times \left[\sum_{\ell=2}^{\ell=900} \tilde{G}_{\ell k}^{\text{un-binned}} \left\{ \left(\frac{C_\ell^D - C_\ell^{T(i)}}{C_\ell^{T(i)}} \right) \tanh^2 \left[Q_\ell (C_\ell^D - C_\ell^{T(i)}) \right] \right\}_{\text{un-binned}} + \sum_{\ell_{\text{binned}} > 900} \tilde{G}_{\ell k}^{\text{binned}} \left\{ \left(\frac{C_\ell^D - C_\ell^{T(i)}}{C_\ell^{T(i)}} \right) \tanh^2 \left[\frac{C_\ell^D - C_\ell^{T(i)}}{\sigma_\ell^D} \right]^2 \right\}_{\text{binned}} \right], \quad (1)$$

Shafieloo & Souradeep PRD 2004 ;
Shafieloo et al, PRD 2007;
Shafieloo & Souradeep, PRD 2008;
Nicholson & Contaldi JCAP 2009
Hamann, Shafieloo & Souradeep JCAP 2010
Hazra, Shafieloo & Souradeep PRD 2013
Hazra, Shafieloo & Souradeep JCAP 2013
Hazra, Shafieloo & Souradeep JCAP 2014

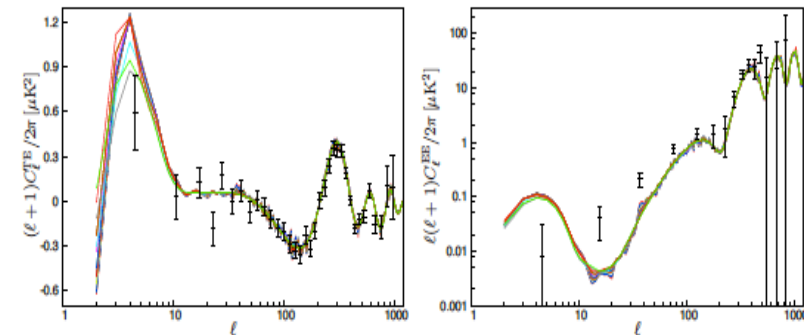
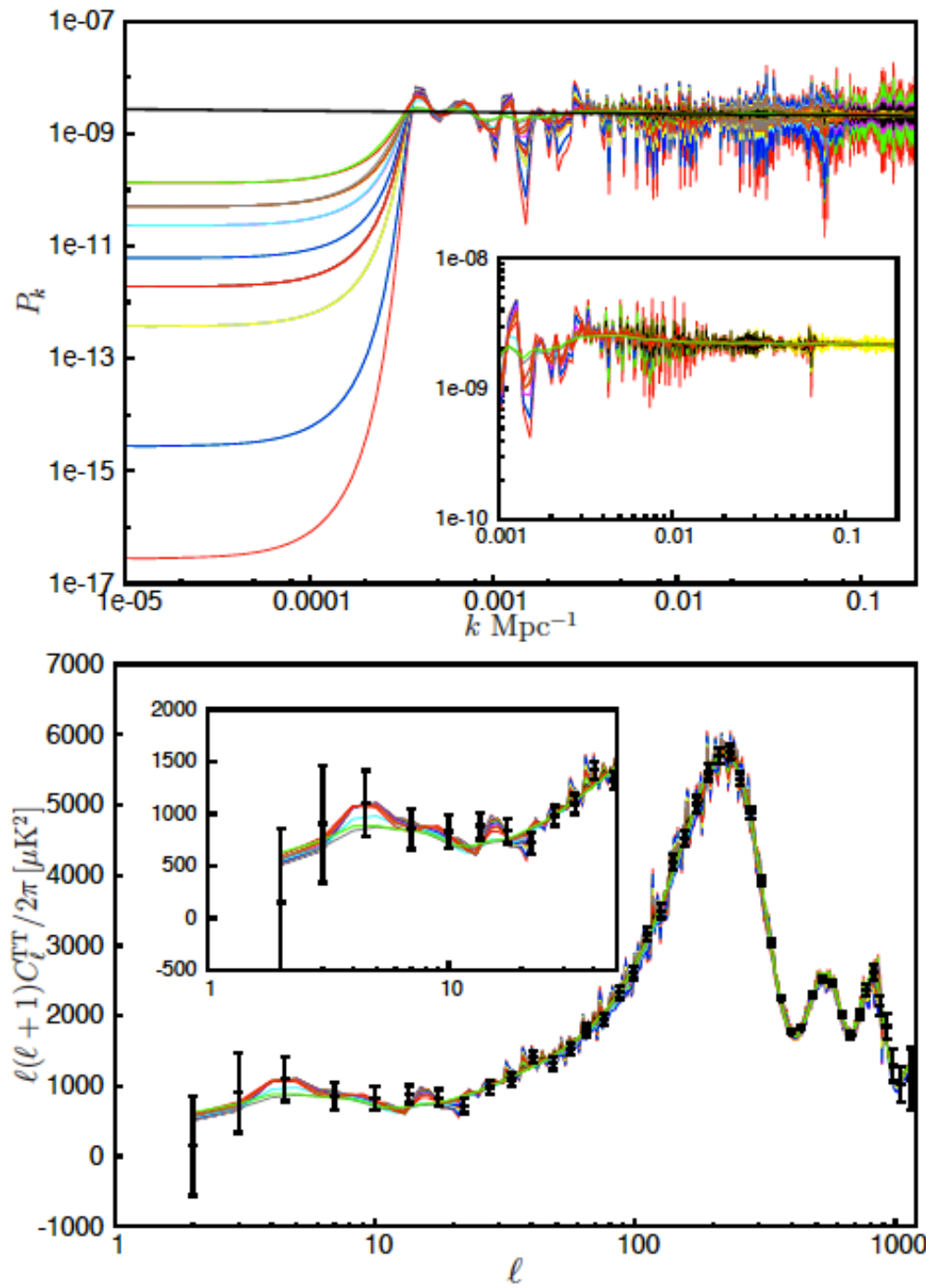
$$Q_\ell = \sum_{\ell'} (C_{\ell'}^D - C_{\ell'}^{T(i)}) COV^{-1}(\ell, \ell'),$$

Theoretical Implication: Importance of the Features in the primordial spectrum

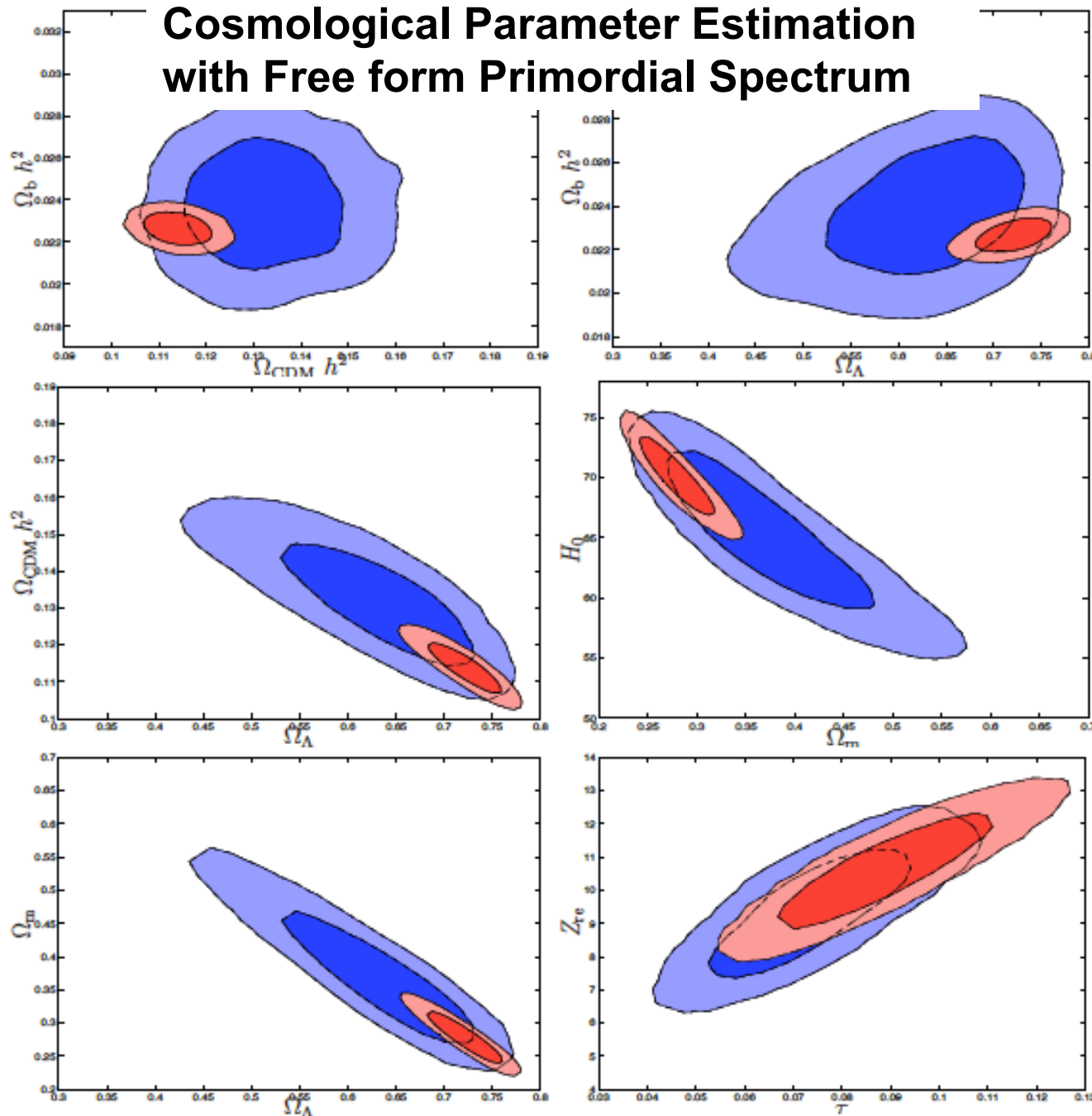
WMAP 9 analysis

The reconstructed primordial power-spectra (on top) and the corresponding angular power spectra (at the bottom) that provide a better fit ranging from **2– 300** in effective chi square (derived from WMAP 9 likelihood code) compared to the power law model.

Hazra, Shafieloo & Souradeep, JCAP 2013



Cosmological Parameter Estimation with Free form Primordial Spectrum



**Red Contours:
Power Law PPS**

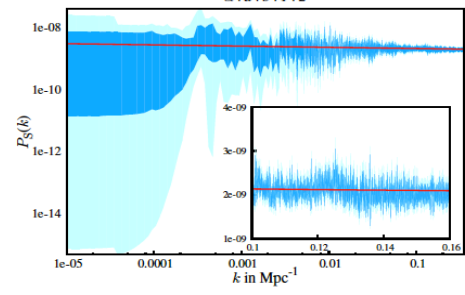
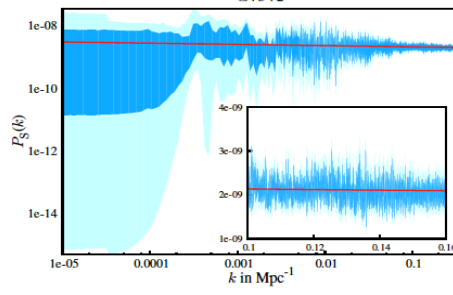
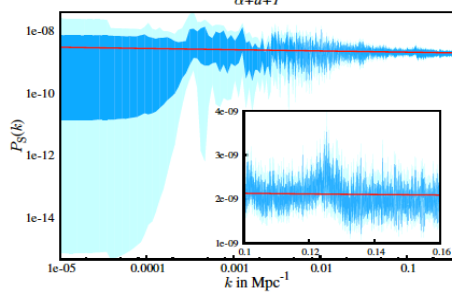
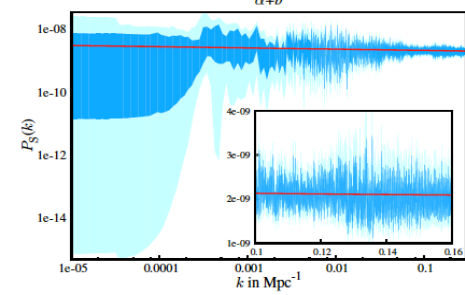
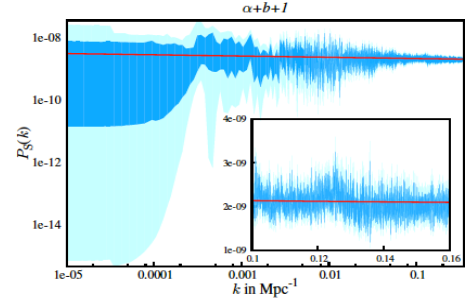
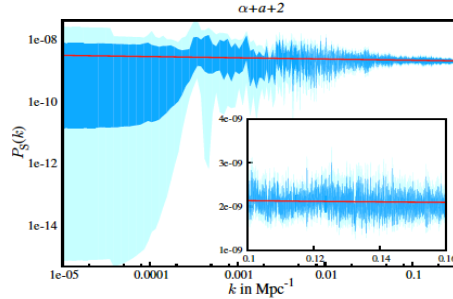
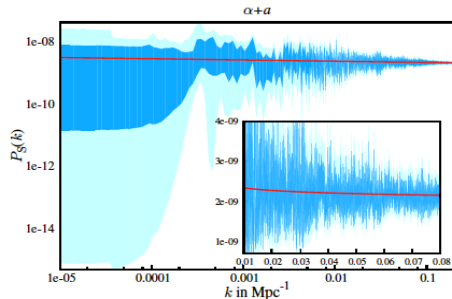
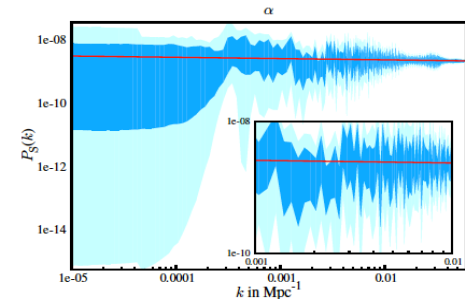
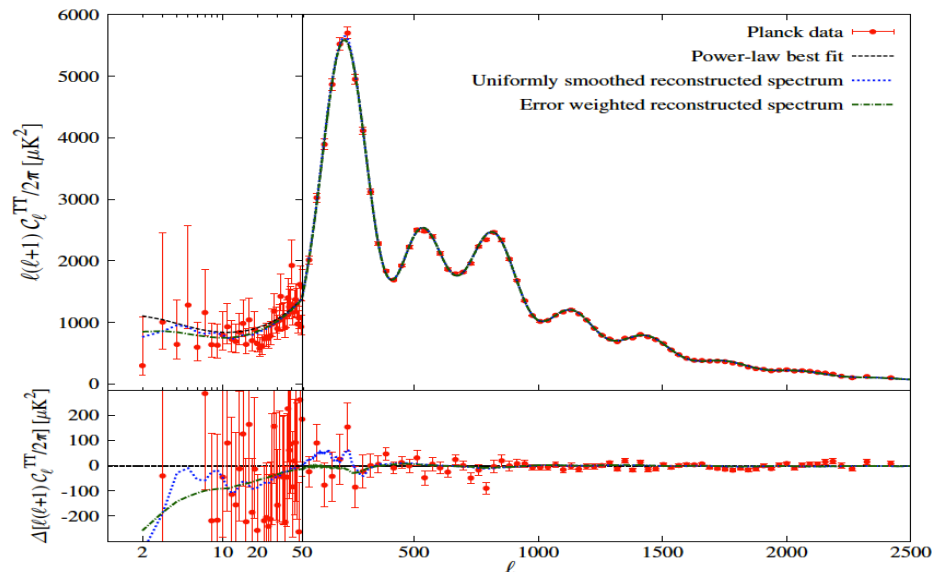
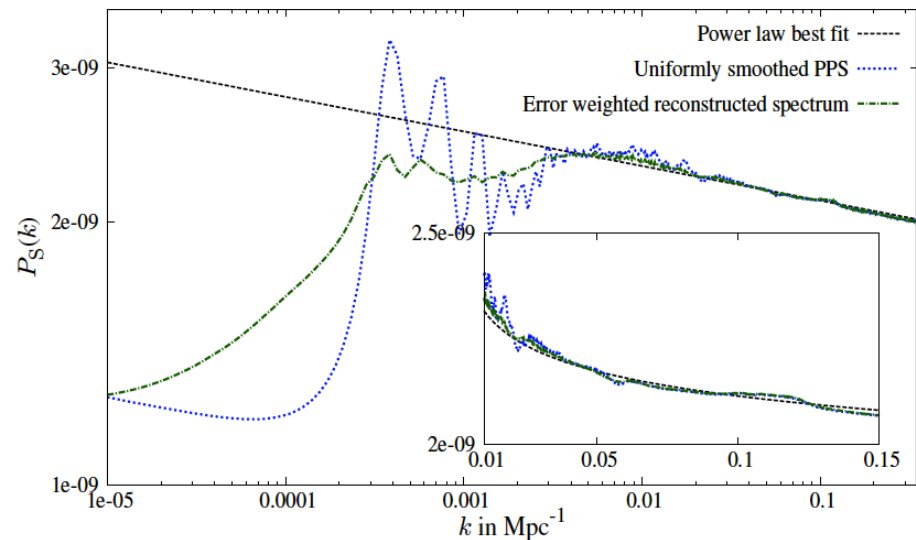
**Blue Contours:
Free Form PPS**

Hazra, Shafieloo & Souradeep,
PRD 2013

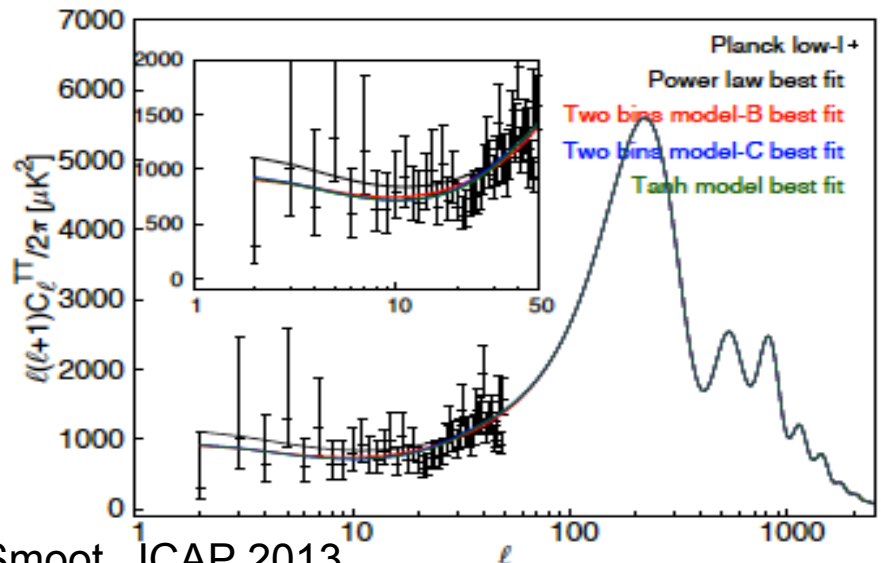
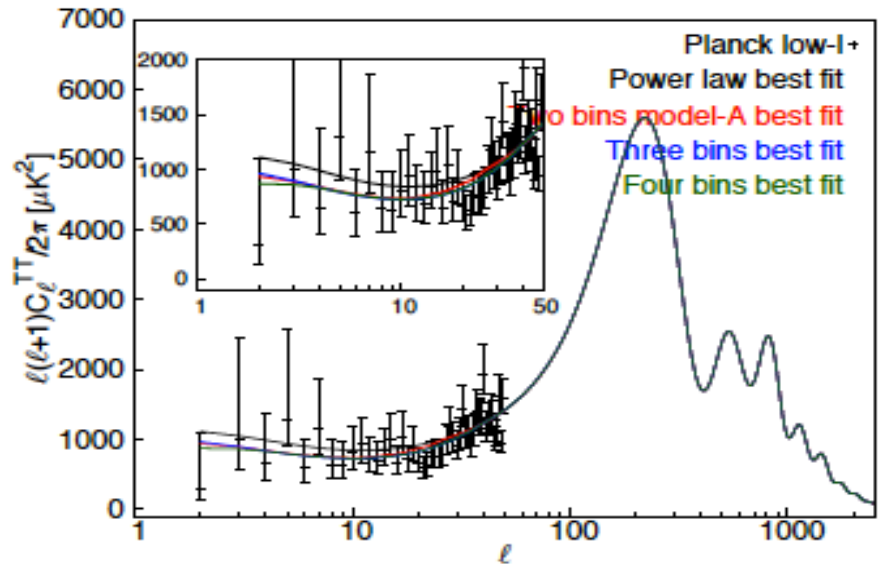
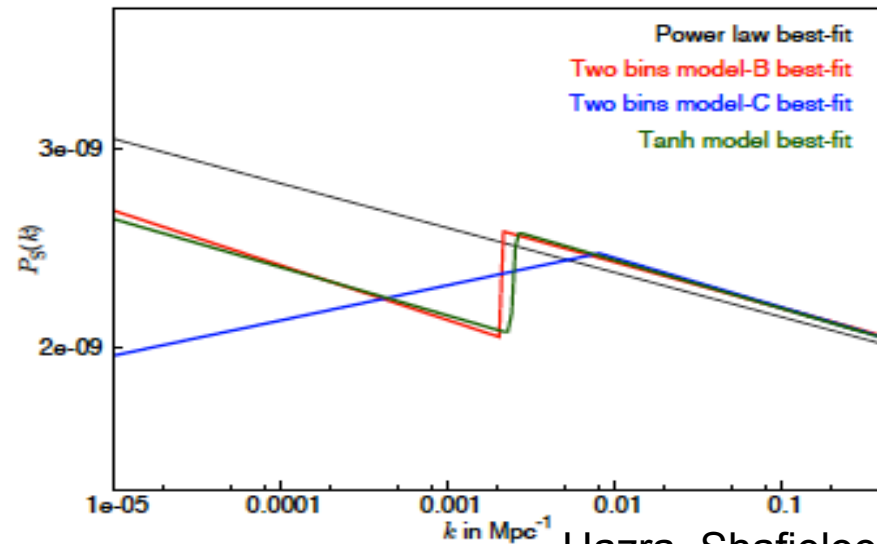
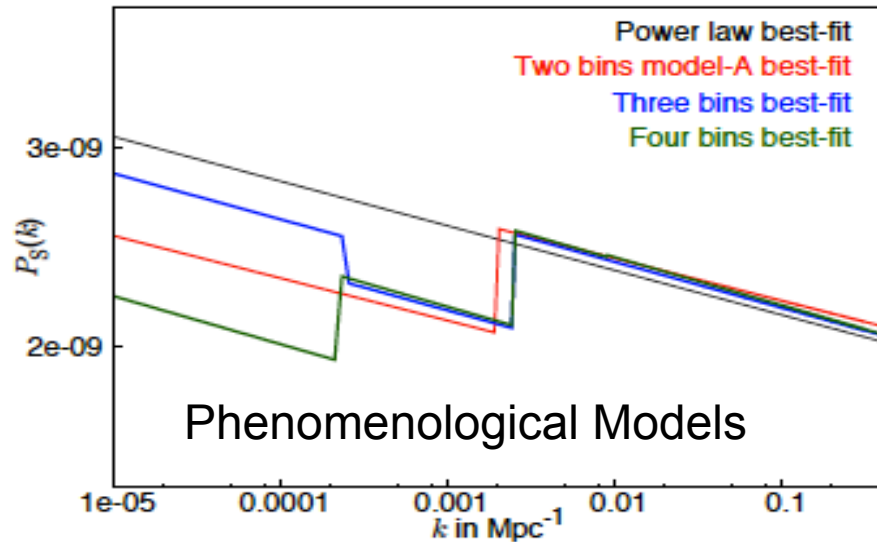
Our symbol	Spectra	Multipoles(ℓ)	Scales
α	low- ℓ	2-49	Largest scales
a	100 GHz \times 100 GHz	50-1200	Intermediate scales
b	143 GHz \times 143 GHz	50-2000	Intermediate scales
1	217 GHz \times 217 GHz	500-2500	Small scales
2	143 GHz \times 217 GHz	500-2500	Small scales

Primordial Power Spectrum from Planck

Hazra, Shafieloo & Souradeep, JCAP 2014

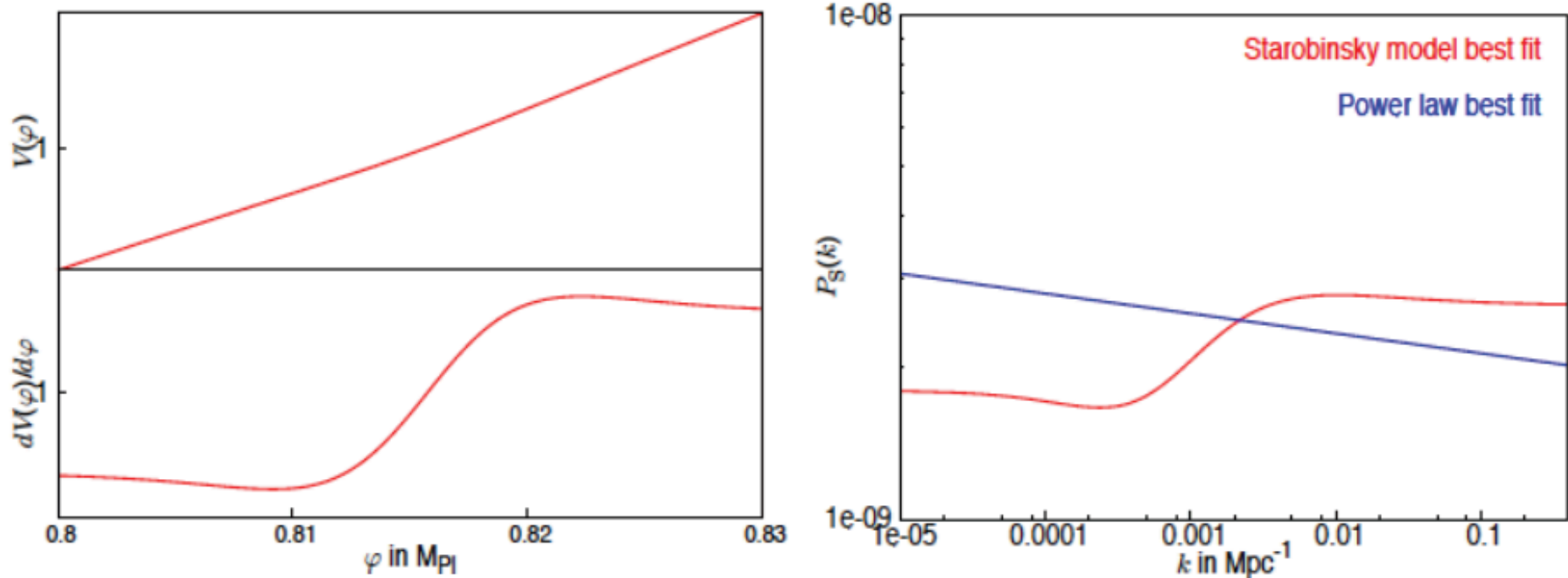


Beyond Power-Law: there are some other models consistent to the data.

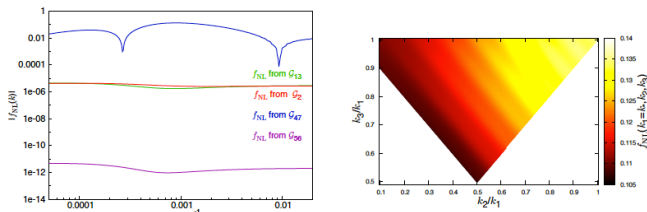


Beyond Power-Law: there are some other models consistent to the data.

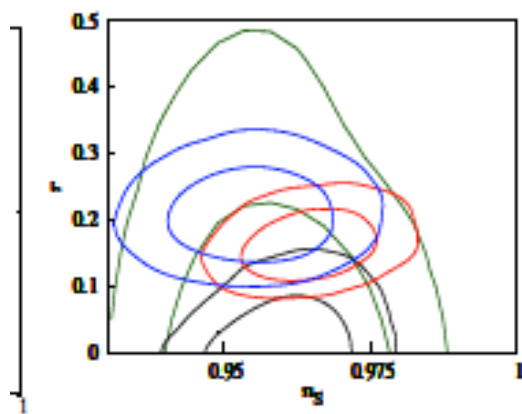
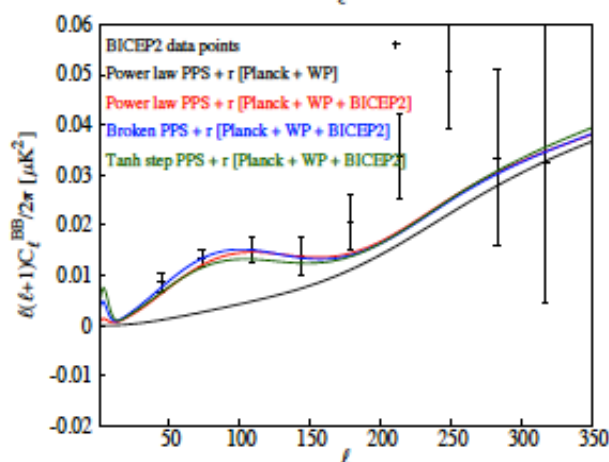
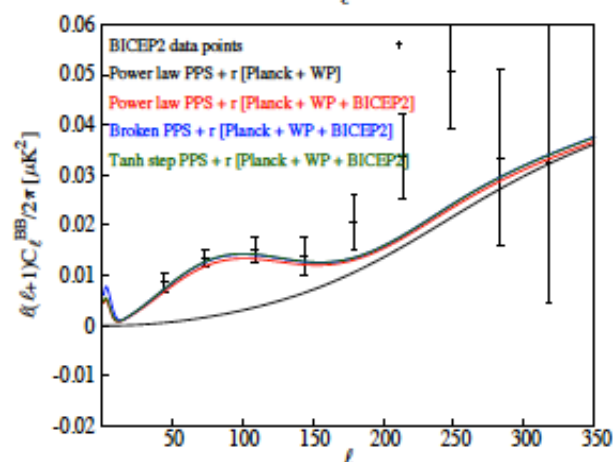
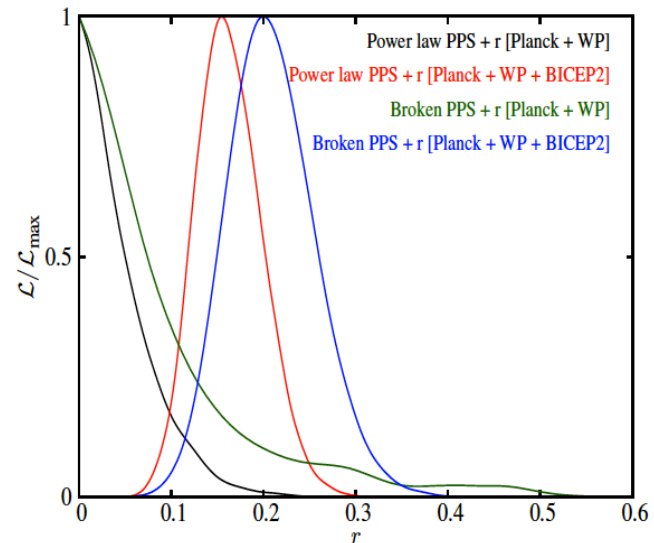
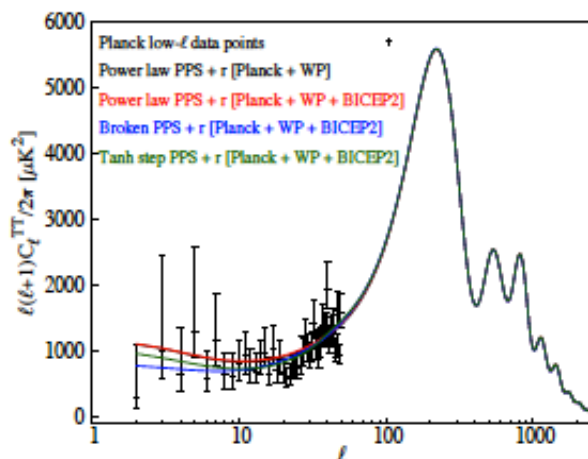
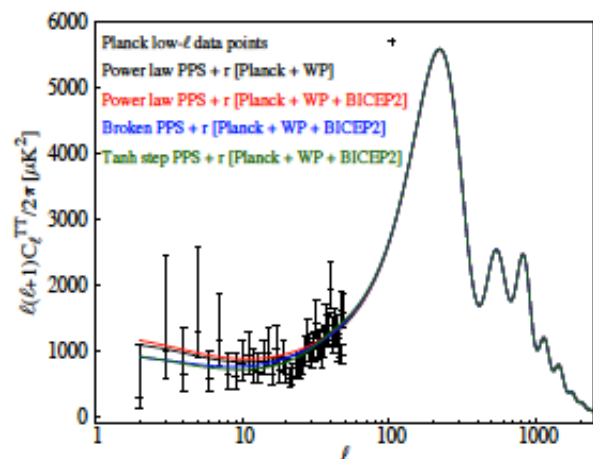
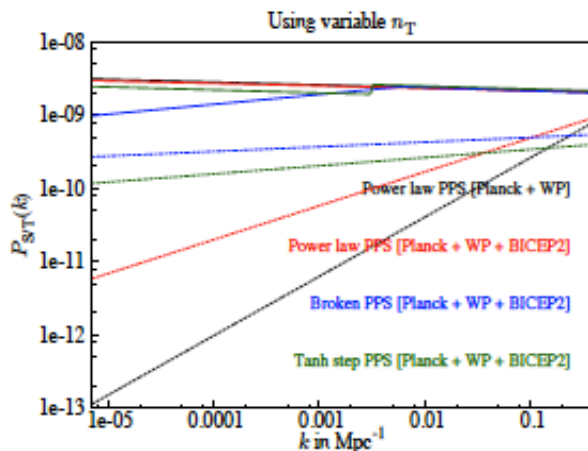
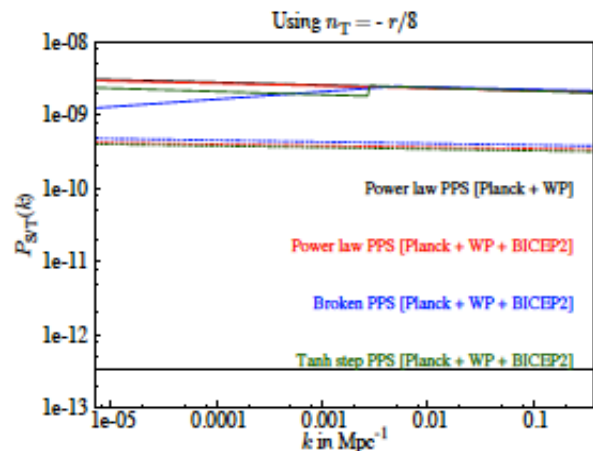
Starobinsky linear field potential, with broken power law.

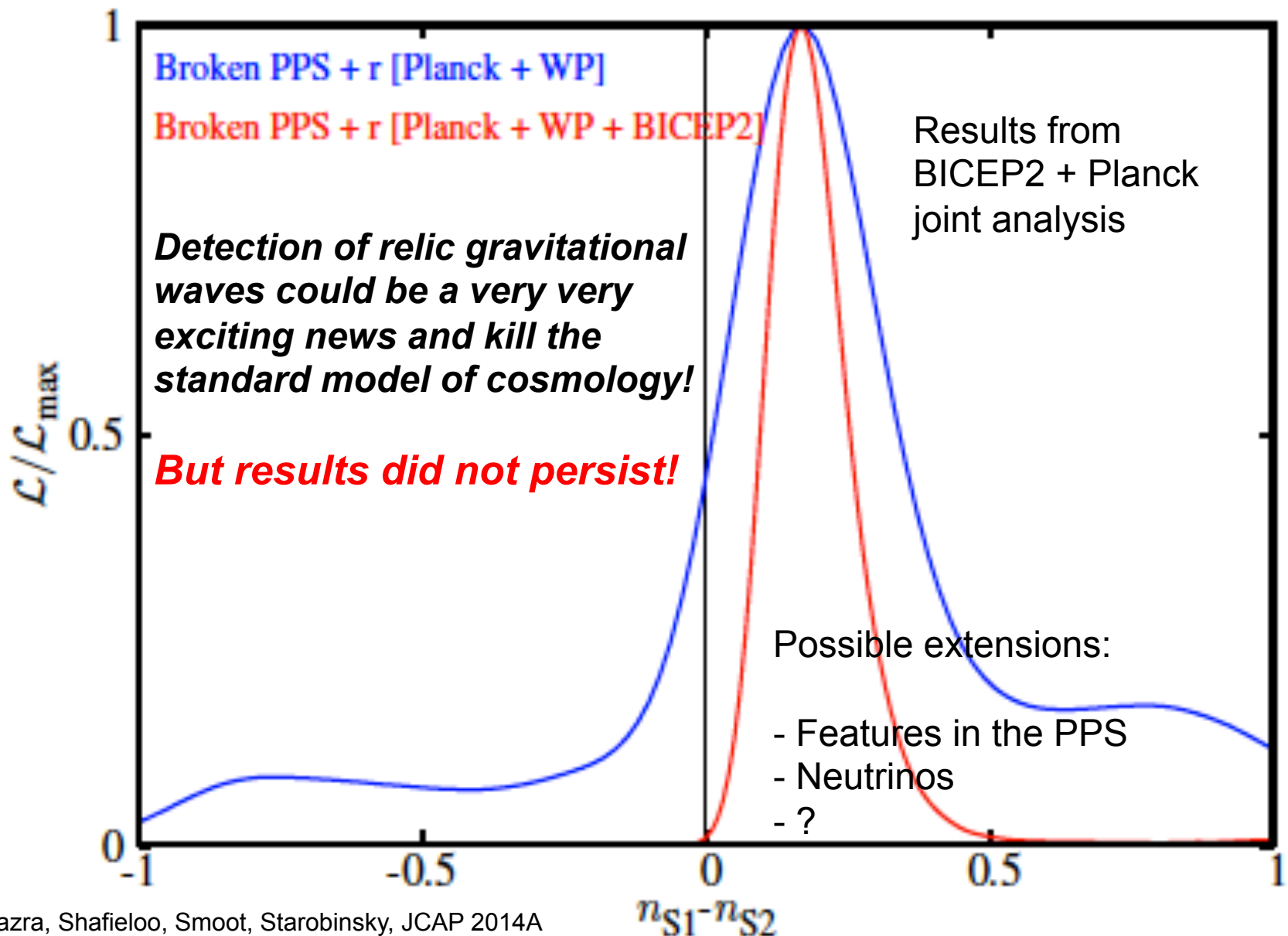


Hazra, Shafieloo, Smoot 1310.3038 (JCAP 2013)



Results from BICEP2 + Planck joint analysis





Hazra, Shafieloo, Smoot, Starobinsky, JCAP 2014A

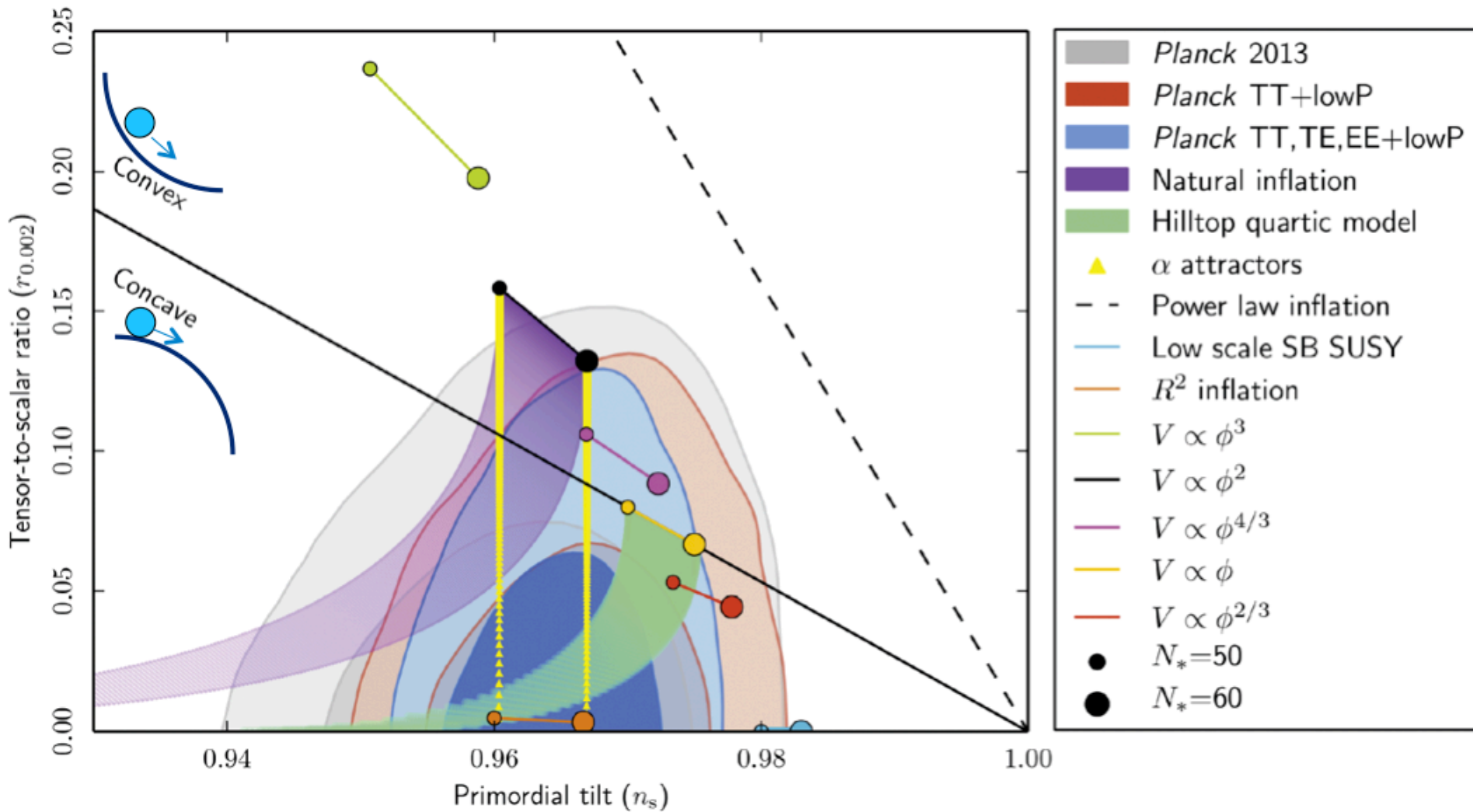
Hazra, Shafieloo, Smoot, Starobinsky, JCAP 2014B

Hazra, Shafieloo, Smoot, Starobinsky, Phys. Rev. Lett 2014

Planck 2015: No detectable primordial G-waves



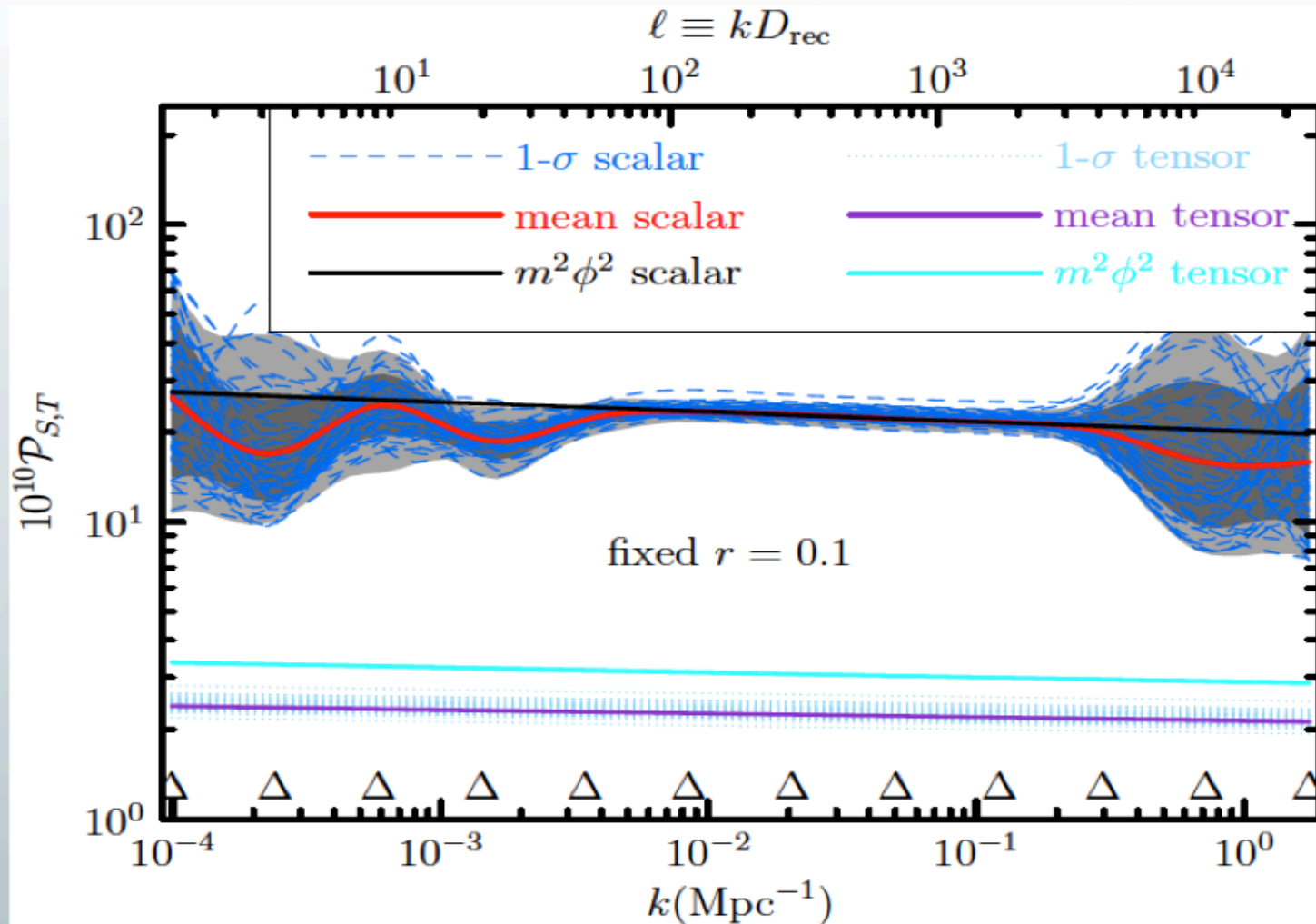
Planck 2015: n_s vs r



Planck 2015: No feature



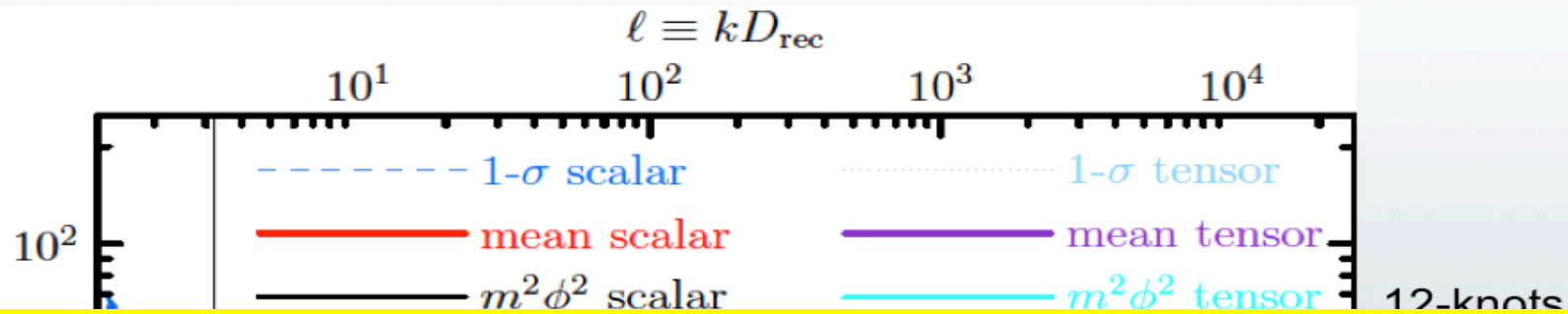
Power spectra reconstruction



Planck 2015: No feature

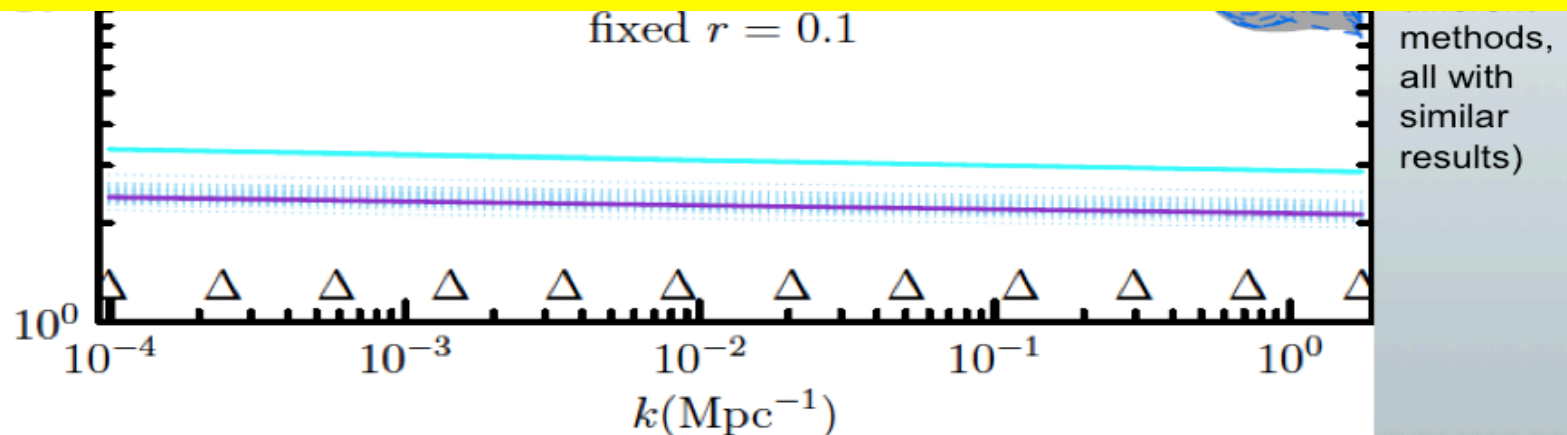


Power spectra reconstruction



Planck likelihood codes just recently released. Analysis are going on.

+BAO+JLA
+Hlow



(Present)_t

Standard Model of Cosmology

Universe is Flat

Universe is Isotropic

Universe is Homogeneous (large scales)

Dark Energy is Lambda ($w=-1$)

Power-Law primordial spectrum ($n_s=\text{const}$)

Dark Matter is cold

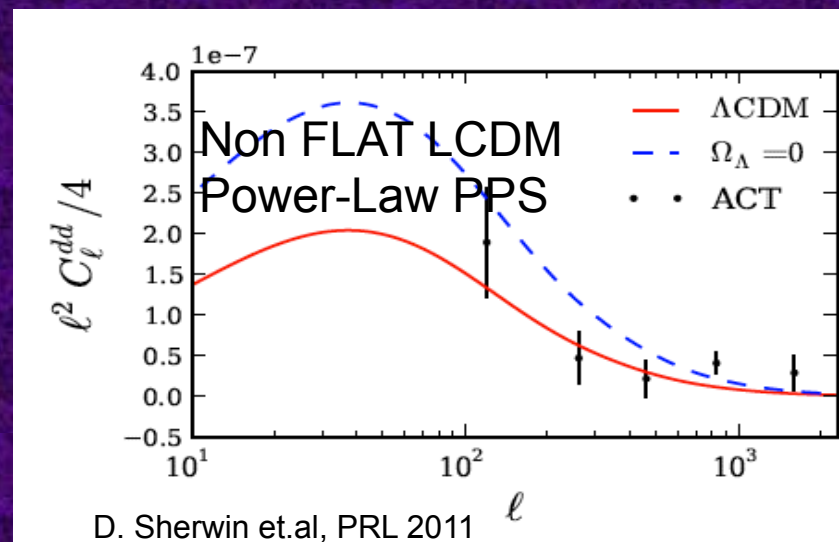
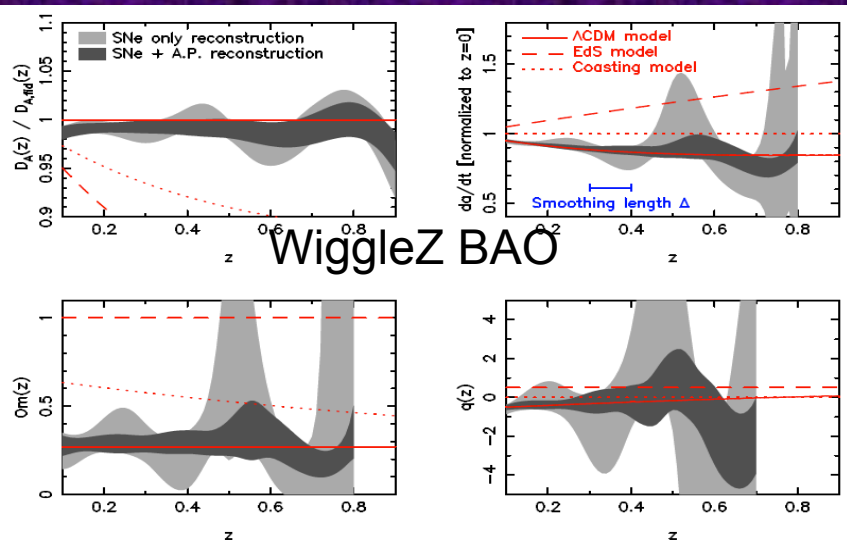
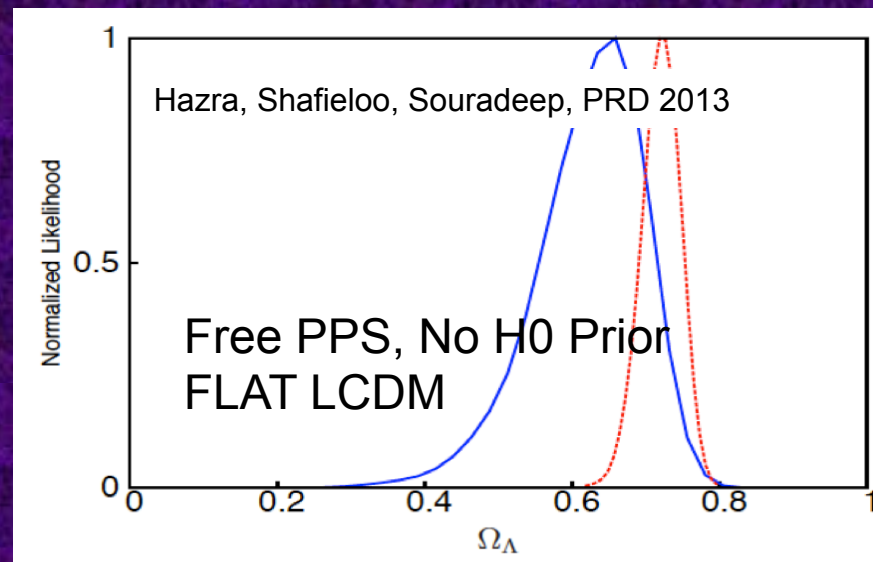
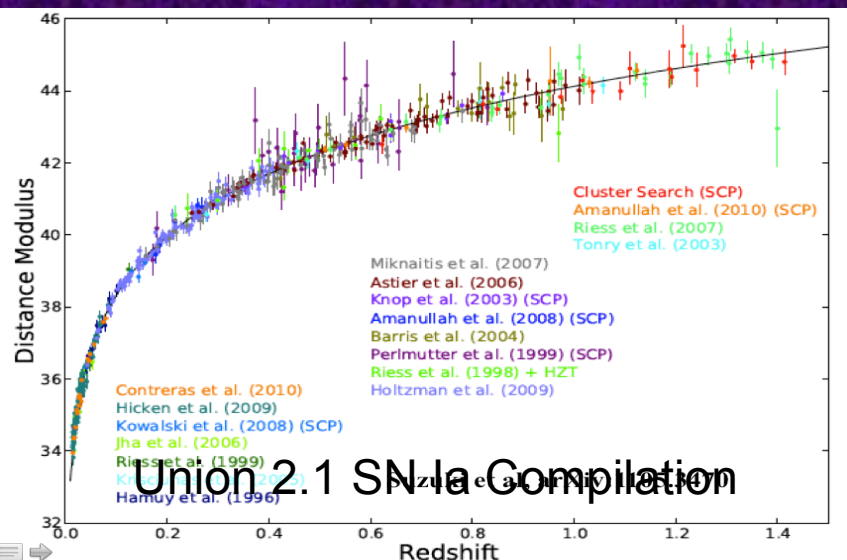
All within framework of FLRW

Era of Accelerating Universe

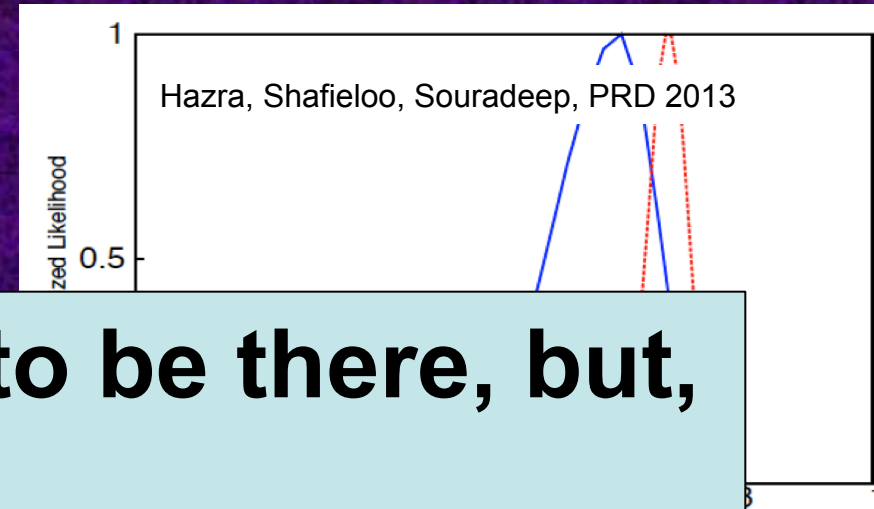
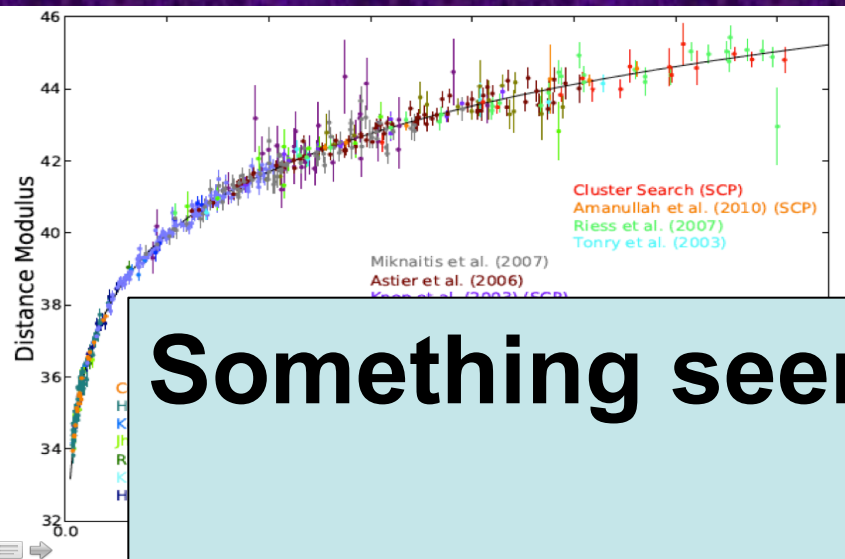
- Mid 90's: Indirect evidences were seen in the distribution of the galaxies where Λ CDM could not explain the excess of power at large scales.
- 1998: Direct evidence came by Supernovae Type Ia Observations. *Going to higher redshifts, supernovae are fainter than expected. One can explain this only (?!=Nobel Prize) by considering an accelerating universe.*

Accelerating Universe, Now-2015

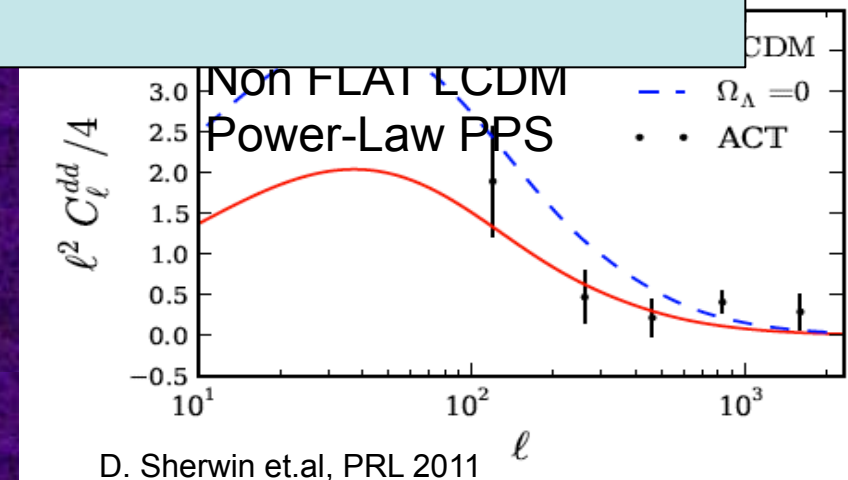
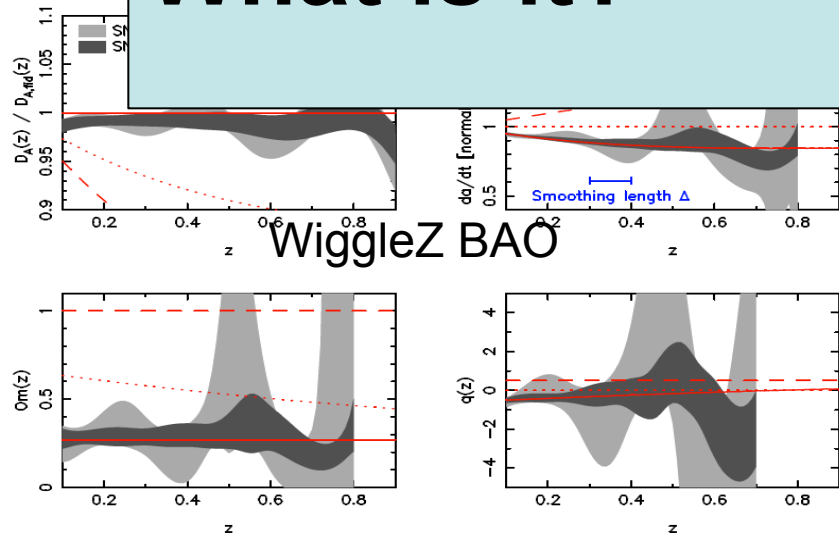
Or better to say, ruling out zero-Lambda Universe



Accelerating Universe, Now



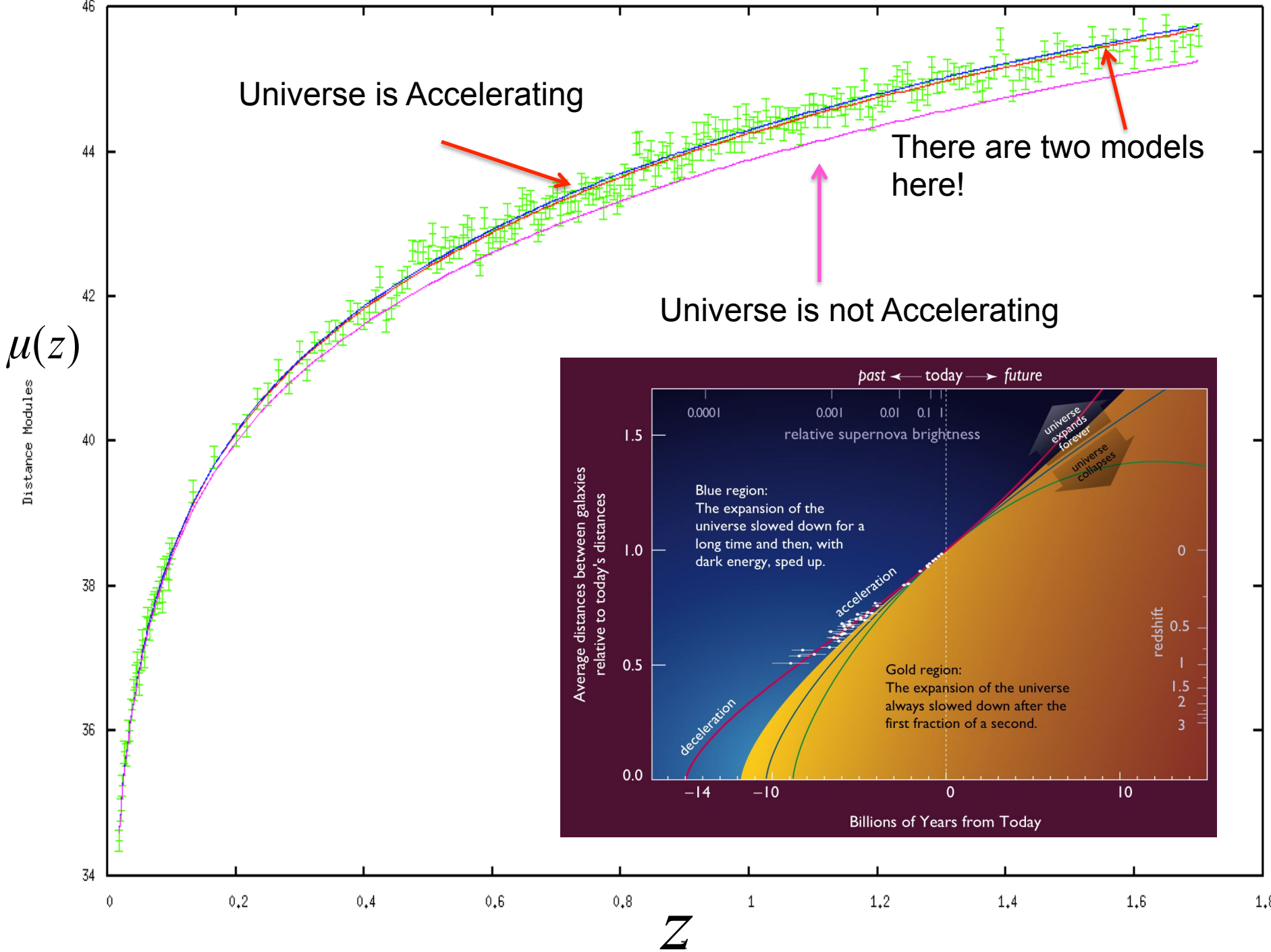
**Something seems to be there, but,
What is it?**



Dark Energy Models

- Cosmological Constant
- Quintessence and k-essence (scalar fields)
- Exotic matter (Chaplygin gas, phantom, etc.)
- Braneworlds (higher-dimensional theories)
- Modified Gravity
-

But which one is really responsible for the acceleration of the expanding universe?!



Reconstructing Dark Energy

To find cosmological quantities and parameters there are two general approaches:

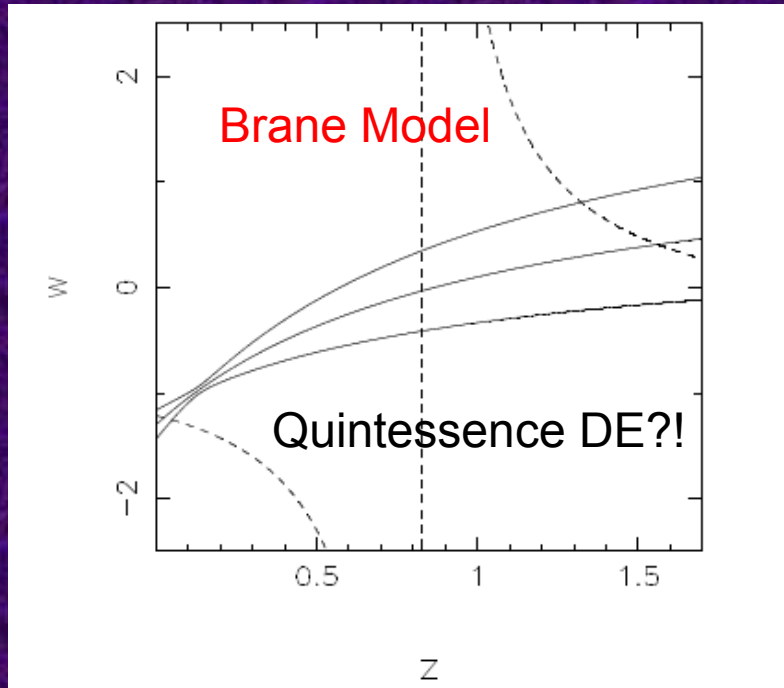
1. Parametric methods

Easy to confront with cosmological observations to put constraints on the parameters, but the results are highly biased by the assumed models and parametric forms.

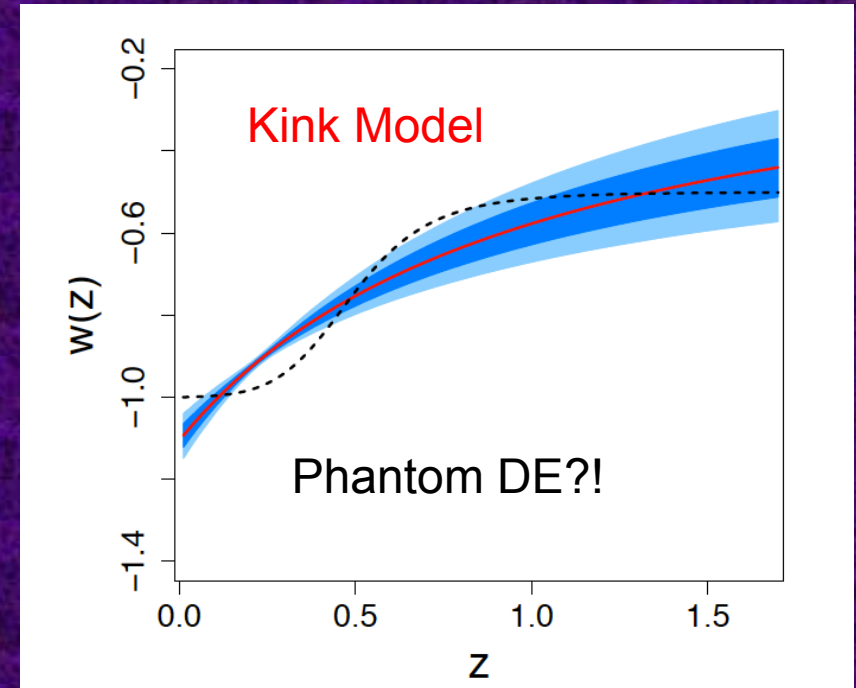
2. Non Parametric methods

Difficult to apply *properly* on the raw data, but the results will be less biased and more reliable and independent of theoretical models or parametric forms.

Problems of Dark Energy Parameterizations (model fitting)



Shafieloo, Alam, Sahni &
Starobinsky, MNRAS 2006



Holsclaw et al, PRD 2011

$$w(z) = w_0 - w_a \frac{z}{1+z}.$$

Chevallier-Polarski-Linder ansatz (CPL).

Non Parametric methods of Reconstruction

Usually involves binning and smoothing

$$F = \frac{L}{4\pi d_L^2}$$

$$d_L(z) = (1+z) \int_0^z \frac{dz'}{H(z')}$$

$$H(z) = \left[\frac{d}{dz} \left(\frac{d_L(z)}{1+z} \right) \right]^{-1}$$

$$\frac{H^2(z)}{H_0^2} = \left[\Omega_{0M} (1+z)^3 + (1 - \Omega_{0M}) \exp \left[\int 3 \left(1 + w(z) \right) \frac{dz}{1+z} \right] \right]$$

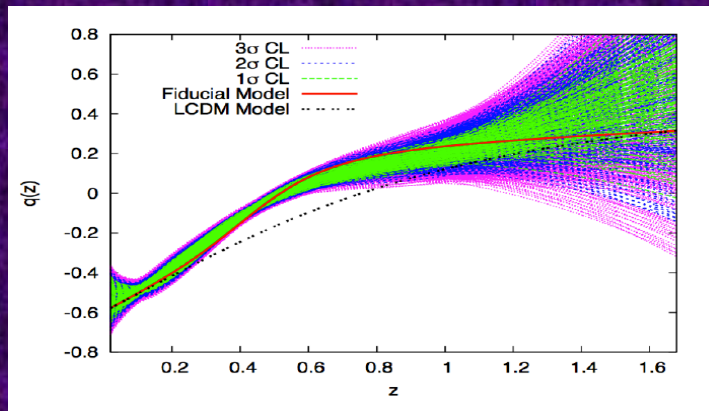
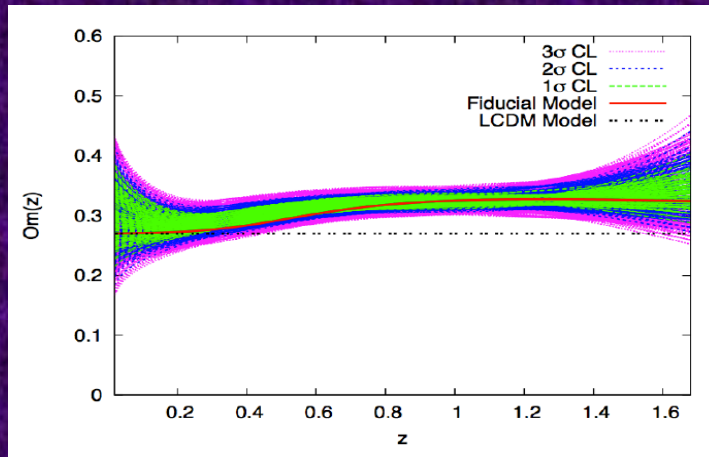
$$\omega_{DE} = \frac{\left(\frac{2(1+z)}{3} \frac{H'}{H} \right) - 1}{1 - \left(\frac{H_0}{H} \right)^2 \Omega_{0M} (1+z)^3}$$

$$H(z) = \left[\frac{d}{dz} \left(\frac{d_L(z)}{1+z} \right) \right]^{-1}$$

$$q(z) = (1+z) \frac{H'(z)}{H(z)} - 1$$

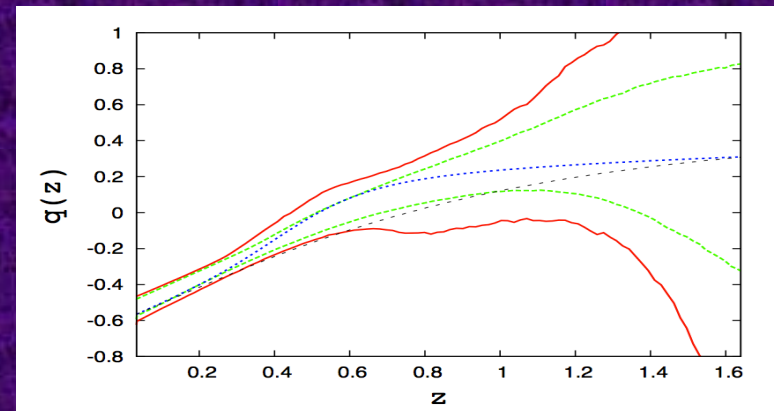
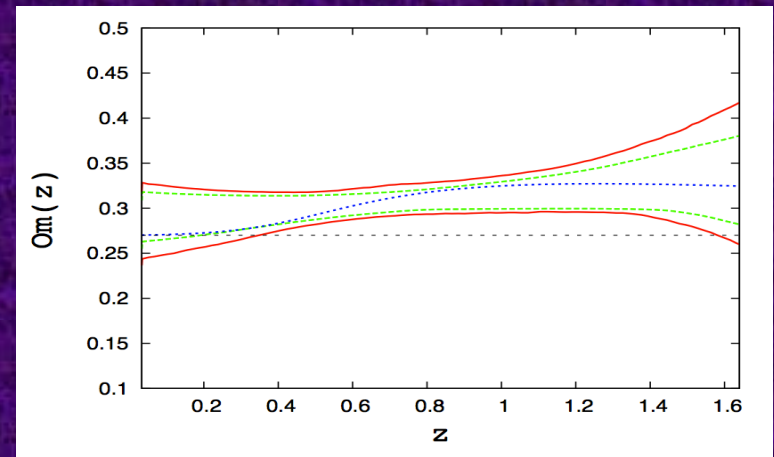
Model independent reconstruction of the expansion history

Crossing Statistic + Smoothing



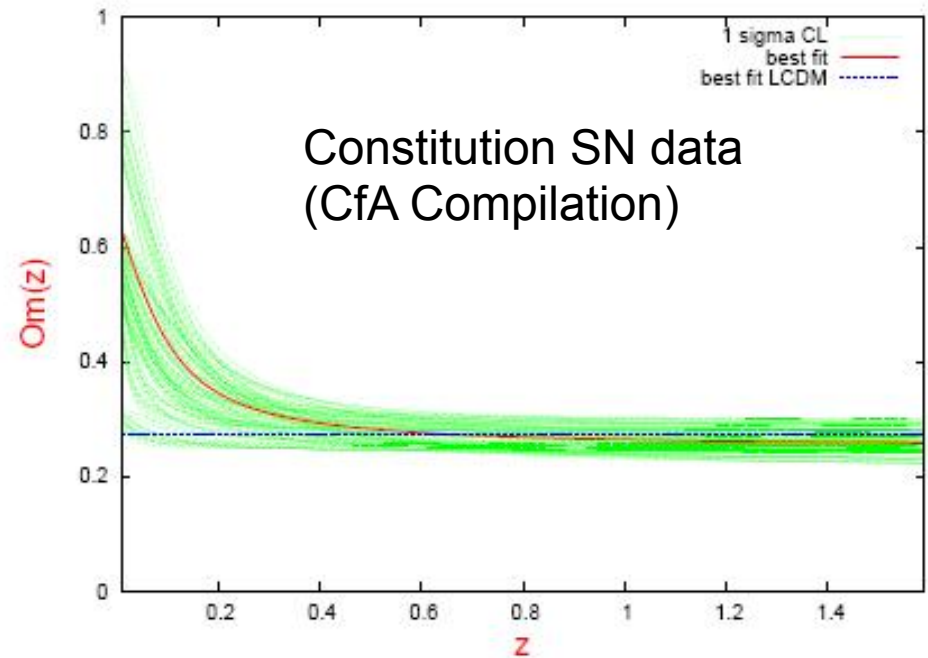
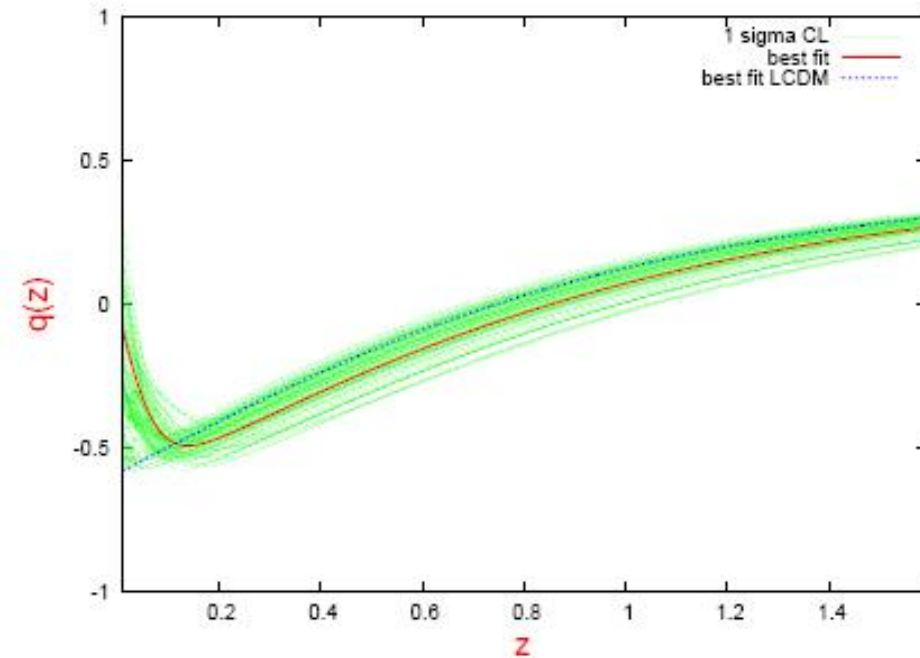
Shafieloo, JCAP (b) 2012

Gaussian Processes



Shafieloo, Kim & Linder, PRD 2012

IS COSMIC ACCELERATION SLOWING DOWN?



$$w(z) = -\frac{1 + \tanh \left[(z - z_t) \Delta \right]}{2}$$

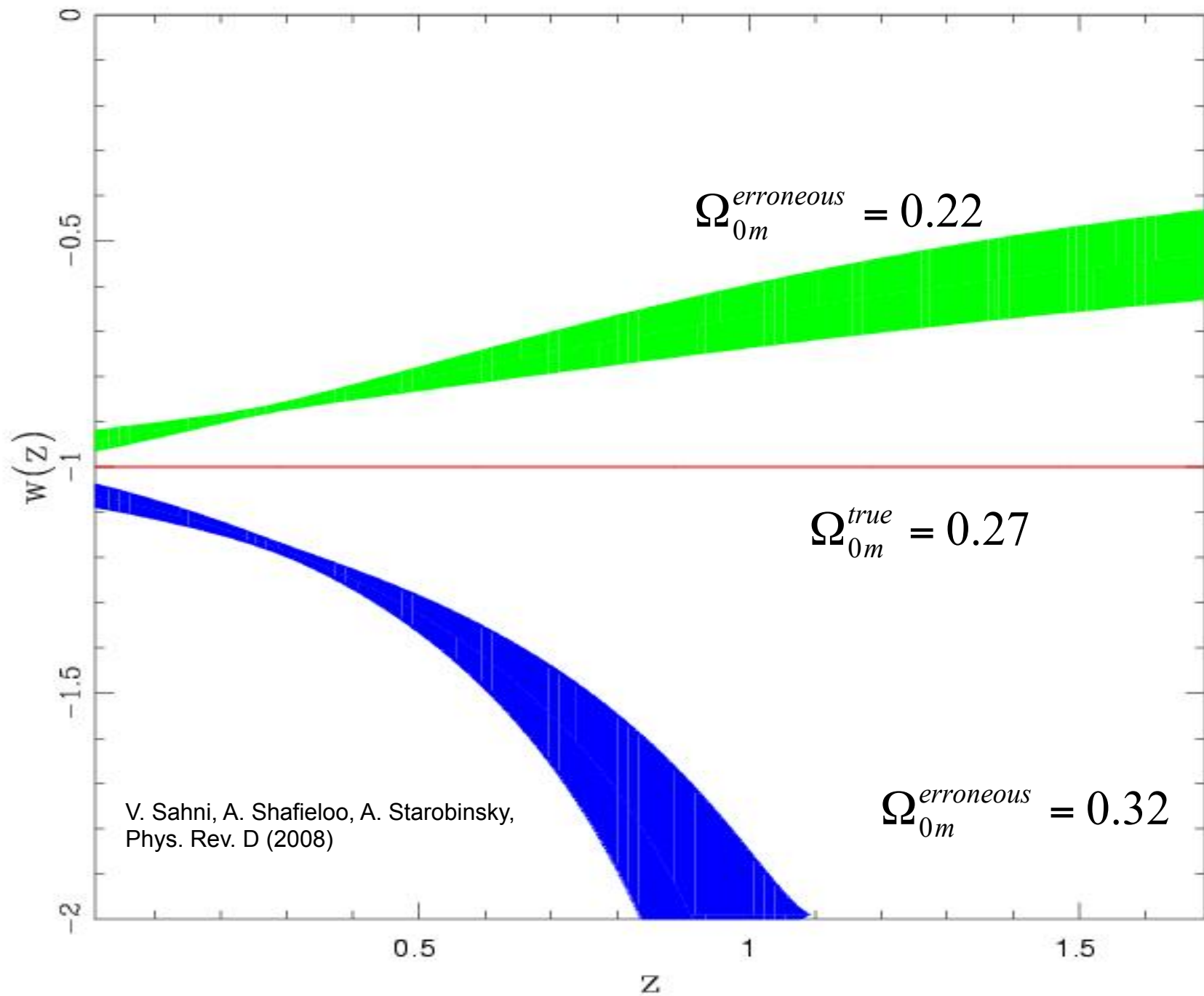
$$\Delta\chi^2 = -0.6 \text{ with respect to CPL}$$

Dealing with observational uncertainties in matter density (and curvature)

- Small uncertainties in the value of matter density affects the reconstruction exercise quite dramatically.
- Uncertainties in matter density is in particular bound to affect the reconstructed $w(z)$.

$$H(z) = \left[\frac{d}{dz} \left(\frac{d_L(z)}{1+z} \right) \right]^{-1}$$

$$\omega_{DE} = \frac{\left(\frac{2(1+z)}{3} \frac{H'}{H} \right) - 1}{1 - \left(\frac{H_0}{H} \right)^2 \Omega_{0M} (1+z)^3}$$



Full theoretical picture:

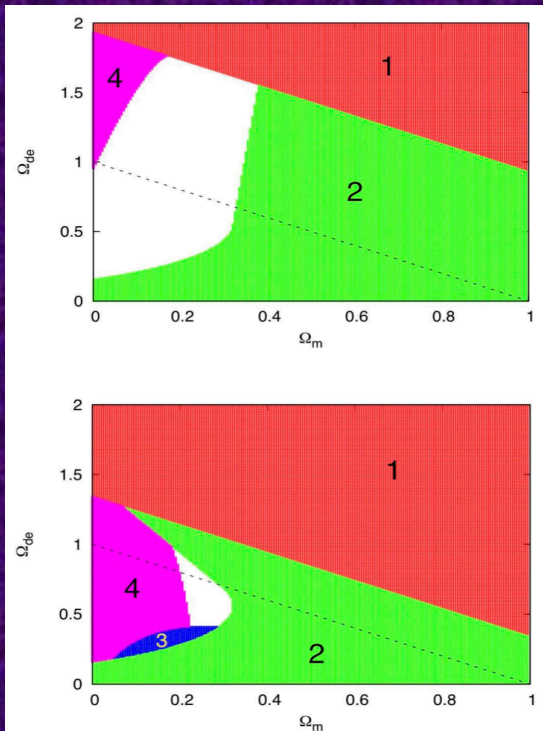
Cosmographic Degeneracy

$$d_l(z) = \frac{1+z}{\sqrt{1 - \Omega_m - \Omega_{de}}} \sinh \left(\sqrt{1 - \Omega_m - \Omega_{de}} \int_0^z \frac{dz'}{h(z')} \right)$$

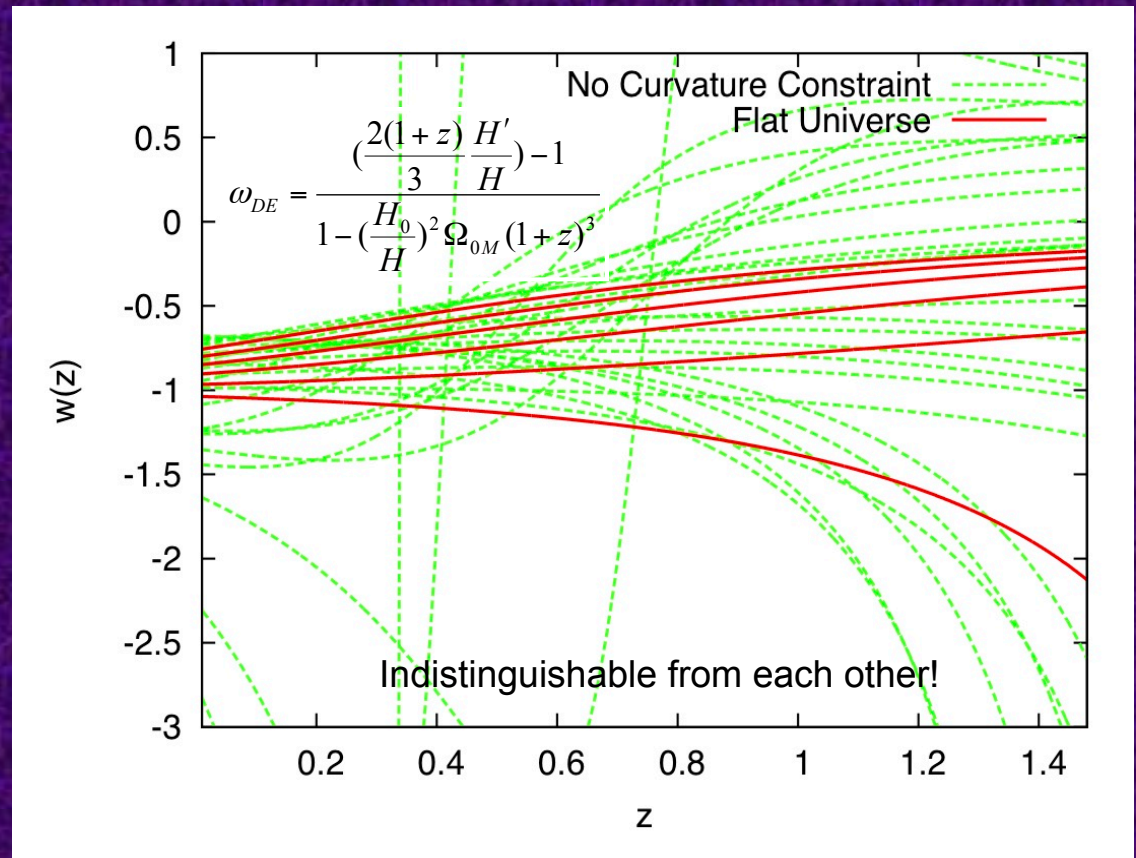
$$\begin{aligned} h(z)^2 &\equiv [H(z)/H_0]^2 \equiv (\dot{a}/a)^2 \\ &= \Omega_m (1+z)^3 + (1 - \Omega_m - \Omega_{de})(1+z)^2 \\ &\quad + \Omega_{de} \exp \left[3 \int_0^z \frac{dz'}{1+z'} [1 + w(z')] \right], \end{aligned}$$

Cosmographic Degeneracy

- **Cosmographic Degeneracies** would make it so hard to pin down the actual model of dark energy even in the near future.



Shafieloo & Linder, PRD 2011



Reconstruction & *Falsification*

Considering (low) quality of the data and cosmographic degeneracies we should consider a new strategy sideways to reconstruction: **Falsification.**

Yes-No to a hypothesis is easier than characterizing a phenomena.

We should look for special characteristics of the standard model and relate them to observables.

But, How?

Falsification of Cosmological Constant

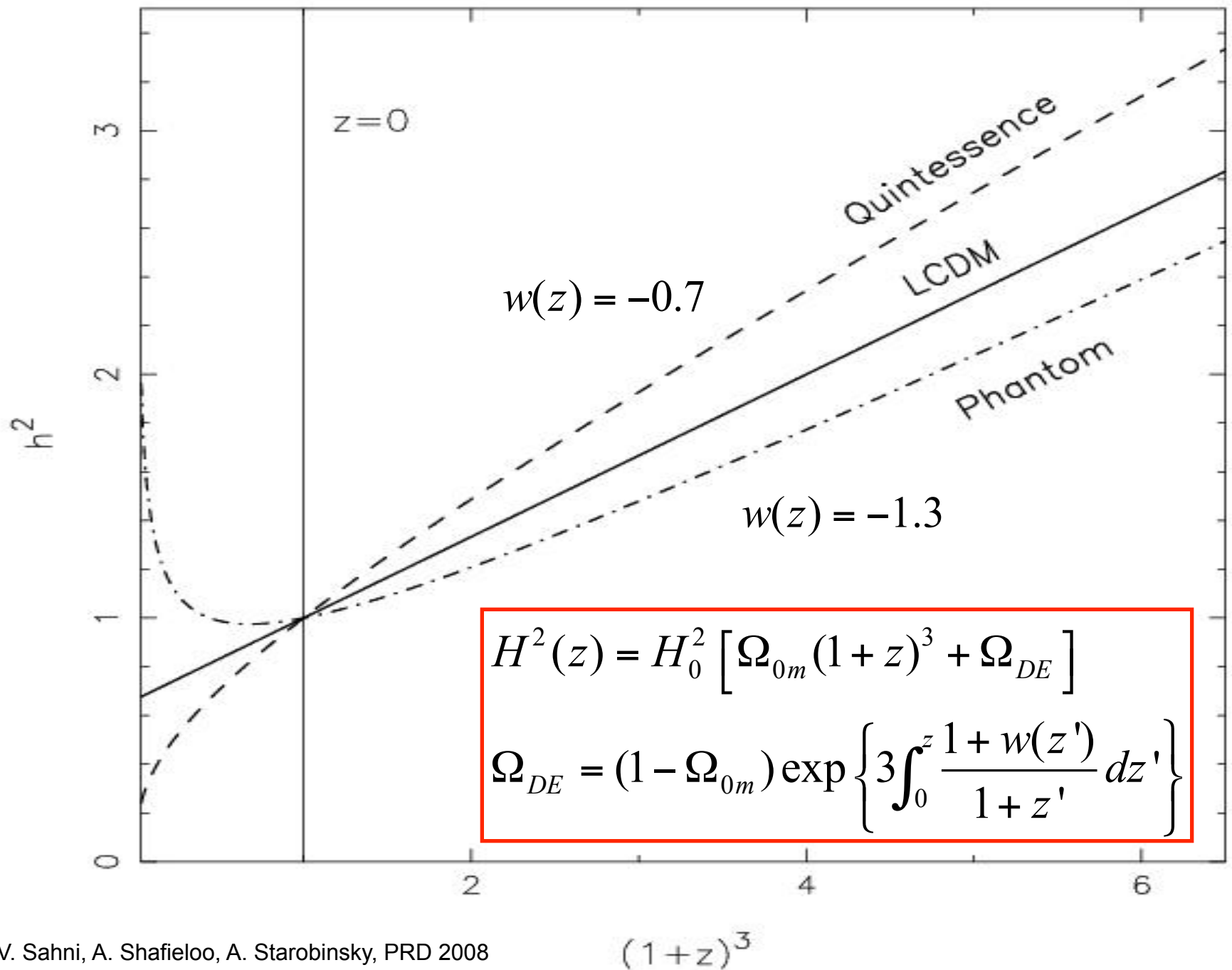
- Instead of looking for $w(z)$ and exact properties of dark energy at the current status of data, we can concentrate on a more reasonable problem:



OR NOT



Yes-No to a hypothesis is easier than characterizing a phenomena



Falsification: Null Test of Lambda

Om diagnostic

$$Om(z) = \frac{h^2(z) - 1}{(1+z)^3 - 1}$$

Om(z) is constant only
for FLAT LCDM model

We Only Need h(z)

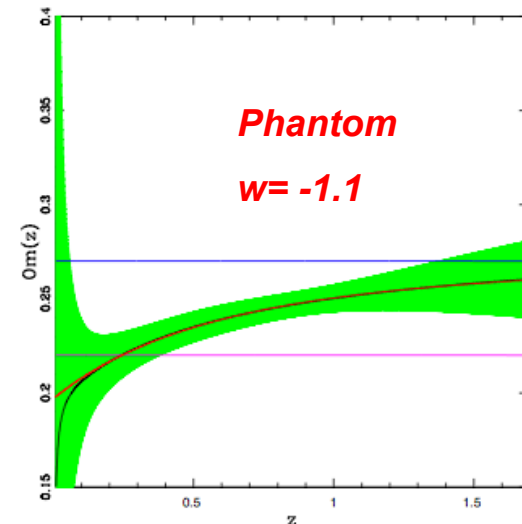
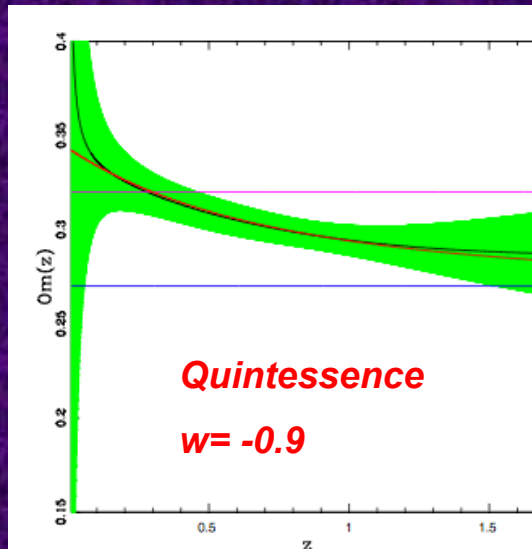
$$h(z) = H(z)/H_0$$

V. Sahni, A. Shafieloo, A. Starobinsky,
PRD 2008

$$w = -1 \rightarrow Om(z) = \Omega_{0m}$$

$$w < -1 \rightarrow Om(z) < \Omega_{0m}$$

$$w > -1 \rightarrow Om(z) > \Omega_{0m}$$



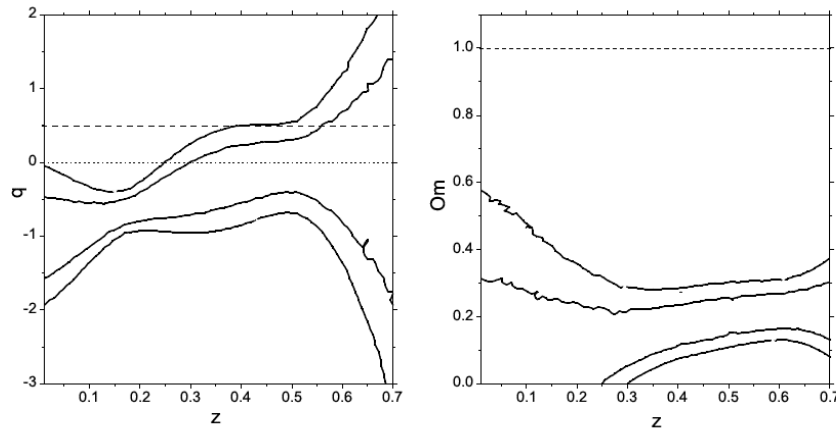


Figure 12. Confidence levels (1σ and 2σ) for the deceleration parameter as a function of redshift and $Om(z)$ reconstructed from the compilation of geometric measurements in tables 2 and 3. H_0 is marginalised over with an HST prior. The dotted line in the left panel demarcates accelerating expansion (below the line) from decelerated expansion (above the line). The dashed line in both panels shows the expectation for an EdS model.

Om diagnostic is very well established

SDSS III / BOSS collaboration
L. Samushia et al, MNRAS 2013

WiggleZ collaboration
C. Blake et al, MNRAS 2011
(Alcock-Paczynski measurement)

10 Blake et al.

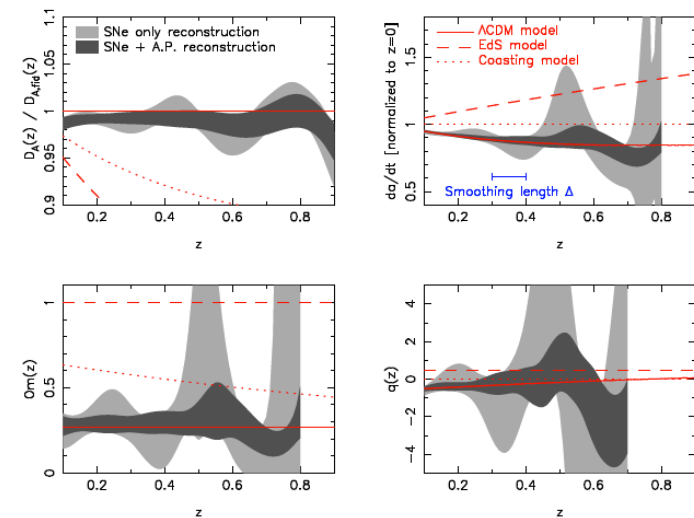


Figure 6. This Figure shows our non-parametric reconstruction of the cosmic expansion history using Alcock-Paczynski and supernovae data. The four panels of this figure display our reconstructions of the distance-redshift relation $D_A(z)$, the expansion rate \dot{a}/H_0 , the $Om(z)$ statistic and the deceleration parameter $q(z)$ using our adaptation of the iterative method of Shafieloo et al. (2006) and Shafieloo & Clarkson (2010). The distance-redshift relation in the upper left-hand panel is divided by a fiducial model for clarity, where the model corresponds to a flat Λ CDM cosmology with $\Omega_m = 0.27$. This fiducial model is shown as the solid line in all panels; Einstein de-Sitter and coasting models are also shown as in Figure 5. The shaded regions illustrate the 68% confidence range of the reconstructions of each quantity obtained using bootstrap resamples of the data. The dark-grey regions illustrate a combination of the Alcock-Paczynski and supernovae data and the light-grey regions are based on the supernovae data alone. The redshift smoothing scale $\Delta = 0.1$ is also illustrated. The reconstructions in each case are terminated when the SNe-only results become very noisy; this maximum redshift reduces with each subsequent derivative of the distance-redshift relation [i.e. is lowest for $q(z)$].

Om3

A null diagnostic customized for reconstructing the properties of dark energy directly from BAO data

$$Om3(z_1, z_2, z_3) = \frac{Om(z_2, z_1)}{Om(z_3, z_1)} = \frac{\frac{h^2(z_2) - h^2(z_1)}{(1+z_2)^3 - (1+z_1)^3}}{\frac{h^2(z_3) - h^2(z_1)}{(1+z_3)^3 - (1+z_1)^3}} = \frac{\frac{\frac{h^2(z_2)}{h^2(z_1)} - 1}{(1+z_2)^3 - (1+z_1)^3}}{\frac{\frac{h^2(z_3)}{h^2(z_1)} - 1}{(1+z_3)^3 - (1+z_1)^3}} = \frac{\frac{\frac{\frac{H^2(z_2)}{H_0^2} - 1}{\frac{H^2(z_2)}{H^2(z_1)}}}{(1+z_2)^3 - (1+z_1)^3}}{\frac{\frac{\frac{H^2(z_3)}{H_0^2} - 1}{\frac{H^2(z_3)}{H^2(z_1)}}}{(1+z_3)^3 - (1+z_1)^3}} = \frac{\frac{\frac{H^2(z_2)}{H^2(z_1)} - 1}{(1+z_2)^3 - (1+z_1)^3}}{\frac{\frac{H^2(z_3)}{H^2(z_1)} - 1}{(1+z_3)^3 - (1+z_1)^3}}$$

$$d(z) = \frac{r_s(z_{\text{CMB}})}{D_V(z)}$$

Observables

Shafieloo, Sahni, Starobinsky, PRD 2013

$$H(z_i; z_j) := \frac{H(z_i)}{H(z_j)} = \frac{z_i}{z_j} \left[\frac{D(z_i)}{D(z_j)} \right]^2 \left[\frac{D_V(z_j)}{D_V(z_i)} \right]^3 = \frac{z_i}{z_j} \left[\frac{D(z_i)}{D(z_j)} \right]^2 \left[\frac{d(z_i)}{d(z_j)} \right]^3,$$

Characteristics of Om3

Om is constant only for Flat LCDM model

Om3 is equal to one for Flat LCDM model

$$Om3(z_1; z_2; z_3) = \frac{H(z_2; z_1)^2 - 1}{x_2^3 - x_1^3} \bigg/ \frac{H(z_3; z_1)^2 - 1}{x_3^3 - x_1^3}, \quad \text{where } x = 1 + z,$$

$$H(z_i; z_j) = \left(\frac{z_j}{z_i} \right)^2 \left[\frac{D(z_i)}{D(z_j)} \right]^2 \left[\frac{A(z_j)}{A(z_i)} \right]^3 = \frac{z_i}{z_j} \left[\frac{D(z_i)}{D(z_j)} \right]^2 \left[\frac{d(z_i)}{d(z_j)} \right]^3,$$

Om3 is independent of H0 and the distance to the last scattering surface and can be derived directly using BAO observables.

Om h^2

A very recent result.

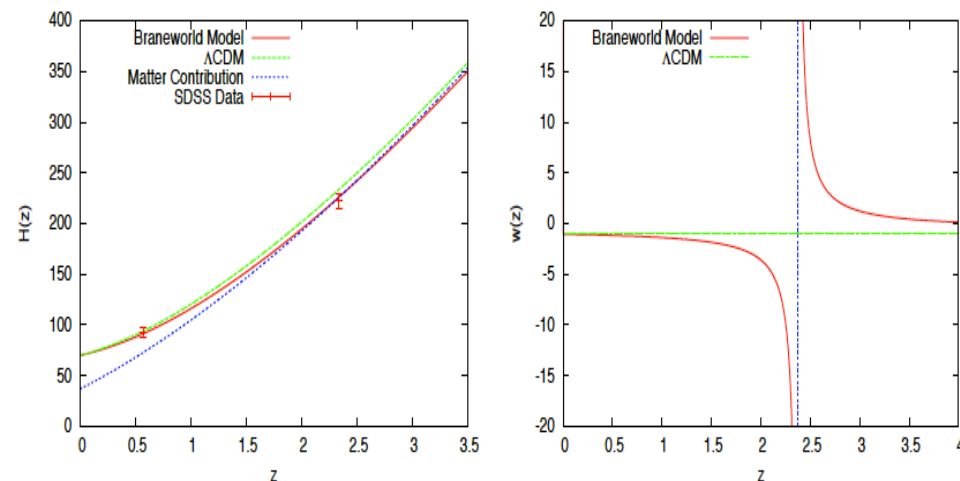
Important discovery if no systematic in the SDSS Quasar BAO data

Model Independent Evidence for Dark Energy Evolution from Baryon Acoustic Oscillation

$$Om h^2(z_1, z_2) = \frac{H^2(z_2) - H^2(z_1)}{(1+z_2)^3 - (1+z_1)^3} = \Omega_{0m} H_0^2$$

Only for LCDM

Sahni, Shafieloo, Starobinsky, ApJ Lett 2014



$$Om h^2 = 0.1426 \pm 0.0025$$

LCDM
+Planck+WP

$$Om h^2(z_1; z_2) = 0.124 \pm 0.045$$

$$Om h^2(z_1; z_3) = 0.122 \pm 0.010$$

$$Om h^2(z_2; z_3) = 0.122 \pm 0.012$$

BAO+H0

$$H(z = 0.00) = 70.6 \pm 3.3 \text{ km/sec/Mpc}$$

$$H(z = 0.57) = 92.4 \pm 4.5 \text{ km/sec/Mpc}$$

$$H(z = 2.34) = 222.0 \pm 7.0 \text{ km/sec/Mpc}$$

(Present)_t

Standard Model of Cosmology

Universe is Flat

Universe is Isotropic

Universe is Homogeneous (large scales)

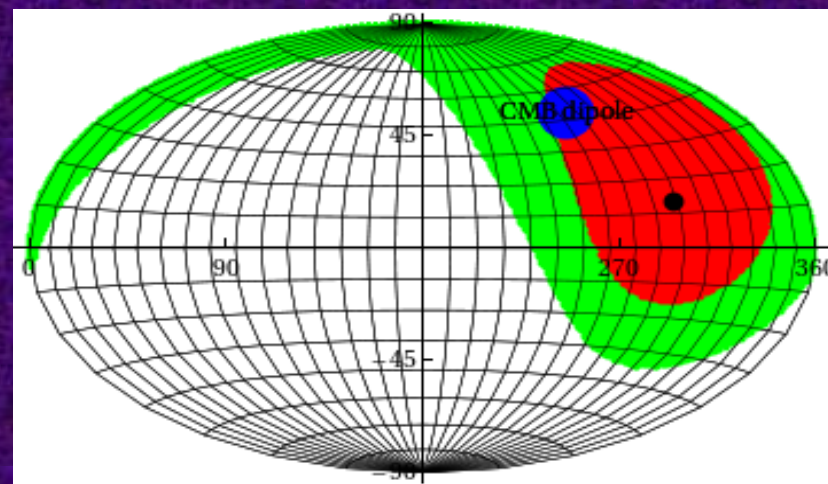
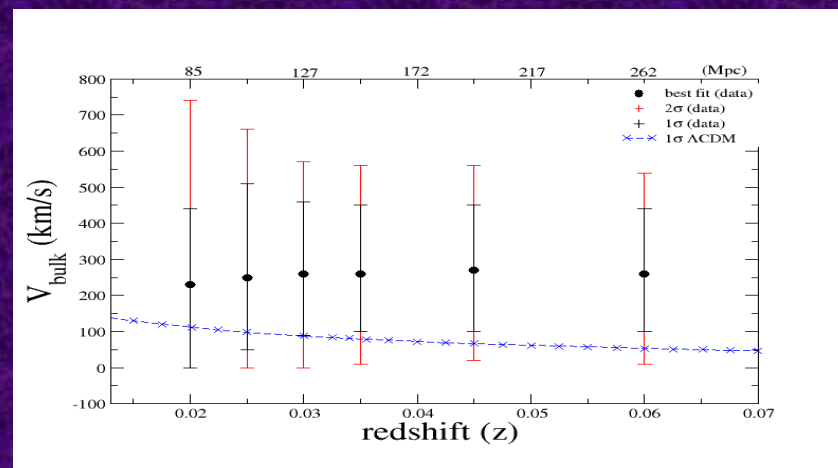
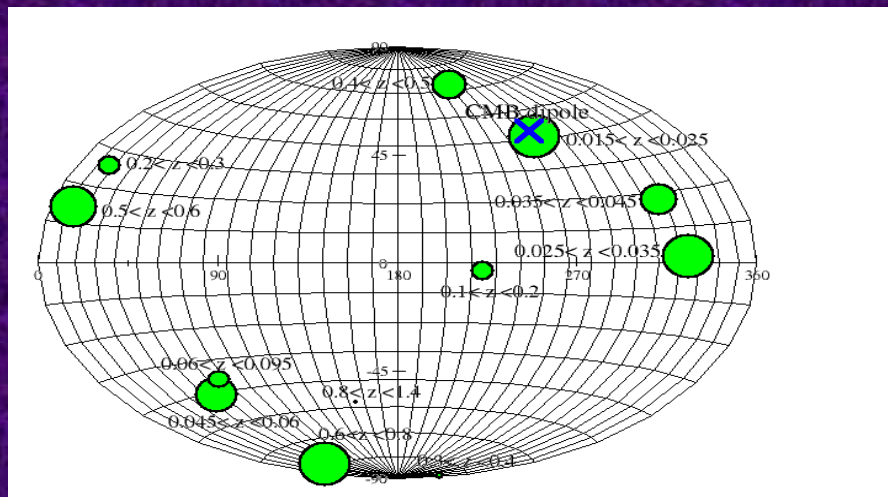
Dark Energy is Lambda ($w=-1$)

Power-Law primordial spectrum ($n_s=\text{const}$)

Dark Matter is cold

All within framework of FLRW

Falsification: Is Universe Isotropic?



Method of Smoothed Residuals

- Residual Analysis,
- Tomographic Analysis,
- 2D Gaussian Smoothing,
- Frequentist Approach
- Insensitive to non-uniform distribution of the data

Measuring cosmic bulk flows with Type Ia Supernovae from the Nearby Supernova Factory

U. Feindt^{1*}, M. Kerschhaggl^{1*}, M. Kowalski¹, G. Aldering², P. Antilogus³, C. Aragon², S. Bailey², C. Baltay⁴, S. Bongard³, C. Buton¹, A. Canto⁵, F. Cellier-Holzem³, M. Childress⁵, N. Chotard⁶, Y. Copin⁶, H. K. Fakhouri^{2,7}, E. Gangler⁶, J. Guy³, A. Kim², P. Nugent^{8,9}, J. Nordin^{2,10}, K. Paech¹, R. Pain³, E. Pecontal¹¹, R. Pereira⁶, S. Perlmutter^{2,7}, D. Rabinowitz², M. Rigault⁴, K. Runge², C. Saunders², R. Scalzo⁵, G. Smadja⁶, C. Tao^{12,13}, R. C. Thomas⁸, B. A. Weaver¹⁴, C. Wu^{3,15}

¹ Physikalisches Institut, Universität Bonn, Nuffallee 12, 53115 Bonn, Germany

² Physics Division, Lawrence Berkeley National Laboratory, 1 Cyclotron Road, Berkeley, CA, 94720

³ Laboratoire de Physique Nucléaire et des Hautes Énergies, Université Pierre et Marie Curie Paris 6, Université Paris Diderot Paris 7, CNRS-IN2P3, 4 place Jussieu, 75252 Paris Cedex 05, France

⁴ Department of Physics, Yale University, New Haven, CT, 06250-8121

⁵ Research School of Astronomy and Astrophysics, Australian National University, Canberra, ACT 2611, Australia.

⁶ Université de Lyon, F-69622, Lyon, France ; Université de Lyon 1, Villeurbanne ; CNRS-IN2P3, Institut de Physique Nucléaire de Lyon.

⁷ Department of Physics, University of California Berkeley, 366 Le Conte Hall MC 7300, Berkeley, CA, 94720-7300

⁸ Computational Cosmology Center, Computational Research Division, Lawrence Berkeley National Laboratory, 1 Cyclotron Road MS 50B-4206, Berkeley, CA, 94720

⁹ Department of Astronomy, B-20 Hearst Field Annex # 3411, University of California, Berkeley, CA 94720-3411, USA

¹⁰ Space Sciences Laboratory, University of California Berkeley, 7 Gauss Way, Berkeley, CA 94720, USA

¹¹ Centre de Recherche Astronomique de Lyon, Université Lyon 1, 9 Avenue Charles André, 69561 Saint Genis Laval Cedex, France

¹² Centre de Physique des Particules de Marseille, 163, avenue de Luminy - Case 902 - 13288 Marseille Cedex 09, France

¹³ Tsinghua Center for Astrophysics, Tsinghua University, Beijing 100084, China

¹⁴ Center for Cosmology and Particle Physics, New York University, 4 Washington Place, New York, NY 10003, USA

¹⁵ National Astronomical Observatories, Chinese Academy of Sciences, Beijing 100012, China

Received 12 May 2013, Accepted 10 Oct, 2013

ABSTRACT

Context. Our Local Group of galaxies appears to be moving relative to the cosmic microwave background with the source of the peculiar motion still uncertain. While in the past this has been studied mostly using galaxies as distance indicators, the weight of type Ia supernovae (SNe Ia) has increased recently with the continuously improving statistics of available low-redshift supernovae.

Aims. We measured the bulk flow in the nearby universe ($0.015 < z < 0.1$) using 117 SNe Ia observed by the Nearby Supernova Factory, as well as the Union2 compilation of SN Ia data already in the literature.

Methods. The bulk flow velocity was determined from SN data binned in redshift shells by including a coherent motion (dipole) in a cosmological fit. Additionally, a method of spatially smoothing the Hubble residuals was used to verify the results of the dipole fit. To constrain the location and mass of a potential mass concentration (e.g., the Shapley supercluster) responsible for the peculiar motion, we fit a Hubble law modified by adding an additional mass concentration.

Results. The analysis shows a bulk flow that is consistent with the direction of the CMB dipole up to $z \sim 0.06$, thereby doubling the volume over which conventional distance measures are sensitive to a bulk flow. We see no significant turnover behind the center of the Shapley supercluster. A simple attractor model in the proximity of the Shapley supercluster is only marginally consistent with our

Method of Smoothed Residuals is well received and was used recently by Supernovae Factory collaboration

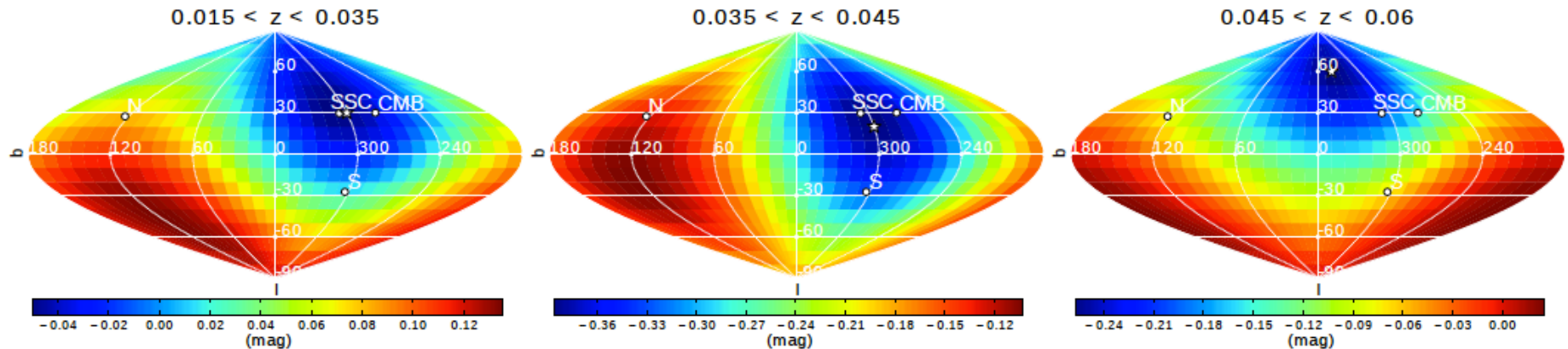
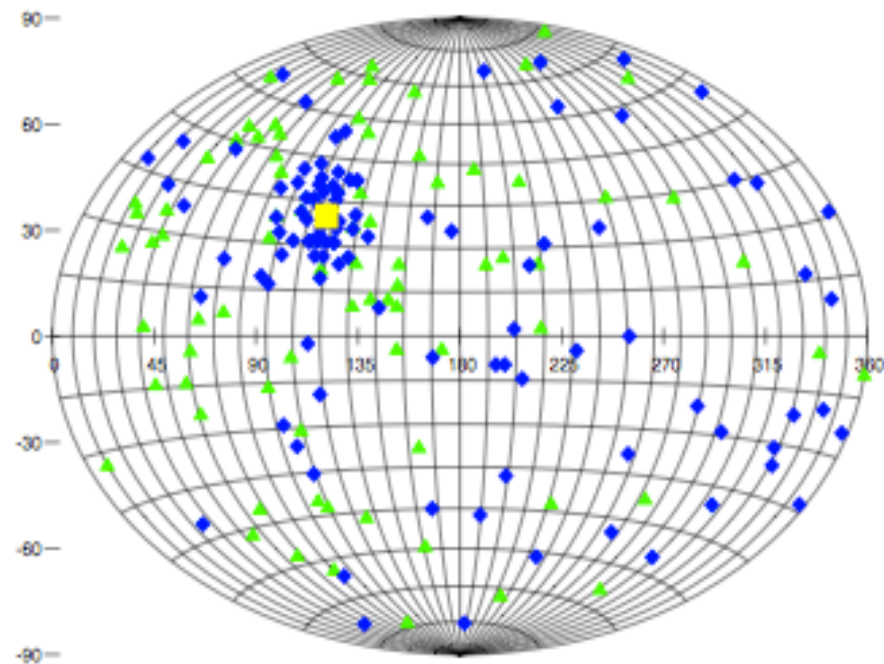
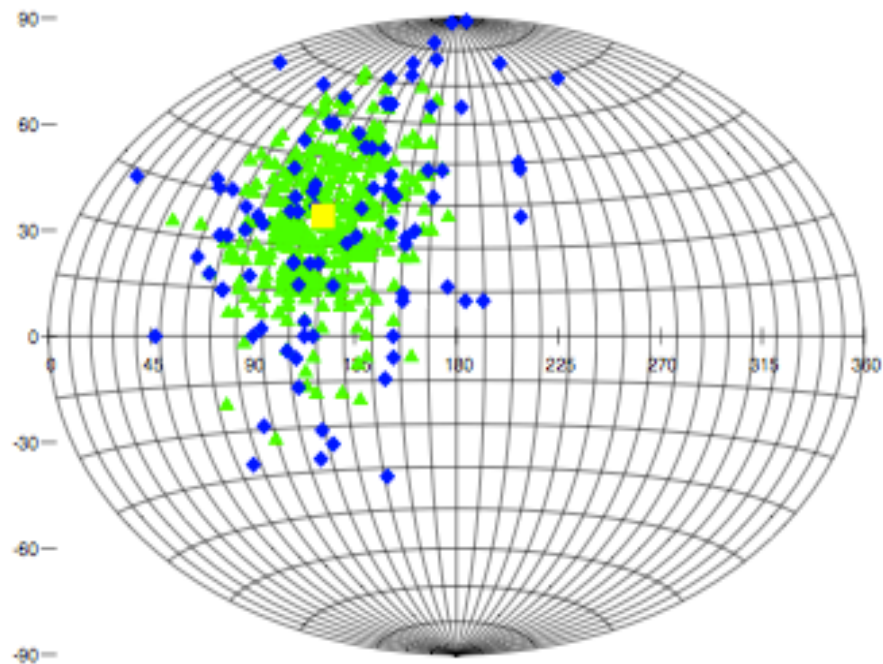
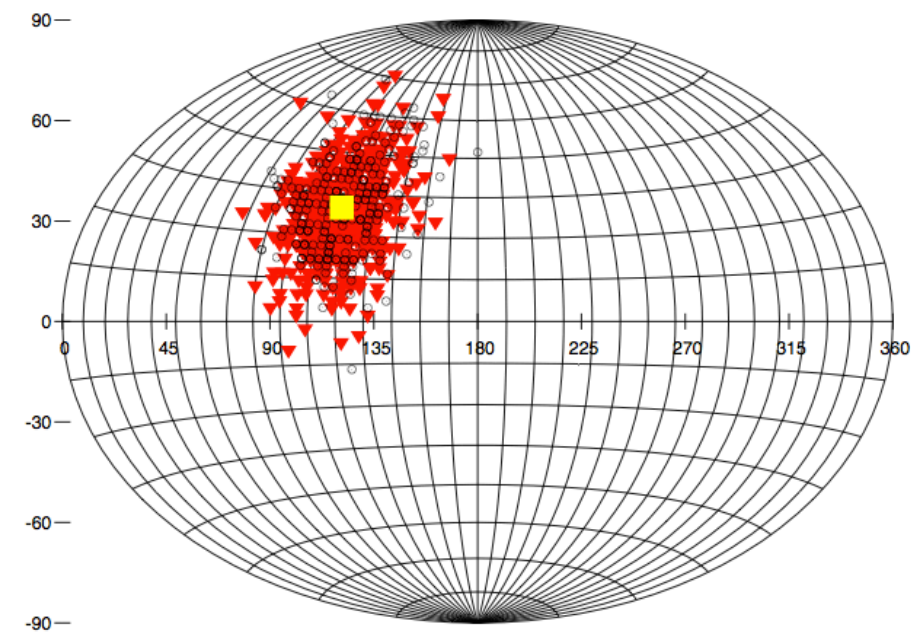


Fig. 3. Magnitude residuals of SNe Ia from the combined Union2 and SN_{FACTORY} dataset as a function of galactic coordinates (l, b) after smoothing with a Gaussian window function of width $\delta = \frac{\pi}{2}$ in the redshift range $0.015 < z < 0.035$ (left), $0.035 < z < 0.045$ (middle) and $0.045 < z < 0.06$ (right). The bulk flow direction is marked by a star.



Distribution	N_{exc} (method A)	N_{exc} (method B)
Isotropic	404	406
Anisotropic I	239	212
Anisotropic II	<u>838</u>	<u>189</u>



Appleby & Shafieloo, JCAP 2014

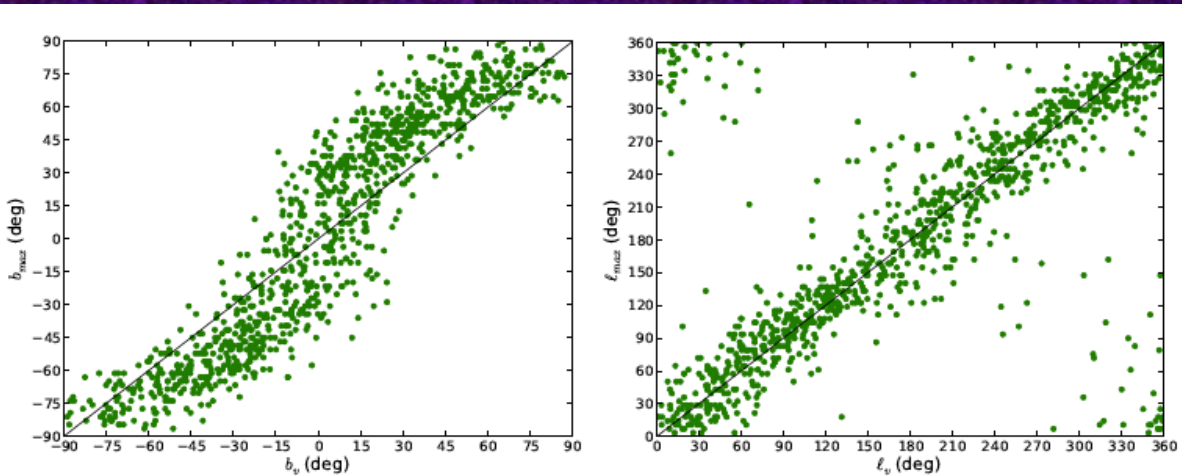
Catalog	$0.015 \leq z < 0.025$	$0.025 \leq z < 0.035$	$0.035 \leq z < 0.045$	$0.045 \leq z < 0.06$	$0.06 \leq z < 0.1$
Union 2.1	61	51	15	17	19
Constitution	53	40	11	12	8
LOSS	76	64	23	17	19
Combined	98	67	22	27	12

Method of Smoothed Residuals

New Results and Bias Control

Δz	Catalog	b_{\max}	ℓ_{\max}	p	Δz	Catalog	b_{\max}	ℓ_{\max}	p
$0.015 \leq z < 0.025$	Union 2.1	49°	259°	0.084	$0.015 < z \leq 0.025$	Union 2.1	49°	259°	0.084
	Const (SALT II)	20°	284°	0.624		Const (SALT II)	20°	284°	0.624
	Const (MLCS 17)	67°	241°	0.692		Const (MLCS 17)	67°	241°	0.692
	LOSS	4°	247°	0.412		LOSS	4°	247°	0.412
	Combined	27°	241°	0.179		Combined	27°	241°	0.179
$0.025 \leq z < 0.035$	Union 2.1	−29°	289°	0.665	$0.015 < z \leq 0.035$	Union 2.1	29°	274°	0.166
	Const (SALT II)	36°	320°	0.271		Const (SALT II)	27°	322°	0.201
	Const (MLCS 17)	40°	313°	0.202		Const (MLCS 17)	52°	288°	0.201
	LOSS	38°	320°	0.156		LOSS	39°	283°	0.177
	Combined	56°	328°	0.339		Combined	41°	266°	0.119
$0.035 \leq z < 0.045$	Union 2.1	27°	320°	0.172	$0.015 < z \leq 0.045$	Union 2.1	31°	284°	0.063
	Const (SALT II)	25°	306°	0.672		Const (SALT II)	27°	301°	0.123
	Const (MLCS 17)	36°	316°	0.192		Const (MLCS 17)	49°	299°	0.083
	LOSS	−27°	292°	0.534		LOSS	20°	284°	0.149
	Combined	11°	313°	0.381		Combined	38°	276°	0.070
$0.045 \leq z < 0.06$	Union 2.1	−49°	58°	0.412	$0.015 < z \leq 0.06$	Union 2.1	25°	295°	0.198
	Const (SALT II)	−54°	55°	0.572		Const (SALT II)	22°	310°	0.216
	Const (MLCS 17)	−59°	68°	0.074		Const (MLCS 17)	38°	315°	0.372
	LOSS	54°	3°	0.457		LOSS	22°	288°	0.159
	Combined	−12°	94°	0.495		Combined	39°	281°	0.176
$0.06 \leq z < 0.1$	Union 2.1	−5°	43°	0.426	$0.015 < z \leq 0.1$	Union 2.1	25°	306°	0.295
	Const (SALT II)	54°	32°	0.574		Const (SALT II)	27°	317°	0.197
	Const (MLCS 17)	−4°	65°	0.352		Const (MLCS 17)	41°	342°	0.431
	LOSS	52°	349°	0.532		LOSS	27°	295°	0.114
	Combined	−54°	65°	0.788		Combined	36°	280°	0.270

Δz	p_A	p_B
$0.015 \leq z < 0.025$	0.179	0.371
$0.015 \leq z < 0.035$	0.119	0.355
$0.015 \leq z < 0.045$	0.070	0.290
$0.015 \leq z < 0.060$	0.176	0.412
$0.015 \leq z < 0.100$	0.270	0.531

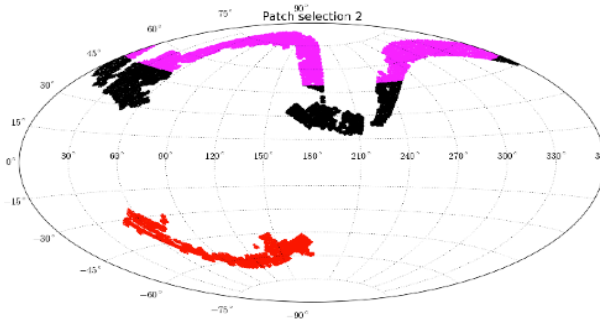
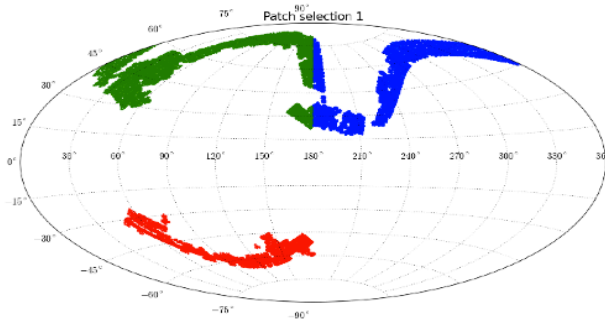


Bias in the Sky

$V_{\text{bulk}}(\text{kms}^{-1})$	North ($b_v > 20^\circ$)		South ($b_v < -20^\circ$)	
	$(\Delta b, \Delta \ell)$	$(\delta b, \delta \ell)$	$(\Delta b, \Delta \ell)$	$(\delta b, \delta \ell)$
400	$(13^\circ, -3^\circ)$	$(14^\circ, 28^\circ)$	$(-12^\circ, 2^\circ)$	$(14^\circ, 29^\circ)$
800	$(15^\circ, -4^\circ)$	$(9^\circ, 22^\circ)$	$(-13^\circ, 2^\circ)$	$(9^\circ, 21^\circ)$

Appleby, Shafieloo, Johnson,
ApJ 2015

Falsification: Testing Isotropy of the Universe in Matter Dominated Era through Lyman Alpha forest



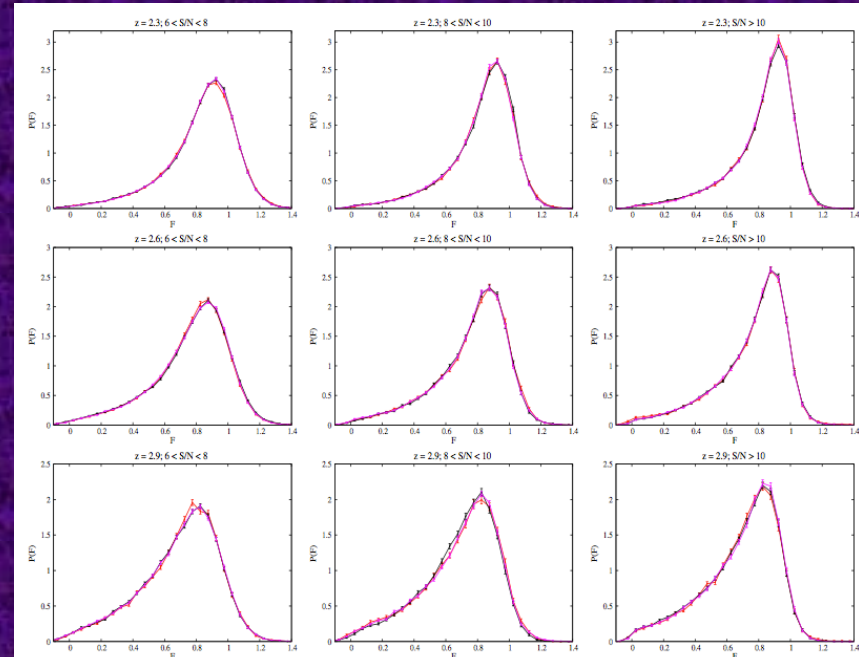
Redshift range(z)	SNR	$\bar{F} \pm \Delta F$
2.15 – 2.45 ($\bar{z} = 2.3$)	6 – 8	$0.826^{+0.154}_{-0.375}$
	8 – 10	$0.822^{+0.138}_{-0.405}$
	> 10	$0.819^{+0.129}_{-0.487}$
2.45 – 2.75 ($\bar{z} = 2.6$)	6 – 8	$0.762^{+0.172}_{-0.39}$
	8 – 10	$0.758^{+0.159}_{-0.427}$
	> 10	$0.756^{+0.152}_{-0.454}$
2.75 – 3.05 ($\bar{z} = 2.9$)	6 – 8	$0.69^{+0.191}_{-0.377}$
	8 – 10	$0.687^{+0.181}_{-0.396}$
	> 10	$0.686^{+0.176}_{-0.413}$

→ Comparing statistical properties of the PDF of the Lyman-alpha transmitted flux in different patches

→ Different redshift bins and different signal to noise

→ Results for BOSS DR9 quasar sample
Results consistent to Isotropy

Hazra and Shafieloo, arXiv:1506.03926



Falsification: Test of Statistical Isotropy in CMB

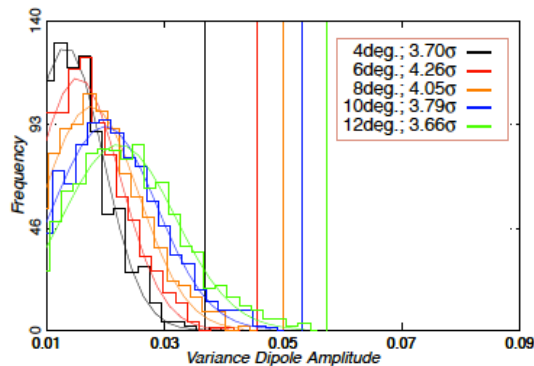


FIG. 3.— Histograms of the local-variance dipole amplitudes from the 1000 FFP6 simulations for disk radii 4° , 6° , 8° , 10° and 12° , together with the best-fit Gaussian distributions in all cases. Vertical lines indicate the corresponding amplitudes measured from the Planck data. The legend shows the rough estimates of detection significances derived from the Gaussian fits.

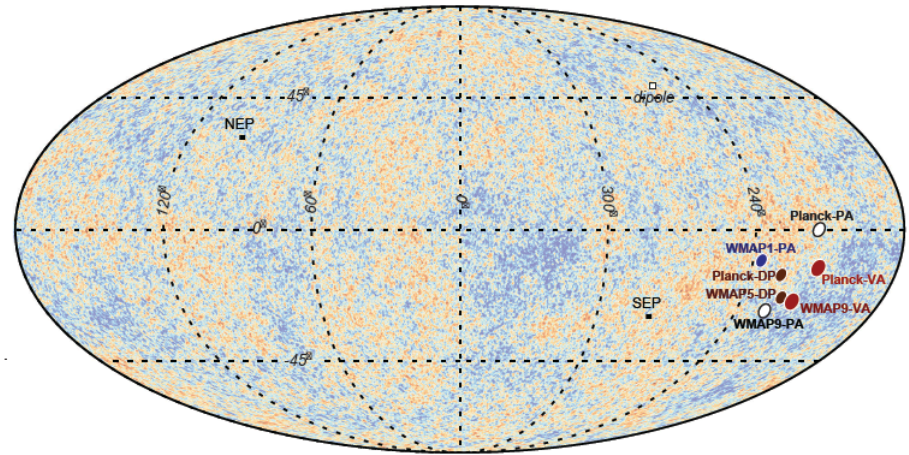


FIG. 6.— Asymmetry directions found in this work by analyzing the local variance of the WMAP 9-year and Planck 2013 data [denoted by *WMAP9-VA* and *Planck-VA*], as well as the directions found previously from the latest likelihood analyses of the dipole modulation model [denoted by *WMAP5-DP* (Hoftuft *et al.* 2009) and *Planck-DP* (Ade *et al.* 2013a)] and the local-power spectrum analyses [denoted by *WMAP1-PA* (Eriksen *et al.* 2004), *WMAP9-PA* (Axelsson *et al.* 2013) and *Planck-PA* (Ade *et al.* 2013a)] for the WMAP and Planck data.

Using Local Variance to Test Statistical Isotropy in CMB maps

- Based on Crossing Statistic
- Residual Analysis,
- Real Space Analysis
- Low Sensitivity to Systematics
- 2D Adaptive Gaussian Smoothing
- Frequentist Approach

TABLE 1
ASYMMETRY DIRECTIONS

Map	(l, b) [$^\circ$]	Significance or p -value	Reference
Planck-VA	(212, -13)	0/1000	present work
WMAP9-VA	(219, -24)	10/1000	present work
Planck-DP	(227, -15)	3.5σ	Ade <i>et al.</i> (2013a)
WMAP5-DP	(224, -22)	3.3σ	Hoftuft <i>et al.</i> (2009)
Planck-PA	(224, 0)	0/500	Ade <i>et al.</i> (2013a)
WMAP9-PA	(227, -27)	7/10000	Axelsson <i>et al.</i> (2013)

Testing deviations from an assumed model (without comparing different models)

Gaussian Processes:

Modeling of the data around a mean function searching for likely features by looking at the the likelihood space of the hyperparameters.

Bayesian Interpretation of Crossing Statistic:

Comparing a model with its own possible variations.

REACT:

Risk Estimation and Adaptation after Coordinate Transformation

Gaussian Process

- Efficient in statistical modeling of stochastic variables
- Derivatives of Gaussian Processes are Gaussian Processes
- Provides us with all covariance matrices

Shafieloo, Kim & Linder, PRD 2012
Shafieloo, Kim & Linder, PRD 2013

Data

Mean Function

$$\begin{bmatrix} \mathbf{y} \\ \mathbf{f} \\ \mathbf{f}' \\ \mathbf{f}'' \end{bmatrix} \sim \mathcal{N} \left(\begin{bmatrix} \mathbf{m}(\mathbf{Z}) \\ \mathbf{m}(\mathbf{Z}_1) \\ \mathbf{m}'(\mathbf{Z}_1) \\ \mathbf{m}''(\mathbf{Z}_1) \end{bmatrix}, \begin{bmatrix} \Sigma_{00}(\mathbf{Z}, \mathbf{Z}) & \Sigma_{00}(\mathbf{Z}, \mathbf{Z}_1) & \Sigma_{01}(\mathbf{Z}, \mathbf{Z}_1) & \Sigma_{02}(\mathbf{Z}, \mathbf{Z}_1) \\ \Sigma_{00}(\mathbf{Z}_1, \mathbf{Z}) & \Sigma_{00}(\mathbf{Z}_1, \mathbf{Z}_1) & \Sigma_{01}(\mathbf{Z}_1, \mathbf{Z}_1) & \Sigma_{02}(\mathbf{Z}_1, \mathbf{Z}_1) \\ \Sigma_{10}(\mathbf{Z}_1, \mathbf{Z}) & \Sigma_{10}(\mathbf{Z}_1, \mathbf{Z}_1) & \Sigma_{11}(\mathbf{Z}_1, \mathbf{Z}_1) & \Sigma_{12}(\mathbf{Z}_1, \mathbf{Z}_1) \\ \Sigma_{20}(\mathbf{Z}_1, \mathbf{Z}) & \Sigma_{20}(\mathbf{Z}_1, \mathbf{Z}_1) & \Sigma_{21}(\mathbf{Z}_1, \mathbf{Z}_1) & \Sigma_{22}(\mathbf{Z}_1, \mathbf{Z}_1) \end{bmatrix} \right),$$

$$\Sigma_{\alpha\beta} = \frac{d^{(\alpha+\beta)} K}{dz_i^\alpha dz_j^\beta},$$

$$\begin{bmatrix} \bar{\mathbf{f}} \\ \bar{\mathbf{f}}' \\ \bar{\mathbf{f}}'' \end{bmatrix} = \begin{bmatrix} \mathbf{m}(\mathbf{Z}_1) \\ \mathbf{m}'(\mathbf{Z}_1) \\ \mathbf{m}''(\mathbf{Z}_1) \end{bmatrix} + \begin{bmatrix} \Sigma_{00}(\mathbf{Z}_1, \mathbf{Z}) \\ \Sigma_{10}(\mathbf{Z}_1, \mathbf{Z}) \\ \Sigma_{20}(\mathbf{Z}_1, \mathbf{Z}) \end{bmatrix} \Sigma_{00}^{-1}(\mathbf{Z}, \mathbf{Z}) \mathbf{y}$$

Kernel

$$k(z, z') = \sigma_f^2 \exp \left(-\frac{|z - z'|^2}{2l^2} \right),$$

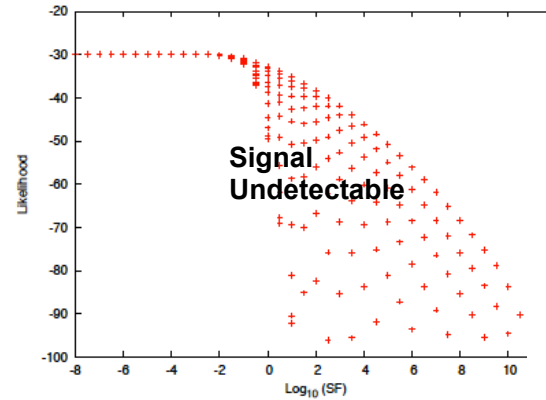
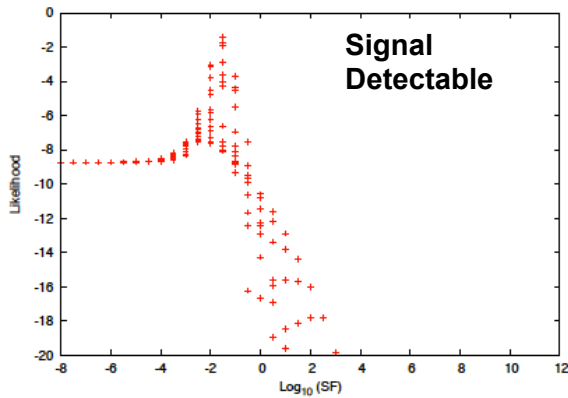
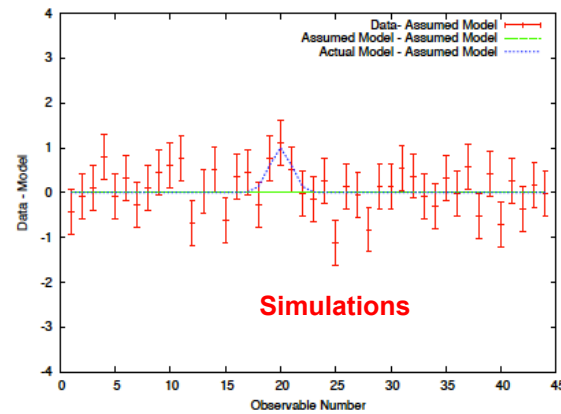
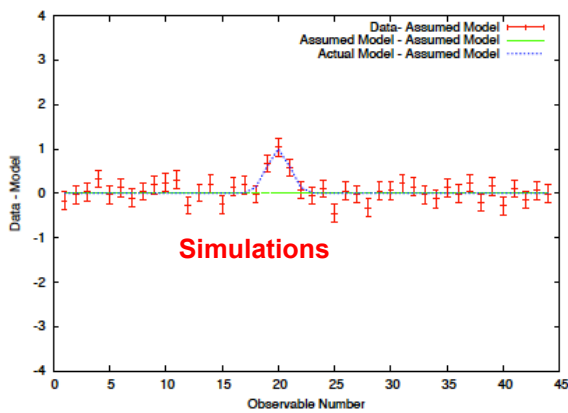
GP Hyper-parameters

$$\text{Cov} \left(\begin{bmatrix} \mathbf{f} \\ \mathbf{f}' \\ \mathbf{f}'' \end{bmatrix} \right) = \begin{bmatrix} \Sigma_{00}(\mathbf{Z}_1, \mathbf{Z}_1) & \Sigma_{01}(\mathbf{Z}_1, \mathbf{Z}_1) & \Sigma_{02}(\mathbf{Z}_1, \mathbf{Z}_1) \\ \Sigma_{10}(\mathbf{Z}_1, \mathbf{Z}_1) & \Sigma_{11}(\mathbf{Z}_1, \mathbf{Z}_1) & \Sigma_{12}(\mathbf{Z}_1, \mathbf{Z}_1) \\ \Sigma_{20}(\mathbf{Z}_1, \mathbf{Z}_1) & \Sigma_{21}(\mathbf{Z}_1, \mathbf{Z}_1) & \Sigma_{22}(\mathbf{Z}_1, \mathbf{Z}_1) \end{bmatrix} - \begin{bmatrix} \Sigma_{00}(\mathbf{Z}_1, \mathbf{Z}) \\ \Sigma_{10}(\mathbf{Z}_1, \mathbf{Z}) \\ \Sigma_{20}(\mathbf{Z}_1, \mathbf{Z}) \end{bmatrix} \Sigma_{00}^{-1}(\mathbf{Z}, \mathbf{Z}) [\Sigma_{00}(\mathbf{Z}, \mathbf{Z}_1), \Sigma_{01}(\mathbf{Z}, \mathbf{Z}_1), \Sigma_{02}(\mathbf{Z}, \mathbf{Z}_1)].$$

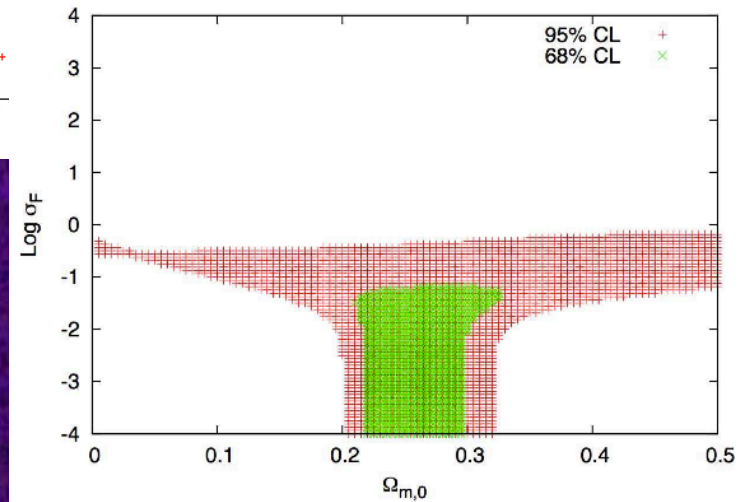
$$2 \ln p(\mathbf{y}|\mathbf{f}) = -\mathbf{y}^T \Sigma_{00}(\mathbf{Z}, \mathbf{Z})^{-1} \mathbf{y} - \ln \det \Sigma_{00}(\mathbf{Z}, \mathbf{Z}) - n \ln(2\pi),$$

GP Likelihood

Detection of the features in the residuals



GP to test GR
Shafieloo, Kim, Linder, PRD 2013



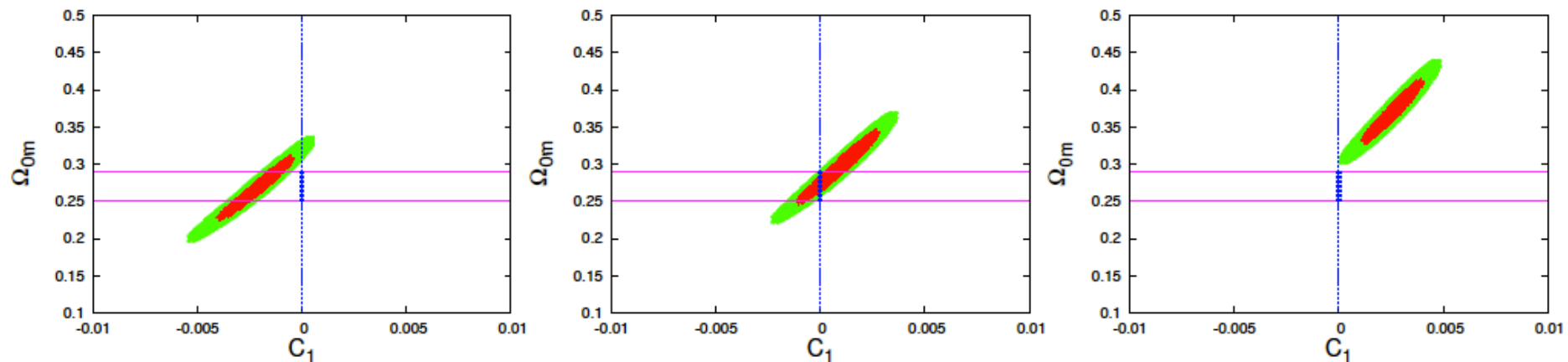
Crossing Statistic (Bayesian Interpretation)

Theoretical model

Crossing function

Comparing a model
with its own variations

$$\mu_M^{T_N}(z) = \mu_M(p_i, z) \times T_N(C_1, \dots, C_N, z)$$



$$T_I(C_1, z) = 1 + C_1 \left(\frac{z}{z_{max}} \right)$$

Chebyshev Polynomials
as Crossing Functions

$$T_{II}(C_1, C_2, z) = 1 + C_1 \left(\frac{z}{z_{max}} \right) + C_2 \left[2 \left(\frac{z}{z_{max}} \right)^2 - 1 \right],$$

Shafieloo, JCAP 2012 (a)

Shafieloo, JCAP 2012 (b)

Crossing Statistic (Bayesian Interpretation)

Theoretical model

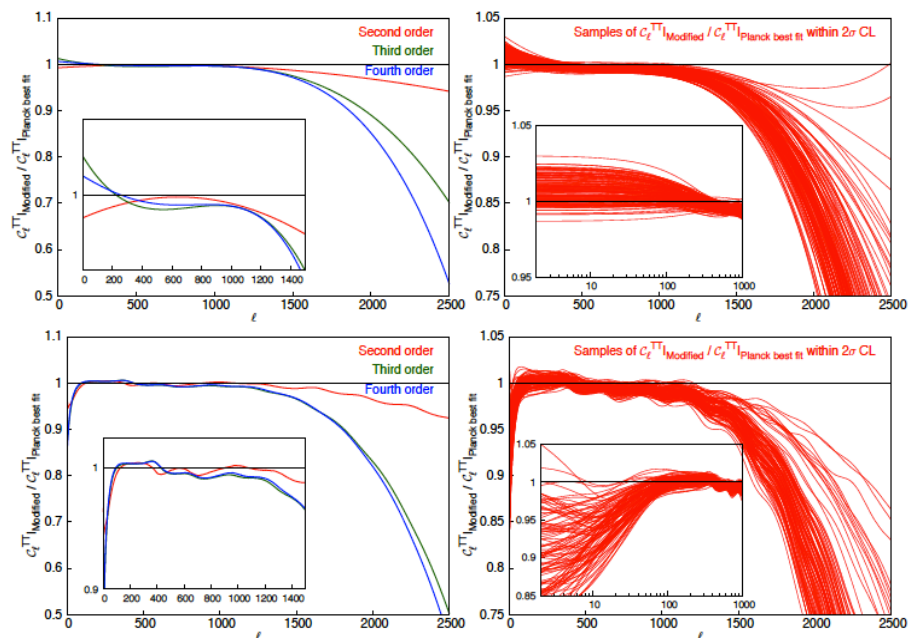
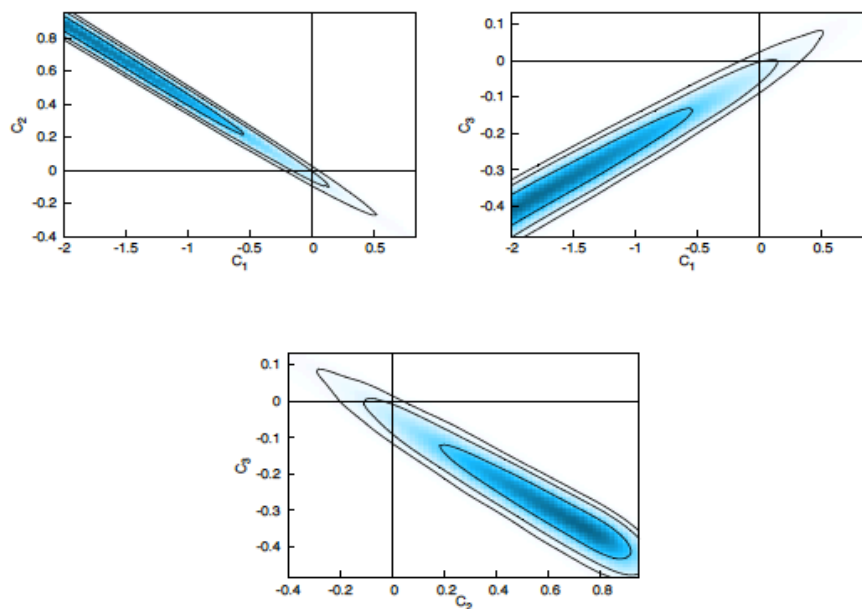
Crossing function

$$C_{\ell}^{\text{TT}}|_{\text{modified}}^N = C_{\ell}^{\text{TT}}|_{\Omega_b, \Omega_{\text{CDM}}, H_0, \tau, A_S, n_S, \ell} \times T_i(C_0, C_1, C_2, \dots, C_N, \ell).$$

Confronting the concordance model of cosmology with Planck data

Hazra and Shafieloo, JCAP 2014

Consistent only at 2~3 sigma CL



Dates

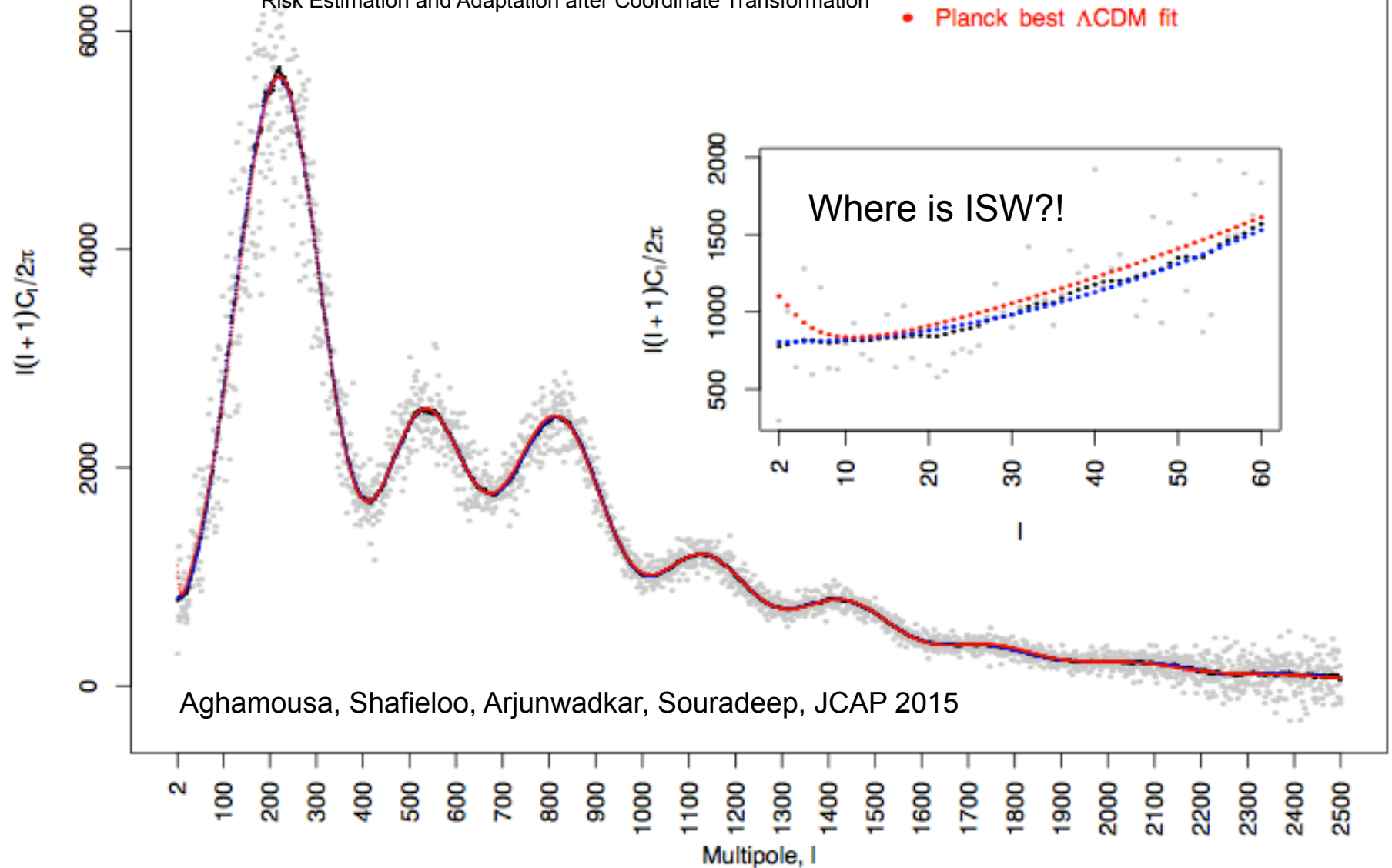
Issue 01 (January 2014)

Received 13 January 2014, accepted for publication 14 January 2014

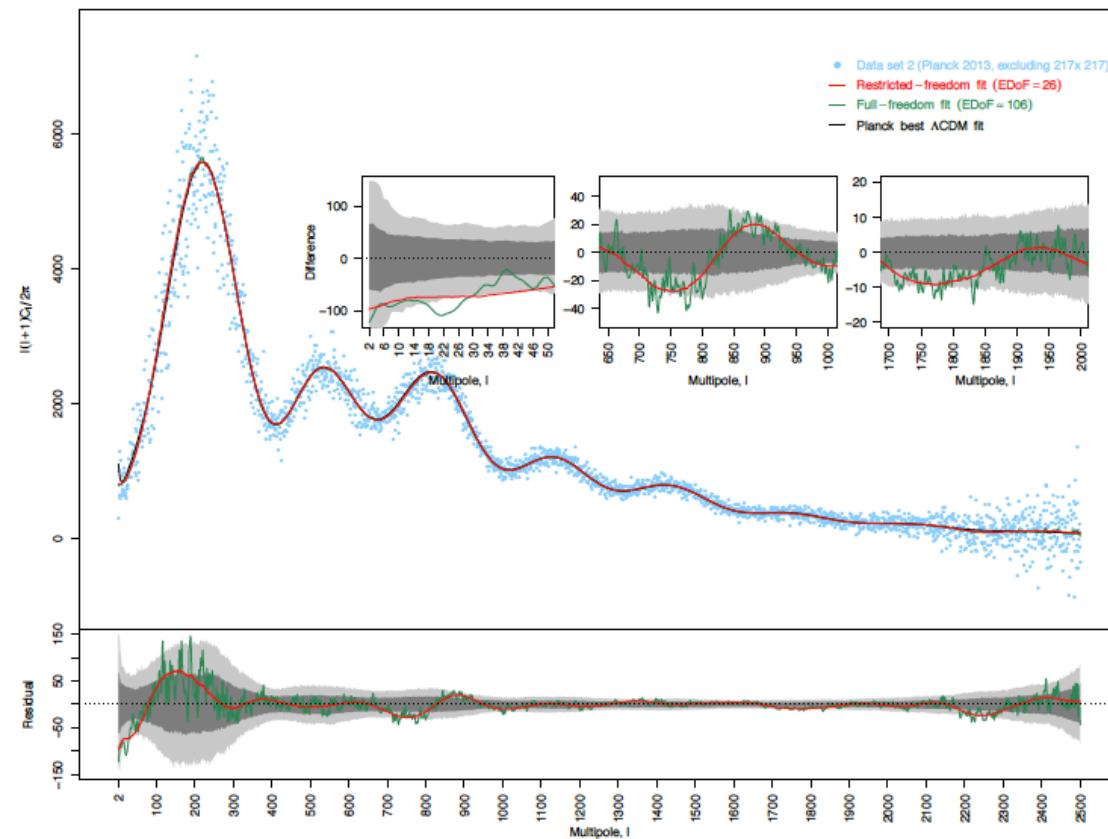
Published 28 January 2014

REACT Non-parametric fit

Risk Estimation and Adaptation after Coordinate Transformation



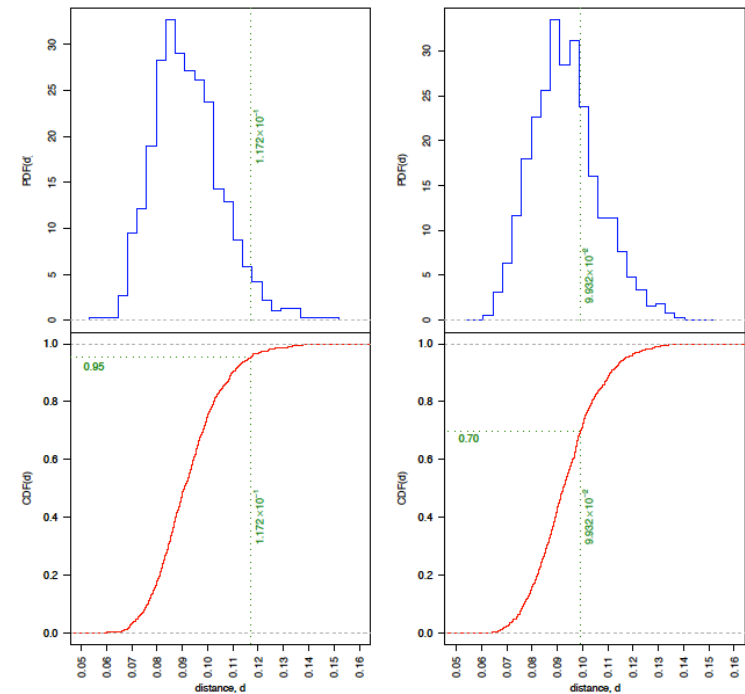
Calibrated REACT



Aghamousa and Shafieloo, JCAP 2015

Consistent only at 2~3 sigma CL

Excluding 217 Ghz, consistent at 1~2 sigma CL



Conclusion

- The current standard model of cosmology seems to work fine but this does not mean all the other models are wrong. Data is not yet good enough to distinguish between various models.
- Using parametric methods and model fitting is tricky and we may miss features in the data. Non-parameteric methods of reconstruction can guide theorist to model special features.
- First target can be rigorous testing of the standard 'Vanilla' model. If it is not '*Lambda*' dark energy or power-law primordial spectrum then we can look further. It is possible to focus the power of the data for the purpose of falsification.